UNIVERSITY OF CAPE TOWN
IYUNIVESITHI YASEKAPA • UNIVERSITEIT VAN KAAPSTAD

Medical Biotechnology & Immunotherapy Research Unit
Institute of Infectious Disease & Molecular Medicine
South African Research Chair in Cancer Biotechnology
Department of Integrative Biomedical Sciences
Faculty of Health Sciences
University of Cape Town

Masters Thesis

Development of recombinant immunodiagnostics and -therapeutics for Triple Negative Breast Cancer (TNBC)

Takunda Lameck Ngwenya

Supervisor:

Prof. Dr. Dr. Stefan Barth

Declaration

I, **Takunda Ngwenya**, hereby declare that the work on which this dissertation/thesis is based is my original work (except where acknowledgments indicate otherwise) and that neither the whole work nor any part of it has been, is being, or is to be submitted for another degree in this or any other university.

I empower the university to reproduce for the purpose of research either the whole or any portion of the contents in any manner whatsoever.

Signature: Signed by candidate

Date: 20/06/2023

Acknowledgments

I would like to thank God for granting me the ability to see this work through to completion.

I would like to express my deepest appreciation and gratitude to My supervisor, Professor Dr. Dr. Stefan Barth, for his unwavering support, invaluable guidance, mentorship, and continuous encouragement throughout the entire research journey. Thank you for believing in me from the moment I embarked on my master's journey at the MB&I research unit. You have imparted invaluable knowledge on innovative methods utilizing medical biotechnology in the pursuit of cancer treatment. Your wealth of experience and expertise has been a tremendous source of learning for me.

I would like to thank the members of my MB&I for their valuable input, constructive criticism, and scholarly advice and for being exceptional lab mates. I want to thank Marc Henry and Dr. Alex for their thorough review and thoughtful suggestions that have significantly enhanced this work's quality.

I would like to thank the National Research Foundation (NRF), of South Africa, the South African Research Chair Initiative (SARChI) in Cancer Biotechnology, and the University of Cape Town (UCT) for the financial assistance and for making this project a reality.

I am indebted to my family, particularly my parents Tambudzai and Kundai, and my siblings Tafara, Tadiwa, Tanaka, Tawanda and Tatenda, for their unconditional love, unwavering belief in my abilities, and constant encouragement. Their support, prayers and sacrifices have been the foundation for this thesis.

Lastly, I would like to express my gratitude to all the authors, researchers, and scholars whose work I have referenced in this thesis. Their groundbreaking research and insightful contributions have paved the way for this study and have been a source of inspiration.

Contents

List of Abbreviations

TNBC	Triple Negative Breast Cancer
scFv	Single chain variable fragment
ADC	Antibody-drug conjugate
CSC's	Cancer stem cells
IKB	NF-kB kinase complex
IKK	inhibitor of nuclear factor kappa -ß- kinase subunit
EGF	epidermal growth factor
VH	variable heavy chain
VL	variable light chain
CAR	Chimeric Antigen Receptor
TM	transmembrane
TCR	T cell receptors
CDR's	complementarity determining regions
mAb	Monoclonal antibody
ETA	Pseudomonas Exotoxin A immunotoxin
dETA	deimmunised Pseudomonas Exotoxin A immunotoxin
wt	Wildtype
LGR5	Leucine-rich repeat-containing G protein-coupled receptor 5
CD90	Cluster differentiation 90
EpCAM	Epithelial cell adhesion molecule
HIV	Human Immunodeficiency virus
AIDS	Acquired Immunodeficiency Syndrome
rIT	Recombinant Immunotoxin

List of Figures

List of Tables

List of Publications

1. Dogbey DM, Torres VES, Fajemisin E, Mpondo L, **Ngwenya T**, Akinrinmade OA, Perriman AW, Barth S. Technological advances in the use of viral and non-viral vectors for delivering genetic and non-genetic cargos for cancer therapy. Drug Deliv Transl Res. 2023 Jun 10:1–20. doi: 10.1007/s13346-023-01362-3. Epub ahead of print. PMID: 37301780; PMCID: PMC10257536.

Abstract

Breast cancer is the most common form of female malignancy globally. There are several subtypes of breast cancers including Triple-negative breast cancer (TNBC), which is mainly characterized by a lack of expression of the estrogen receptor (ER), progesterone receptor (PR) and human epidermal growth factor receptor 2 (HER2). TNBC is one of the most aggressive subtypes of breast cancer, with a 20% lower disease-free and overall survival rates than is observed for non-TNBC patients. It is characterized by higher rates of aggressive relapse, high metastatic potential, shorter survival rate and an overall aggressive and invasive clinical course. This subtype is most prevalent in young ($\leqslant$ 50 years) female patients of African ancestry compared to other ethnicities. TNBC poses a significant challenge due to the lack of molecular targets. The current treatment of TNBC is achieved by chemotherapy, surgery and radiotherapy, collectively referred to as tri-modality therapy. However, tri-modality therapy results in disease relapse and adverse side effects. As a result, an ongoing need exists to develop a range of targeted therapeutics to effectively treat the majority of TNBC tumours. These targeted anti-cancer therapies aim to enable the selective killing of cancer cells while minimizing harm to healthy cells. This selective cytotoxicity would result in a significant improvement in TNBC treatment efficacy while reducing the side effects. The development of targeted anticancer therapies for TNBC is an active area of research and scientists are currently exploring various approaches to develop targeted anticancer therapies for TNBC and other cancer types.

Antibody-Drug-Conjugates (ADCs) are proteins that combine an antibody and a toxin designed to selectively target and kill cancerous cells respectively. These are promising alternatives to conventional cancer treatment. This approach takes advantage of the specific cell surface receptors (CSRs) that are often present on cancerous cells and absent in healthy tissues. Among several CSRs that have been identified to be overexpressed in TNBC, CD90, LGR5 and EpCAM were considered for this study. Due to the limited effectiveness of full mAbs penetration into tumours, smaller antibody fragments such as scFv and Fabs have shown a greater ability to penetrate tumour tissues. These smaller antibody formats can be used to develop recombinant immunotoxins (rITs) using protein toxins as cell-killing moieties to achieve targeted destruction of cancer cells. Pseudomonas exotoxin A (ETA) is a potent enzyme that disrupts the function of

eukaryotic elongation factor 2, causing inhibition of protein synthesis and leading to cell death. Due to the bacterial origin of ETA, scientists have discovered that it often triggers an unwanted humoral response in patients during clinical trials. To address this challenge, researchers have introduced mutations in the ETA gene to reduce the risk of causing an immunogenic response while preserving the cytotoxicity activity.

This study aimed at developing single chain fragments of variability (scFvs) derived from publicly available sequences of antibodies that target three CSRs overexpressed in TNBC, genetically fused to wild-type ETA (wt ETA) or a mutant version of ETA that was generated using advanced computer simulation by our collaborating partner, Professor Paolo Carloni from Forschungszentrum Jülich, Germany. The mutated version is described as de-immunized ETA (dETA). The recombinant immunotoxins were generated by constructing a bacterial periplasmic expression plasmid, which included ETA or dETA fused to an scFv antibody fragment targeting each of the three biomarkers (CD90, LGR5 and EpCAM). The plasmid also contained the corresponding scFv that was inserted before the transformation of the plasmid into *Escherichia coli* (*E. coli*) BL21 for bacterial protein expression under osmotic stress conditions in the presence of compatible solutes. The rITs were then purified by immobilized metal ion chromatography (IMAC) and size exclusion chromatography (SEC). Confirmation of full-length rITs was done by sodium dodecyl-sulfate polyacrylamide gel electrophoresis (SDS PAGE) and Western blot analysis. Upon successful confirmation of full-length proteins, binding and cytotoxicity studies were conducted on TNBC cell line MDA-MB-468 using the rITs.

In this study, all six designed plasmids were successfully cloned, and recombinant fusion proteins were expressed using the bacterial periplasm of *E. coli* BL21 as evidenced by SDS PAGE and western blot. The rITs displayed a strong binding affinity for MDA-MB-468 TNBC cells. Cytotoxicity results revealed that both ETA and dETA-rITs can both target and kill MDA-MB-468 TNBC cells. ETA-based rITs exhibited more robust killing activity than dETA-based rITs, except for the rITs targeting CD90, in this case exceeding wt ETA enzymatic activity.

This study showed potential for clinical application of the generated rITs' for TNBC immunodiagnostic use and the ability of ETA and dETA toxins to specifically kill TNBC antigen-positive tumour cells indicating targeted therapeutic potential. This work serves as proof of

concept for investigating the use of rITs in TNBC tumour detection and patient stratification to offer personalized therapeutics.

1. CHAPTER 1: LITERATURE REVIEW

1.1. Breast Cancer Overview

According to the World Health Organization (WHO), breast cancer is the most common cancer worldwide and is the leading cause of cancer deaths in women[1]. It accounts for 25% and 30% of all new cancers diagnosed globally and in Africa respectively[2]. Globally, female breast cancer has surpassed lung cancer as the leading cause of cancer incidence in 2020, with an estimated 2.4 million new cases of all cancer cases[3]. Breast cancer patients in Africa experience a mortality rate exceeding 50% [4]. The National Cancer Registry (2014) predicts that women have a 1 in 27-lifetime risk of having breast cancer, making it the most common cancer amongst South African women excluding nonmelanoma skin cancers. The incidence of breast cancer is also on the rise in South Africa[11], [12]. As the second-leading cause of death for women, breast cancer presents a great danger to the socioeconomic well-being of South Africa and the world at large.

Breast cancer refers to the malignant transformation[5], and proliferation of cells originating from breast tissue that are characteristically aberrant [6]. It is a heterogeneous disease whereby the neoplasms originate from various types of breast tissues. Breast cancer is prevalent in women more than in men. It was first identified in 1500 BC, in ancient Egypt[7]. Breast cancers can be characterized as non-invasive or invasive depending on the tissue structure which is indicative of its severity[8]. If the cancer has spread into surrounding breast tissue, it is referred to as invasive breast cancer [9] and if it is confined to the ducts and does not invade surrounding fatty and connective tissues of the breast, it is defined as non-invasive[10] (Figure 1). The two most common types of invasive breast cancer tumours are defined by where in the breast they begin to grow, which are mammary lobules (invasive lobular carcinoma) or mammary ducts (invasive ductal carcinoma)[11], [12].

It is imperative to know the general structure of the normal female breast to understand breast cancer since it is a complex and heterogeneous disease[13]. The breasts of an adult woman are milk-producing, tear-shaped glands, attached to the front of the chest wall on either side of the breastbone by ligaments[14]. They consist of milk-secreting sacs called lobules, and ducts that

drain milk to the nipples (Figure 1) [15]. A lobule is the functional unit of the mammary gland, consisting of a tree of several intralobular ducts (also called alveolar ducts), each of which can merge into terminal alveoli composed of milk-secreting epithelial cells (Figure 1). The lobules and ducts are milk-secreting sacs that drain milk to the nipples[16]. These two most occurring histological breast cancers arise from the malignant transformation of cells lining these ducts and lobules, thereby resulting in ductal and lobular carcinomas respectively[17]. Sarcoma breast cancers are very rare, constituting less than 1% of primary breast cancers that arise from the stromal components of the breast[18]. Phyllode tumours and angiosarcomas are also rare forms of breast cancer that arise from supportive cells[19].

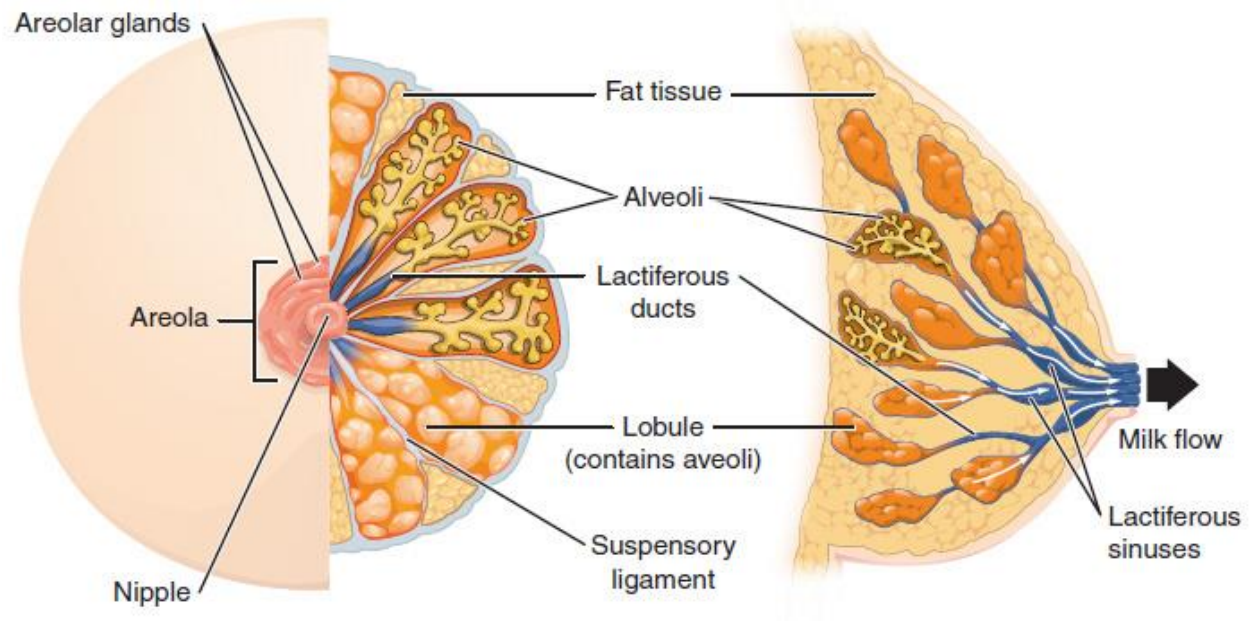

Figure 1: Structure of breast during lactation. The normal female breast is comprised of fatty tissue, ducts, lobules, lymph, and blood vessels. Cancerous cells can start to grow in cells of any breast tissue, but the most common types occur in the lining of the ducts and lobules[20].

1.2. Risk Factors

Breast cancer development is influenced by various risk factors. These factors encompass family history, ethnicity, sex, aging, estrogen exposure, early abortion, oral contraceptives, gene mutations, and an unhealthy lifestyle [21]–[23]. Scientific knowledge has progressively elucidated these risk factors, paving the way for preventive strategies. For example, certain risk factors can be mitigated to decrease the chances of breast cancer occurrence. Despite advancements, the precise mechanisms underlying cancer cell formation remain incompletely understood. A family history of breast cancer emerges as a significant risk factor, contributing to heightened susceptibility [21]. Actually, hereditary gene mutations constitute 10% of all occurrences of breast cancers [22][23]. Unfavourable estrogen-altering lifestyle choices are prevalent risk factors for breast cancer incidence[24]. Behaviours linked to elevated estrogen levels include excessive weight, a sedentary lifestyle, smoking, a high-fat diet, and alcohol consumption [24]. Both exogenous and endogenous estrogen exposure heightens breast cancer risk, further exacerbated by the use of oral contraceptives and hormone replacement therapy. Additionally, genetic factors contribute to the likelihood of breast cancer development [25].

Several gene defects can be implicated in the occurrence of hereditary breast cancer. There are two most popular anti-oncogenes associated with increasing the risk of breast cancer occurrence. The latter are breast cancer-associated genes 1 and 2 (BRCA1 and BRCA2)[25]. BRCA1 and BRCA2 are both tumour suppressor genes or anti-oncogenes located on chromosomes 17q21 and 13q12, respectively. Primarily, they both encode tumour suppressor proteins, and mutation of these would result in tumour pathogenesis and progression[26], [27]. Usually, mutations of these two genes are mostly associated with inheritance and aging (>50 years)[28]. In particular, BRCA1 is more significant since individuals carrying mutations in this gene are more prone to developing TNBC which is the main focus of this research project[29].

In addition, there are more genes related to breast cancer, some of which are Human Epidermal Growth Factor Receptor 2, known as c-erbB-2, Epidermal Growth Factor Receptor (EGFR), also known as c-erbB-1 or HER1 in humans, the genes encoding Myc protein and three members in the Ras gene family: H-ras, K-ras and N-ras, located on the chromosome of 11 (11p15), 12 (12p12) and 1 (1p22), respectively. Ras signalling pathways are found in both benign and malignant

cancerous mammary tissues, giving them limited predictive value although they are mostly associated with TNBC [30][31]. Currently, these are still being investigated to strengthen their prognostic/diagnostic accuracy potential [30]. However, all risk factors combined, tumour pathogenesis is thought to be caused by uncontrolled stem cell division that results in tumour phenotypes, or possibly random gene mutation accumulation that may disrupt the normal cell division processes resulting in benign or potentially metastatic carcinomas. [32][25].

Table 1: An outline of common risk factors

Risk Factor	**Prevalence/Incidence**	**References**
Age	Increases with age, most common in women over 50 [21]	[21]
Gender	Higher risk in women compared to men	[21]
Family history	About 5-10% of breast cancer cases have a hereditary component [22].	[22].
Genetic mutations	BRCA1 and BRCA2 mutations increase the risk significantly	[25].
Personal history	Prior breast cancer increases the risk of a new occurrence	[21].
Race and ethnicity	Higher incidence in white women, but mortality rates are higher in African-American women	[21].
Hormonal factors	Early menarche (onset of menstruation), late menopause, and hormone replacement therapy can increase risk	[24].
Reproductive factors	Late or no pregnancy, never breastfeeding	[21].
Dense breast tissue	Increased breast density is associated with a higher risk	[33].
Radiation exposure	Prior chest radiation therapy, especially during childhood, increases risk	[34].
Obesity	A higher body mass index (BMI) is associated with an increased risk, particularly in postmenopausal women	[35].
Alcohol consumption	Regular and excessive alcohol intake is associated with an increased risk	[36]

Physical inactivity	A sedentary lifestyle and lack of regular physical activity are associated with an increased risk	[37]
Estrogen exposure	Long-term use of estrogen-containing contraceptives or hormone replacement therapy can increase risk	[24]

1.3. Screening and Diagnosis

For many years of research, scientists have discovered that early and precise diagnosis is key for effective management and essential for reduced mortality associated with breast cancers[25], [38][39]. An early breast cancer diagnosis is correlated to the survival rate[40]. Currently, there is a great health burden for TNBC as it is a highly heterogeneous disease with ununiform patterns in biological and morphological features[40]. This poses a great challenge to their clinical classification and detection of different breast cancer subtypes. This research project also speaks to this effect as an attempt to improve the diagnostic and therapeutic procedures for TNBC. Several techniques and methods are currently being used for breast cancer screening. These include physical examination, and affordable imaging techniques including x-ray mammography, magnetic resonance imaging (MRI) and breast ultrasound[39].

Mammography is also referred to as the gold standard for breast cancer imaging because it is the mainstay of breast cancer screening and detection [41][42]. It uses low-energy X-rays to produce high-resolution images of breast tissues to detect abnormalities. However, some researchers are not pro mammography, and they suggest that it also gives false negatives in some cases[43], [44]. Due to human error whilst interpreting images, Artificial intelligence (AI) has been proposed to reduce the error margin whilst interpreting the images[45]. Magnetic resonance imaging and ultrasound have become useful diagnostic adjuncts in select patient populations[42]. MRI is however sensitive but less specific in its detection of cancer in high-risk patients[25]. The use of adjunctive ultrasound screening offers marginal screening benefits in high-risk patients[42][46].

1.4. Tumour staging

Staging determines the primary tumour size and how far it has spread, whilst grading refers to the appearance of the affected cells[47]. Treatment and prognosis of breast cancers are usually

based on tumour staging and grading outcomes[48]. Effective treatment of breast tumours has been correlated with the tumour stage at the time of diagnosis[49]. Several critical aspects are usually considered for the classification and proper monitoring of breast cancer disease. These include the popular TNM system (Figure 2) that accounts for tumour size and locality (T), the presence or absence of Nodal metastasis(N), and the presence of distant Metastasis(M) and the biopsy (pathological assessment)[50].

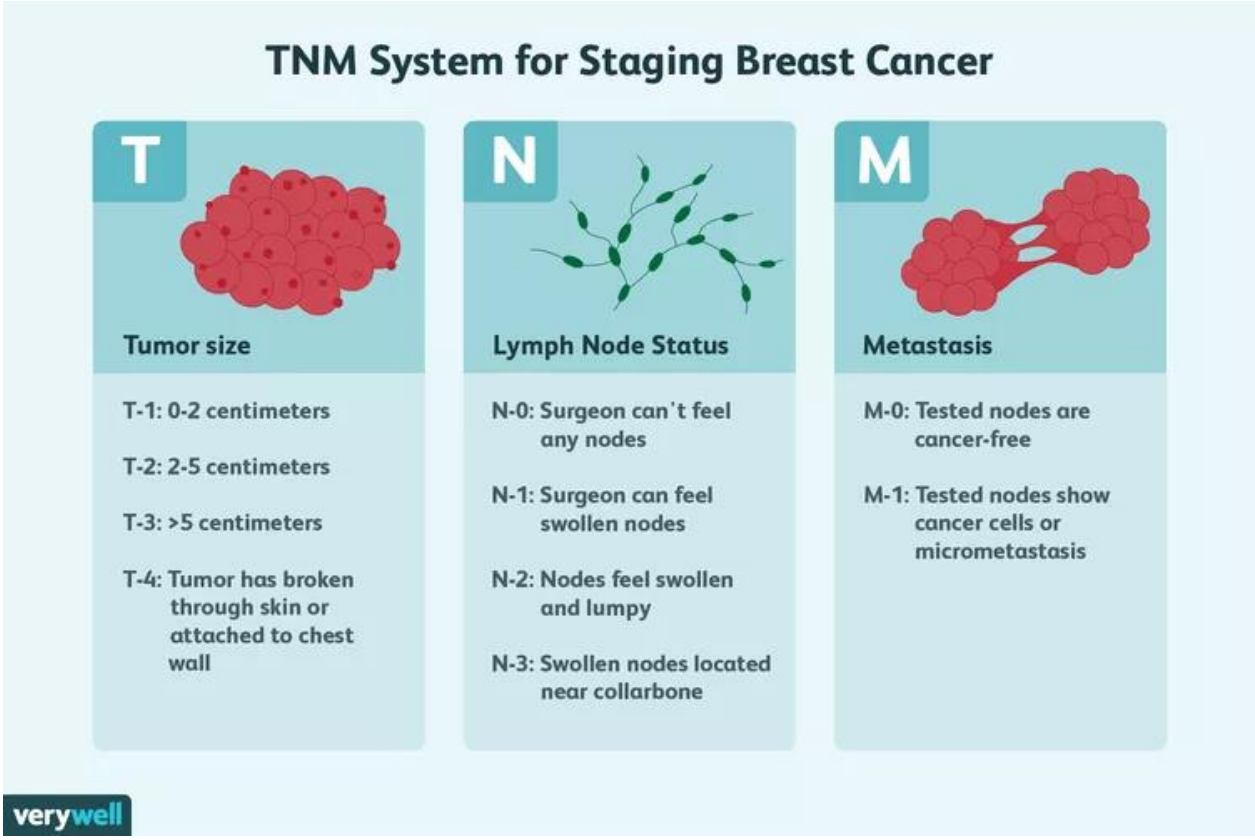

Figure 2: TNM system for breast cancer staging. TNM is an abbreviation for three characteristics used to determine the stage of cancer[51].

If breast screening results suggest that there is a possibility of predisposition to cancer, a biopsy procedure is recommended as a successive step[52]. This procedure is conducted by a pathologist, who examines breast tissues and/or cells to assess the histological features as compared to non-tumourous cells or tissues[53][54]. The standard of comparison for this is derived from the Nottingham modification of the Scarff Bloom Richardson grading system[55].

1.5. Classification and subtypes of Breast cancer

Breast cancer has since been classified into five molecular subtypes which have biological distinctness that is important for tumour management[54]. Pathologists have used immunohistochemistry to analyze and classify molecular subtypes of breast cancer by analyzing the expression of certain key genes[56], [57]. This is done by use of the global gene expression profiling studies by hierarchical clustering[58]. The three main prognostic markers for breast cancers are estrogen receptor (ER), progesterone receptor (PR), and human epidermal growth factor receptor 2 (HER-2)[59]. The five intrinsic subtypes are determined by the presence or absence of these receptors[59]. Below is a short description of each of the five subtypes:

1. Luminal A breast cancer

This is the most common subtype of breast cancer, accounting for 35,6% of all breast cancers. It is characterized by ER and PR expression, and low levels of Ki-67(a proliferation index marker)[60]. These are also known to be slow growing and have the best prognosis and low recurrence risk as compared to other subtypes[60], [61]. Although this subtype is relatively well-characterized, it still presents heterogeneity and still requires further exploration.

2. Luminal B breast cancer

This is the third most common subtype of breast cancer, accounting for 20% of all breast cancers The Luminal B cancers are characterized by the expression of ER and a slightly faster growth rate as compared to Luminal A. It also has greater proliferation rates and poorer survival rates in contrast to the Luminal A subtype.

3. HER2-positive breast cancer

This subtype accounts for 10-15% of breast cancers and the overexpression of the HER2 results in activation and upregulation of the proliferation genes.. It is associated with poor prognosis, but it can be successfully treated with targeted therapies aimed at the HER2 protein, such as trastuzumab and pertuzumab [62].

4. Norma-type breast cancer

This rare subtype is associated with high expression of ER and PR, with low Ki-67 levels. It has a good prognosis due to the low expression of genes involved in cellular proliferation.

5. Basal-like subtype

This subtype is characterized by the absence of 3 key receptors involved in breast cancer, ER, PR, and HER2. They are also known as the 'triple-negative' subtype that is most commonly associated with BRCA1 mutation patients. Unfortunately, there are no known targets available for treatment yet. [63][64]. Basal-like cancers are associated with their aggressive nature and are highly unlikely to benefit from currently available targeted therapies[65]. Particularly, this master's project is focusing on this subtype, and below is an in-depth review of TNBC.

1.6. Triple-negative Breast Cancer

TNBC is one of the most aggressive subtypes of breast cancer, that is mainly characterized by negative expression of ER, PR, and HER2 receptors[66]. It accounts for 10-20% of the approximate total of 1 million new breast cancer cases diagnosed per year, globally[67]. Surprisingly, TNBC constitutes most of the breast cancer-associated deaths. In a study conducted by Montagna *et al*., 2012, TNBC has a high risk of relapse and accounts for most breast cancer-associated deaths [68]. It is more prevalent in African American young women (<50 years of age) and those who have mutations of the BRCA1 gene[69]. However, the explanation behind the tendance of TNBC's preference for the descendants of African ancestry compared to any other subtype is not known[70], [71]. Its occurrence is also associated with a higher grade, high mitotic index, larger tumour size, tumour necrosis, and more advanced stage at diagnosis[72][67]. Lehmann *et al* conducted a meta-analysis of 587 TNBC cases from 21 breast cancer studies to further divide TNBC into six subtypes namely, basal-like 1 (BL1), basal-like 2 (BL2), mesenchymal (M), mesenchymal stem-like (MSL), immunomodulatory (IM), and luminal androgen receptor (LAR)[73]. Each of these six TNBC subtypes is briefly described below.

1. Basal-like 1

This subtype is mainly marked by high gene expression and exhibits upregulation in cell division and proliferation pathways, as well as increased DNA damage response. As such, the majority of TNBCs are of the basal-like molecular subtype, which is marked by elevated levels of basal

cytokeratin expression (cytokeratin 5/6 and 17), higher histological grade, increased mitotic activity, marked cellular pleomorphism, poor differentiation, early relapse and decreased survival[74]. Also, the BSL1 subtype has a high frequency of heterozygous or homozygous deletion of DNA repair-related genes such as *BRCA2*, *PTEN*, *MDM2*, *RB1*, and *TP53*)[75].

2. Basal-like 2

The BL2 subtype is mostly associated with the upregulation of genes involved in growth factor signalling, glycolysis, and gluconeogenesis. This affects several pathways including the MET, NGF, Wnt/-catenin, EGFR, and IGF-1R signalling pathways, among others[73].

3. Immunomodulatory (IM)

This subtype is enriched for factors involved in immune cell processes, including immune cell signalling. It causes upregulation of genes responsible for immune signalling pathways[76]. These include pathways involving T cells, T helper cells, natural killer cells and B cells, as well as cytokines, chemokines, complement cascades, and antigen processing[73].

4. Mesenchymal (M)

This subtype has numerous gene ontologies that are significant in pathways related to cell motility, ECM receptor interaction, and cell differentiation processes[73].

5. Mesenchymal stem-like (MSL)

This subtype resembles the upregulation of genes responsible for the expression of mesenchymal stem cells. It results from the interference of the abnormalities on pathways that promote motility, dedifferentiation (epithelial-mesenchymal transition), and cell growth upregulation. In contrast, claudin expression and proliferation-associated genes are downregulated for this subtype[73].

6. Luminal androgen receptor (LAR)

This subtype exhibits luminal gene expression patterns. Unlike the other hormone receptor-negative subtypes, it is steroid hormone driven via highly elevated expression of the androgen receptor and its downstream targets[73].

Table 2. Classification of TNBC subtypes and signalling pathways associated [73]**.**

TNBC subtype	**Signalling pathway associated**
Basal-like 1	Cell cycle, proliferation, DNA damage pathways
Basal-like 2	Cell cycle, proliferation, growth factor signalling, glycolysis, gluconeogenesis
Immunomodulatory (IM)	Immune cell signalling processes
Mesenchymal (M)	Epithelial-mesenchymal transition (EMT), cell motility, differentiation, proliferation
Mesenchymal stem-like (MSL)	EMT, cell motility, differentiation, growth factor signalling, angiogenesis
Luminal androgen receptor (LAR)	Androgen/estrogen metabolism, steroid synthesis, porphyrin metabolism

Based on genomic and biological analysis across 21 different breast cancer data sets, these subtypes were identified and characterized according to gene expression profiles and their implicated signalling pathways.

1.6.1. Standard diagnosis and treatment

Unlike other subtypes of breast cancer, TNBC tumours may be detected during normal screenings using mammography and ultrasound, however, the rapid growth of these type of tumours may hamper early identification, or when identified maybe at an advanced stage. Immunohistochemistry is used for confirmatory diagnosis following biopsy of the suspected tumour tissue. [77]. [78]. This is subsequently followed by genetic testing of the BRCA mutation status of the patient[79]. TNBC disproportionately affects young females, below the age of 40 who are not routinely screened as screening sessions are more encouraged for women above the age of 40[80]. Therefore, clinical examinations are often recommended to detect and diagnose TNBC[81]. Unfortunately, these methods usually detect TNBC at an advanced tumour progression stage. This in turn poses a great challenge because early detection of TNBC is critical for patient survival[82], and once the disease metastasizes, the prognosis is significantly poorer[81], [83].

Current treatment modalities for TNBC include surgery, radiation therapy, chemotherapy and immunotherapy. Unlike other breast cancer subtypes, TNBC treatment is further complicated because it lacks therapeutic targets, specifically ER, PR and HER2 which are typically used as targets for breast cancer treatments. This means that there are fewer available targeted therapies for TNBC, making it more difficult to treat than other breast cancer types. The tri-modality treatment (cytotoxic chemotherapy, radiation therapy and surgical excisions), therefore remains as the current mainstay of TNBC therapy[84]. Although presurgical chemotherapy response rates are higher, there is a higher risk of recurrence and the prognosis deteriorates after metastatic relapse [78][85].

The lack of effective targeted therapies for TNBC, in addition to its poor prognosis, results in a significant social and economic burden[85]. TNBC patients may require more aggressive treatments which usually lead to adverse side effects that may also require hospitalization. These treatments can be too expensive, posing a great financial and psychological burden on the patient and their families[85], [86]. In developing countries, limited healthcare facilities and poverty can lead to low survival rates of patients with TNBC as patients may not afford the costs

associated with the treatment. This underscores the need for novel detection and therapeutic methods that can help identify TNBC early and provide targeted therapies[87].

1.6.2. Immunotherapy for TNBC

Cancer immunotherapy is a form of treatment that manipulates the body's immune system to selectively recognize and attack cancer cells without damaging healthy cells. There are two types of immunotherapy approaches, passive and active immunotherapy[88]. Active immunotherapy works by reactivating the body's immune response against cancer cells. On the other hand, passive immunotherapy utilizes immune components such as monoclonal antibodies (mAbs) and immune cells that have been generated outside the body to specifically target cancer cells. In this study, a passive immunotherapy approach has been employed to target TNBC cells. It has been identified as a potential option to explore new targeted treatments that may improve the TNBC patient outcome[89].

Such an immunotherapeutic approach has several advantages, including improved prognosis, survival rates, and potency in therapy-resistant tumours[90]. It has the potential to greatly enhance the quality of life for patients receiving treatment for aggressive malignancies like TNBC. Various studies have been conducted on the effectiveness of immunotherapy for TNBC patients, including immune checkpoint inhibitors, monoclonal antibodies (mAbs), T-cell activation, and immune vaccines[91]. Clinical trial results have demonstrated immense potential although many of these studies are still in the preliminary research stages and require further exploration and clinical validation[90].

Pembrolizumab (Keytruda) is an immunotherapeutic drug in phase 3 clinical trials studies. Its efficacy when used in combination with chemotherapy showed significant improvement in progression-free survival in patients with advanced TNBC tumours expressing programmed death ligand 1 (PD-L1) compared to chemotherapy alone[92]. Pembrolizumab is a monoclonal antibody that targets the programmed death 1 (PD-1) receptor on T cells, thereby preventing it from binding to its ligands, PD-L1, and PD-L2, on the surface of tumour cells. PD-L1 and PD-L2 are typically found on healthy cells to prevent their destruction by activated T-cells, but cancer cells

mimic this to evade the immune system. By blocking this interaction, the T-cells remain active against tumour cells expressing PD-L1 and PD-L2, a form of immunotherapy known as immune checkpoint inhibition. Pembrolizumab is now approved for combination therapy in patients with advanced TNBC and high PD-L1 expression in tumours[92], [93].

Another prominent immunotherapeutic approach involves the use of antibodies or antibody derivatives that recognize tumour-associated antigens (TAAs) that are differentially overexpressed. This technique involves using antibodies or antibody fragments combined with a toxic moiety to generate antibody-drug conjugates (ADCs)[94]. Sacituzumab govitecan (Trodelvy) is an example of a recently FDA-approved ADC that shows high therapeutic potential for metastatic TNBC[95]. This ADC was developed to target a TAA human trophoblast cell surface receptor 2 (Trop-2). Trop-2 is a transmembrane protein that has been reported to be overexpressed in several types of cancers, including TNBC. The toxin moiety of the ADC is SN-38 which is a topoisomerase inhibitor[95]. In phase III clinical trials, Sacituzumab govitecan (Trodelvy) significantly improved the survival rates and progression-free of metastatic TNBC patients as compared to chemotherapy. This promising result shows the great potential of TAA-based ADCs[96].

Given the challenges in targeting TNBC through HER2 and the hormonal receptors, there is a need to identify new alternative targets that for immunotherapy. To this end, gene expression profiling and other technologies have been used to identify several cell surface receptors (CSRs) that can be explored as potential targets for TNBC-targeted therapy[97]. The TAAs selection criterion considers the differential expression, binding, and internalization ability. This is mainly because some TAAs are also expressed in normal tissues, but in comparatively minimal levels than in tumourous cells[98], [99]. CSRs are more beneficial because antigens secreted by target cells would isolate in the extracellular environment causing very little to no effect on the cancerous cells. The identification of tumor-associated CSRs as potential TNBC biomarkers aid in the diagnosis and treatment of the disease[100].

1.7. Potential targets for TNBC

1.7.1. Leucine-rich repeat-containing G protein-coupled receptor 5 (LGR5)

There is evidence to suggest that LGR5 plays a role in the development and progression of TNBC[101]. LGR5 has been identified as a cancer stem cell (CSC)-associated Wnt pathway-regulated gene (Figure 3). Researchers have shown that LGR5 is overexpressed in TNBC cells, compared to non-TNBC cells. The LGR5 expression in TNBC has also been associated with poor prognosis in TNBC patients. Its overexpression has also been associated with tumour size (greater than 2 cm), lymph node metastasis, and advanced stage in TNBC patients[102].

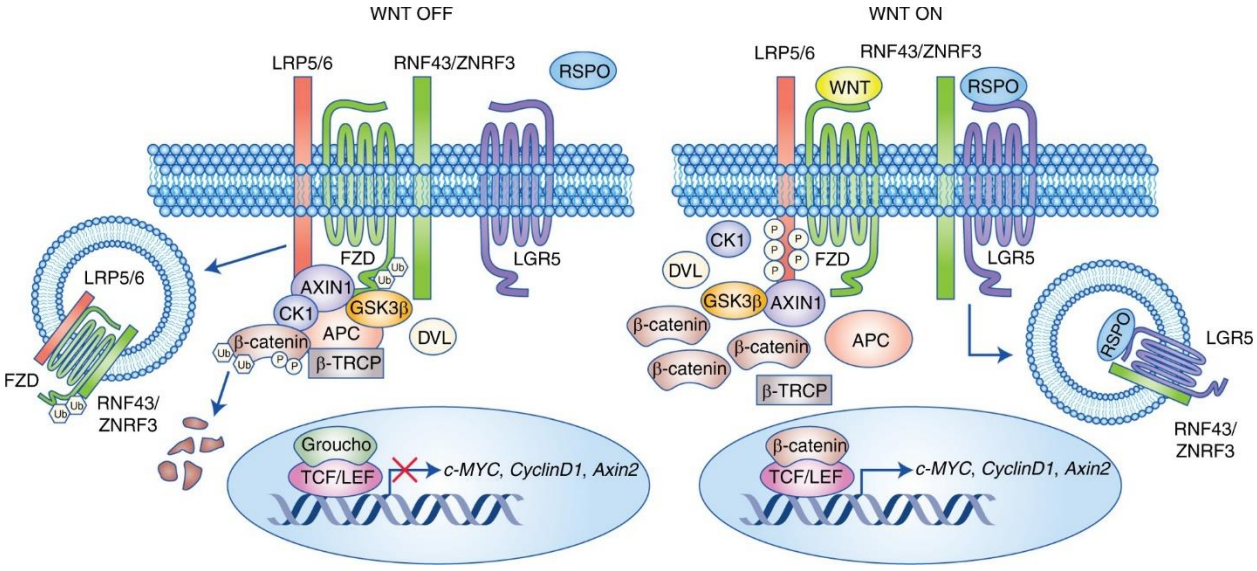

Figure 3: Role of LGR5 in the Wnt/ß-Catenin pathway[103]. LGR5 has a well-defined function in the promotion of Wnt/β-catenin signalling in normal stem cells. Without RSPO bound to LGR5, Wnt signalling is kept low through the action of transmembrane E3 ligases RNF43/ZNRF3, which internalize and degrade the Wnt receptors Frizzled and LRP5/6. This leads to downstream β-catenin degradation and subsequent repression of Wnt target genes. The binding of RSPO to LGR5 sustains Wnt signalling by neutralizing the RNF43/ZNF3 ligases, which can no longer remove Wnt receptors from the cell membrane. FZD and LRP5/6 are free to bind Wnt ligands leading to stabilized β-catenin and downstream activation of Wnt target genes such as *c-MYC, CyclinD1* and *Axin2*of CSCs[103].

Targeting LGR5 could potentially inhibit cancer stem cells, which are thought to be responsible for tumour initiation, maintenance, and resistance to therapy. However, further research is needed to fully understand the role of LGR5 in TNBC and to develop effective therapies targeting

LGR5. There are few examples of tissues where LGR5 expression has been observed in normal cells, for example, in the intestines, hair follicles, stomach and liver[104]–[106].

1.7.2. Cluster differentiation 90 (CD90)

CD90, also referred to as thymocyte differentiation antigen-1 (Thy-1) is a 25-37 kDa small membrane glycophosphatidylinositol (GPI) anchored protein mainly involved in cell-to-cell and cell-to-matrix interactions[107][108]. It also play a role in cell signalling and migration. CD90 is normally expressed in human skin fibroblasts, T Cells and Mesenchymal cells[109]–[111]. High expression of CD90, has been reported to positively correlate with cell transformation and worse prognosis in TNBC patients[112]. Furthermore, high CD90 expression has been linked to increased tumour size, lymph node involvement and distant metastasis, which are all indicators of poor prognosis[108][112]. The exact role of CD90 in TNBC is still not completely understood[113], but some studies have suggested that CD90 may promote tumour cell survival and invasion by interacting with other proteins and signalling pathways[114]. For instance, Thy-1 has been reported to interact with integrin β3 and activate the focal adhesion kinase (FAK) signalling pathway. FAK activation leads to the recruitment activation of Src kinases, which then activate downstream activating pathways for cell adhesion, survival, and migration[115]. In this way, CD90 may play a significant role in the development and progression of TNBC by promoting tumour survival, invasion and resistance to treatment. Therefore, this makes CD90 an appealing therapeutic target for TNBC patients[115][116].

1.7.3. Epithelial Cell Adhesion Molecule (EpCAM)

EpCAM is a 40 kDa transmembrane glycoprotein that is expressed in epithelial tissues and is involved in cell adhesion[117]. It is associated with tumorigenesis, metastasis and cancer stem cells[118]. It is differentially overexpressed in several cancers, including TNBC. It is also involved in cell signalling, proliferation, differentiation, and migration. EpCAM is involved in several molecular pathways that contribute to the suppression of anti-tumor immunity, development, and progression of cancer by activating several signalling pathways[117]. For example, it activates the Wnt/β-catenin pathway (Figure 4)[119]. It is also involved in the activation of the

PI3K/AKT/mTOR signalling pathway that is responsible for cell growth and survival[120]. This makes EpCAM a potential CSR to target for TNBC therapy.

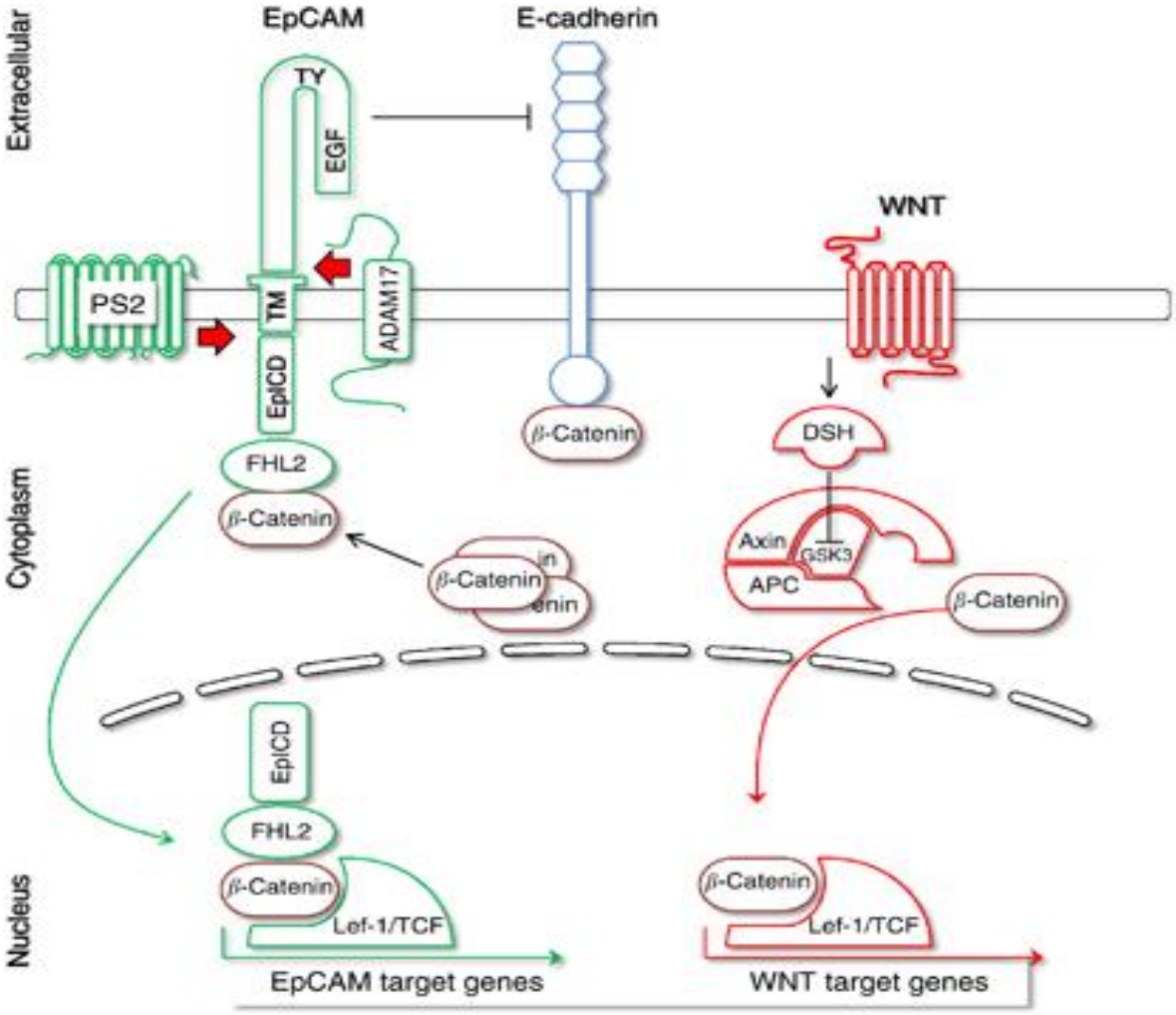

Figure 4: Role of EpCAM in the Wnt signalling pathways[121]. EpCAM activates the Wnt signalling pathway through a process called Regulated Intramembrane Proteolysis (RIP), where EpCAM is cleaved by ADAM17 and PSEN2, releasing intracellular domains (ICDs) that translocate to the nucleus and form a protein complex with FHL2, β-catenin, and Lef-1. This complex activates the transcription of genes involved in cell proliferation, survival, and differentiation. The Wnt signalling pathway activation through EpCAM-mediated RIP has been linked to the development of several types of cancer, including Triple Negative Breast Cancer (TNBC), and targeting EpCAM and the Wnt signalling pathway could be a potential therapeutic strategy for these cancers.

1.8. Monoclonal antibody variants and -derivatives

Monoclonal antibodies (mAbs) have gained popularity as therapeutics due to their high specificity and efficacy in targeting disease-causing agents, such as cancer cells and pathogens[122], [123]. They facilitate several humoral and cellular responses and hence have been used to selectively target diseases. In 1975, Köhler and Milstein pioneered the hybridoma technology which allowed for the production of highly specific (mAbs) in large quantities [124]. The pharmaceutical industry has invested heavily in research and development to create and improve mAbs, resulting in numerous FDA-approved drugs for a range of indications[124]. As of December 2022, 153 mAbs were approved by the FDA, demonstrating the growing importance of these drugs in modern medicine[125].

The therapeutic antibodies used in immunotherapy are referred to as immunoglobulins (Ig) or antibodies, which are large Y-shaped proteins (~150 kDa) that are produced by the immune system in response to foreign antigens (Figure 5)[126]. These Igs are made up of identical two heavy and light chains (~50 kDa and ~25 kDa respectively)[127], that are held together by disulphide bonds, where each of them comprises (VH and VL) and constant domains (CH and CL)[127]. The full antibody can be divided into 3 functional domains, two antigen-biding domains (Fabs) joined by a flexible hinge domain to the fragment crystallizable (Fc) domain of the IgG molecule, which can interact with different CSRs[128].

The mAbs are useful therapeutic tools in passive immunotherapy as they can successfully target tumour cells and induce cell death[129]. This can be achieved by inhibiting downstream signalling of tumour cell surface receptors (CSRs) responsible for proliferation and metastasis, regulating effector functions of the immune system and targeting tumour microenvironment (TME) by inhibiting vasculature and stroma[130]. Although numerous monoclonal antibodies (mAbs) have demonstrated efficacy in enhancing patient outcomes, tumour cells are highly adaptable and can develop resistance to these therapeutic mAbs[176]. Consequently, researchers focused on integrating the tumour-targeting properties of mAbs with cytotoxic drugs to induce cell death directly, circumventing the requirement for an immune response to be activated. However, the mAbs-based drugs that have an antibody domain that possesses an Fc region can mediate Fc-effector function.

The diversity of the human antibody repertoire is based on a unique genetic assembly of the different antibody subdomains that result from the rearrangement and combination of gene segments during B cell development[131], [132]. There are three main gene segments involved in this process: variable (V), diversity (D), and joining (J) segments. These gene segments encode the subdomains of the antibody, including the variable regions responsible for antigen recognition[133]. During B cell development, the V, D, and J gene segments undergo a process called V(D)J recombination. The genetic processes of V(D)J recombination and somatic hypermutation contribute to the remarkable diversity of the human antibody repertoire[133]. This diversity enables the immune system to recognize and respond to a wide range of antigens, providing the basis for effective immune defence against pathogens and other foreign substances[134]. The paratope constituted by VH and VL binding to its target epitope with high affinity is based on a more rigid framework structure combined with highly adjustable complementary determining regions (CDR) [134].

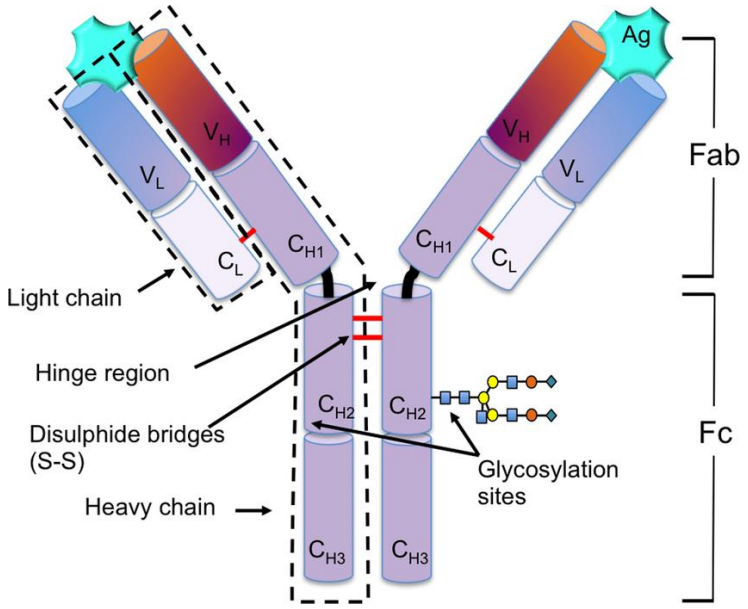

Figure 5: Structural schematic diagram of IgG antibody[135]. Note: The typical IgG molecule consists of four polypeptide chains (two heavy chains and two light chains) joined together by disulphide bridges (shown in red). The light chain consists of a variable light (VL) constant light (CL) region, and the heavy chain consists of one VH chain linked to three constant regions (C H1, C H2, and C H3). The Fc region is important for mediating immune system effector functions, and Protein-A and -G binding.

The clinical effectiveness of conventional full monoclonal antibodies (mAbs) for immunotherapy yielded great results, however, there were challenges and limitations because mouse antibodies used in human patients were found to be immunogenic[136]. Additionally, the relatively large size of these antibodies resulted in inadequate and disproportionate penetration into solid tumours, presenting a significant challenge as well[137]. To overcome the immunological response caused by non-human antibodies, molecular and genetic engineering techniques were employed to develop chimeric or fully humanized antibodies[129]. Furthermore, the challenges caused by the large size of these antibodies led to the creation of smaller antibody derivatives that could better penetrate tumours and still bind to antigens[138]. This informed the evolution of various recombinant antibody formats that have been developed with different molecular weights and derivatives. One type of antibody derivative is the single-chain variable fragment (scFv), which has a molecular weight of ~28 kDa. The scFv is composed of the variable heavy (VH) and variable light (VL) chains of an antibody, connected by a synthetic peptide spacer of 10-20 amino acids[139]. These antibody derivatives can be engineered from conventional monoclonal antibodies or selected from phage-antibody libraries based on the genetic sequences of high affinity and specific VH and VL chains. Studies have shown that scFvs and other small antibody derivatives can penetrate tumours more efficiently and achieve a more widespread distribution within tumours compared to full-length monoclonal antibodies[140]. Due to its smaller size, the (scFv) format has several advantages, including low immunogenicity, better tumour penetration, rapid renal clearance, high tumour specificity, and localization[138]. However, its therapeutic efficacy may be limited by its short retention time in circulation, as it is quickly cleared from the body[141]. This is likely due to the lack of an Fc region, which would otherwise interact with the neonatal Fc receptor (FcRn) and extend the serum half-life of the antibody[142].

The scFvs are gaining attention as key players in the field of targeted anticancer therapeutics by fostering the development of immunotoxins (ITs), as exemplified by this study. In contrast, to improve their killing activity, mAbs are being armed with potent cytotoxic molecules[143].

1.9. Targeted therapy: Recombinant Immunotoxins

Immunotoxins (ITs) are protein molecules formed by a combination of an antibody or antibody fragment (targeting moiety) and a cytotoxic protein component [143], in contrast to synthetic small molecule toxins used in ADC development[144]. The targeting moiety (ligand) is responsible for the selective identification of the target cell population by recognizing a specific antigen on the surface of the targeted cells. The cytotoxic component (toxin) is responsible for inducing cell death in the targeted cell population once it has been internalized [145]. The toxin can achieve cell killing by various mechanisms, such as blocking protein synthesis, inhibiting protein function or disrupting DNA or RNA synthesis.[146]. The toxin molecules used in the development of immunotoxins are usually derived from the plant (e.g., modeccin and abrin)[147] and bacteria (e.g., Pseudomonas exotoxin (PE))[148]. These are extremely active cell-killing agents. The history of immunotoxins dates back to four decades ago when the first generation of immunotoxins was produced by chemically joining a mAb and a toxin[149][150]. These were difficult to produce and had several drawbacks, including non-uniform ligand-to-toxin ratios, low yields, and non-specificity[151]. The second generation considered these limitations for improvement based on cancer patients' clinical trial results. They had only the catalytic domain of the toxin conjugated to an antigen-binding fragment (Fab) to improve tumour penetration and specificity. However, the second generation was also faced with challenges, including chemical heterogeneity and a high cost of production[152]. The third generation, also referred to as recombinant immunotoxins rITs, is made using the genetic fusion of the ligand and the catalytic domain of the toxin. These are fused by peptide linkers to maintain the proper folding and function of the components[153]. Unlike the first and second generations, they are homogeneous and inexpensive to produce, solving most of the major limitations faced by previous generations of immunotoxins. The targeting moiety is often derived from humanized antibody fragments (e.g., single chain variable fragment (scFv)) [151], [154], [155].

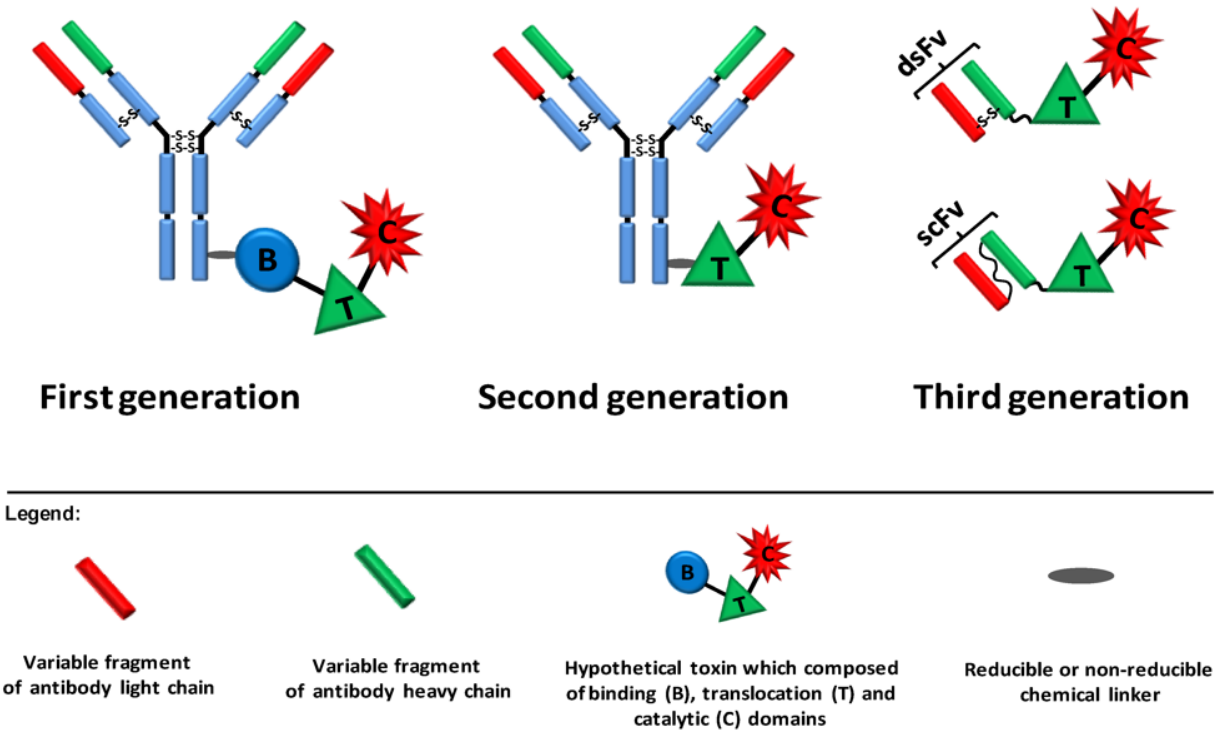

Figure 6: **Structural representation of the three generations of immunotoxins**[145]. The first generation was prepared by chemically linking mAbs or ligands to intact toxins using reducible or non-reducible chemical bonds. The second generation utilized truncated toxins lacking a cell binding domain, which were conjugated to target moieties. Third-generation rITs, mainly produced in *Escherichia coli*, comprise of the cell binding domain of the toxin genetically replaced with a ligand or the Fv section of an antibody. The light and heavy chain variable fragments are either genetically linked as scFv or held together by a disulfide bond as dsFv.

1.9.2 Pseudomonas Exotoxin A (PE/ETA)

Pseudomonas exotoxin A (PE/ETA) is a preferred toxin to consider for the synthesis of immunotoxins, due to its high potency, expression, and purification yields, ease of cloning, and low non-specific toxicity. It is a potent virulence factor secreted by the gram-negative bacteria *Pseudomonas aeruginosa,* that can be used as an anti-cancer agent[148], [156]. This bacterium causes severe acute and chronic infections, particularly in individuals with a compromised immune system. For example, those with cystic fibrosis, cancer, or HIV/AIDS are more susceptible to PE infections[153], [157]. PE/ETA is an enzyme that interferes with protein synthesis in eukaryotic cells, leading to cell death (see detailed description of mechanism of action in the next

section 1.9.2). It is composed of three functional domains, a receptor-binding domain that binds to specific receptors on the surface of target cells, a translocation domain that enables the toxin to cross the cell membrane, and an enzymatic domain that inhibits protein synthesis[158].

ETA has been studied extensively for its potential therapeutic uses, including in the treatment of cancer[156]. Researchers have developed recombinant forms of the toxin that can target cancer cells specifically, and early clinical trials have shown promising results[159]. However, due to its high toxicity, ETA must be carefully dosed and administered to minimize side effects. X-ray crystallographic structure analysis has been used to study the structural domains of ETA. The functions of these domains were studied by isolating each ETA structural gene and expressing them in an *E. coli* host expression system[160].

The ETA protein is composed of 638 amino acids, but only 613 amino acids are present after secretion. The N-terminal domain I (amino acids 1-252) is composed of anti-parallel beta-sheets and serves as the cell recognition site. Domain II (amino acids 253-364) contains six consecutive alpha-helices and facilitates the transfer of the toxin across cell membranes as the translocation domain. Domain Ib (amino acids 365-404) is a structural domain with an unknown function, but studies suggest that it may play a role during the secretion of the toxin. The last four amino acids of Ib (amino acids 400-404) along with domain III (amino acids 405-613) form the catalytic domain, which is responsible for ADP-ribosylation. This process leads to the inhibition of protein synthesis by inactivating eukaryotic EF-2 [161], [162].

1.9.2 Mechanism of action

The mechanism of action of recombinant immunotoxins involves several steps. First, the targeting domain of the rIT recognizes and binds to a specific cell surface receptor (CSR) on the targeted cells. For example, EpCAM, LGR5, and CD90, CSRs are reported to be overexpressed on TNBC cancer cells, making them good targets for immunotoxin therapy. Once the rIT is bound to the targeted cells, it is internalized into the endosomal compartment (Figure 6). The second step includes processing and trafficking of the rIT to reach the cytosol where the antibody fragment is separated from the toxin component, ETA. The retrograde transport from the cellular surface is driven by KDEL like sequence, guiding the protein to the trans-Golgi network. The furin located

at the inner membrane recognizes its consensus sequence on ETA and cleaves the protein, thus separating the binding domain from the catalytic domain which is translocated into the cytosol[163]. In the cytosol, the catalytic domain binds to elongation factor 2 (EF2) to catalyze the ADP-ribosylation of the diphthamide residue of EF2. Diphthamide is required for the toxin to halt protein synthesis because ADP-ribosylation of the diphthamide residue inhibits EF2-dependent chain elongation and protein synthesis. The inhibition of protein synthesis triggers apoptotic signalling and subsequently leads to cell death.

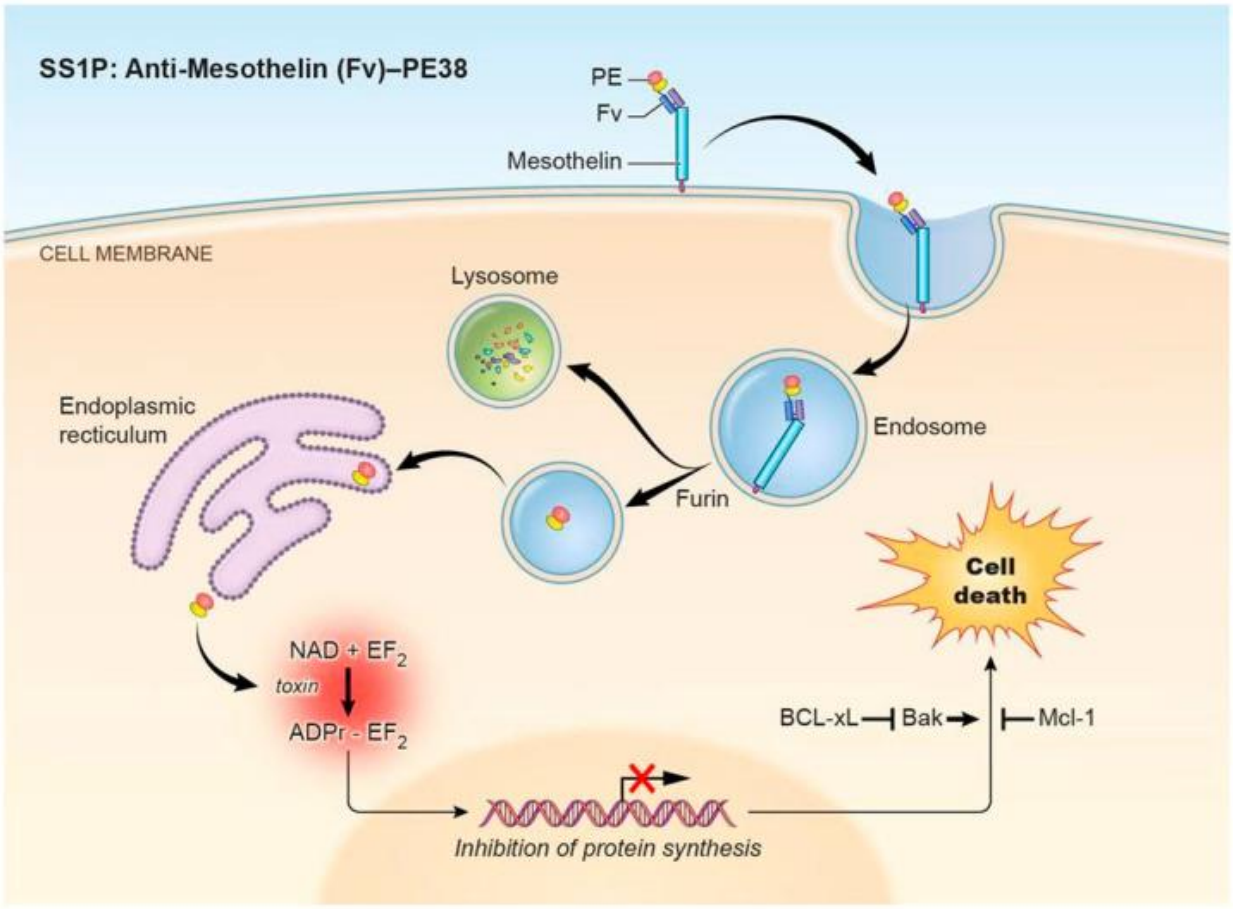

Figure 7: *Pseudomonas exotoxin* A (ETA)-immunotoxin pathway. ETA-based immunotoxins such as the mesothelin-targeting immunotoxin SS1P or LMB-100 act through the Afour step pathway: (I) binding to the target antigen and internalization, (II) processing and trafficking, (III) inhibition of protein synthesis, and (IV) induction of apoptosis[164].

1.9.3 Evolution of ETA-based rITs

There are several ETA-based rITs that have been studied in clinical trials and have yielded promising results. The majority of them have been developed using a truncated form of (PE) called PE38 [165]. Moxetumomab pasudotox (Lumoxiti) is an example of a rIT based on PE38, which has the domain Ia and part of domain Ib missing, in contrast to the native PE[166]. Despite the promising clinical trials results that ETA-based rITs bring as alternative therapeutics, there are limitations associated with the use of such. The major drawback faced by ETA-based rITs in clinical trials is the enhancement of immunogenicity in patients[166]. *P. aeruginosa* is responsible for causing severe acute and chronic infections, particularly in individuals with compromised immune systems. These infections can manifest in various forms, including endophthalmitis (eye inflammation), endocarditis (inflammation of the heart's inner lining), meningitis (inflammation of the membranes surrounding the brain and spinal cord), and septicaemia (bloodstream infection)[167]–[169].

When administered to patients, the toxin component of rITs derived from non-human sources can elicit an immune response that produces human anti-toxin-neutralizing antibodies[170]. Owing to its extreme cytotoxicity, PE-based rITs, the dosage and concentration should be well monitored as high concentrations may lead to side effects, such as vascular leak syndrome[171]. This immune reaction can prevent repeated rIT dosing, limiting its effectiveness in treating the targeted disease. For instance, a clinical trial that administered SSIP (anti-mesothelin PE-based rIT) to mesothelioma patients, achieved no major clinical response because of the neutralizing antibodies that were generated after one treatment cycle[172]. This anti-drug antibody (ADA) formation may result in immune-related adverse side effects in patients such as autoimmunity[173], [174].

1.9.4 Deimmunization of ETA

Efforts have been made to address and attempt to reduce the side effects of ETA-based rITs. Various strategies have been employed to address the immunogenicity challenge. These

strategies include the use of immunosuppressive agents like mAbs, as well as modifying the toxin through site-directed mutagenesis to generate less immunogenic variants[175]. Further attempts have also been considered, including the deimmunization of ETA and altering the ETA domain with macromolecules that induce structural changes within the ETA domain. Deimmunization is a process that is used to identify and remove antigenic epitopes from the recombinant immunotoxins, in this instance, PE. This strategy was used to eliminate B-cell epitopes on PE38 and this was achieved by mapping the location of seven major B-cell epitope groups and then applying an alanine-scanning mutagenesis within these epitopes (R313A, Q332S, R432G, R467A, R490A, R513A, E548A, K590S)[176].

Furthermore, animal-based studies have shown that deleting or mutating certain portions of the ETA toxin domain can remove immunodominant B and T-cell epitopes, leading to reduced immunogenicity and lower production of ADA[177]. In phase 1 clinical trials of SSIP rIT, about 90% of the patients treated produced neutralizing antibodies in the first cycle. The antibodies produced were mostly associated with the ETA part of the rIT, to induce an immunogenic response. In this same study, the researchers screened a phage display library containing the Fv portions of antibodies from patients who produced anti-SS1P antibodies after receiving treatment with SS1P[172]. They used these Fvs to identify B-cell epitopes and mutations that could suppress them. This led to the development of an immunotoxin, SS1-LO10-R, that had high cytotoxic activity but reduced immunogenicity, due to a deletion in domain II and six mutations in domain III. However, this immunotoxin had a short serum half-life, therefore, they replaced the Fv with a Fab, resulting in an immunotoxin called RG7787[178]. This rIT had seven-point mutations on the B cell epitopes (R427A, R456A, D463A, R467A, R490A, R505A and R538A), including one that activates the enzyme (R490A). Although RG7787 was found to have a longer half-life and less immunogenicity, it also showed reduced enzymatic activity and cytotoxicity compared to its wild type. Consequently, our research group, in collaboration with Professor Paolo Carloni used high supercomputer simulations to identify potential mutations within the above-mentioned B cell epitopes that could restore the wild-type enzymatic activity of ETA. Their computer simulations proposed R456T and R456C as possible point mutations with this potential.

2. CHAPTER 2: STUDY AIMS AND OBJECTIVES

2.1. Aims

TNBC patients can hardly benefit from current standard therapies as they lack expression of ER, PR and HER2 receptors[179]. This heterogeneous nature of TNBCs does not allow for proper detection, prognosis[85] and treatment of the tumour and hence they constitute majority of the breast cancer-associated deaths[69], [180]. TNBC has an aggressive and invasive clinical course, with an unexplainable inclination to young women of African ancestry[181].

The current mainstay of TNBC treatment includes chemotherapy, radiotherapy, and surgery options. These treatment methods are associated with a high risk of local and systemic relapses [181] and there is an existing need for the development of targeted therapy for TNBC. However, there is a high socio and economic burden, especially for low-income African countries, as they are mainly affected by poverty and limited healthcare system[182]. Therefore, TNBC represents a major challenge for breast oncologists. Fortunately, molecular and gene expression analyses have enabled the identification of distinct subtypes of TNBCs and their molecular markers[183]. In this study, three such markers that are reported to be overexpressed in TNBC were exploited for antibody-based immunotherapy of TNBC. These markers include Epithelial cell adhesion molecule (EpCAM)[184], Leucine-rich repeat-containing G protein-coupled receptor 5 (LGR5)[102], and cluster differentiation 90 (CD90)[112]. These three biomarkers are cell surface antigens that are potential targets for TNBC therapy.

Recombinant immunotoxins (ITs) are therapeutic proteins that are made by a combination of a disease-specific antibody fragment (ligand) fused to the bacterial Pseudomonas exotoxin A. The ligand (scFv) is derived from the antibody targeting specific cancer CSRs (CD90, LGR5 and EpCAM were considered in this study). After binding to the target CSRs, the rIT is internalized and interacts with elongation factor 2 (EF2), thereby leading to the termination of translation. This will result in cell death by apoptosis. However, recombinant immunotoxins generated from ETA have been shown to elicit immunogenic responses in patients. To overcome this challenge, researchers have also reported that point mutation in the ETA cytotoxic domain has significantly reduced this immunogenicity and anti-drug antibody (ADA) production[185].

The main aim of this study is therefore, to i) develop rITs targeting the CSR (CD90), based on Pseudomonas exotoxin A (ETA) for immunotherapy of TNBC, ii) upon successful establishment of all necessary methods and positive outcome confirming the binding and cell killing effect of the generated recombinant immunotoxin in comparison to a less immunogenic, deimmunized version (dETA) on antigen positive TNBC cells and iii) to optionally use the protocols established in (i) and (ii) to generate up to two additional ETA and dETA-based rITs targeting each of the CSRs, LGR5 and EpCAM, allowing to explore their potential as additional therapeutic agents for immunotherapy of TNBC.

2.2. Specific objectives

The study aims will be achieved by investigating the following objectives.

1. *In silico* plasmid design of bacterial vector plasmids encoding for periplasmic expression of anti-CD90-ETA and anti-CD90-dETA rITs.
2. Molecular cloning of bacterial vector plasmids encoding for periplasmic expression of pMT-anti-CD90(scFv)-ETA and pMT-anti-CD90(scFv)-dETA rITs.
3. Protein expression under osmotic stress conditions in the presence of compatible solutes (well-established protocol in our group), extraction, and 1st step protein purification.
4. Analyse the integrity of the expressed full-length rITs by SDS PAGE and Western blot.
5. Confirm *in vitro* binding of fluorophore-conjugated rITs to antigen-positive TNBC cell lines by confocal microscopy.
6. Evaluate dose-dependent cytotoxicity on antigen-positive TNBC tumour cell line.
7. If successful: apply objectives (1-6), to generate and validate ETA and dETA-based rITs targeting LGR5 and EpCAM on antigen-positive TNBC tumour cell line.

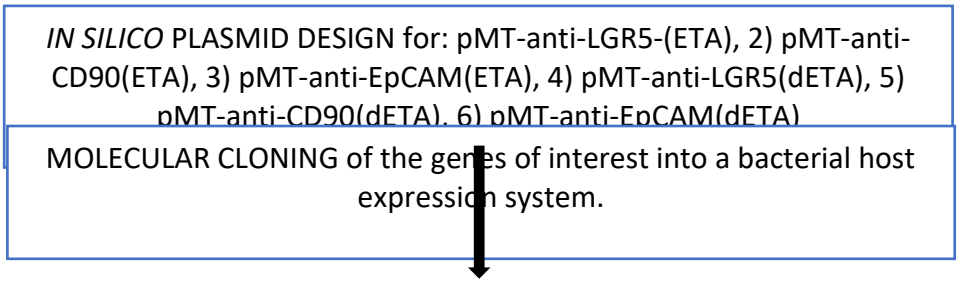

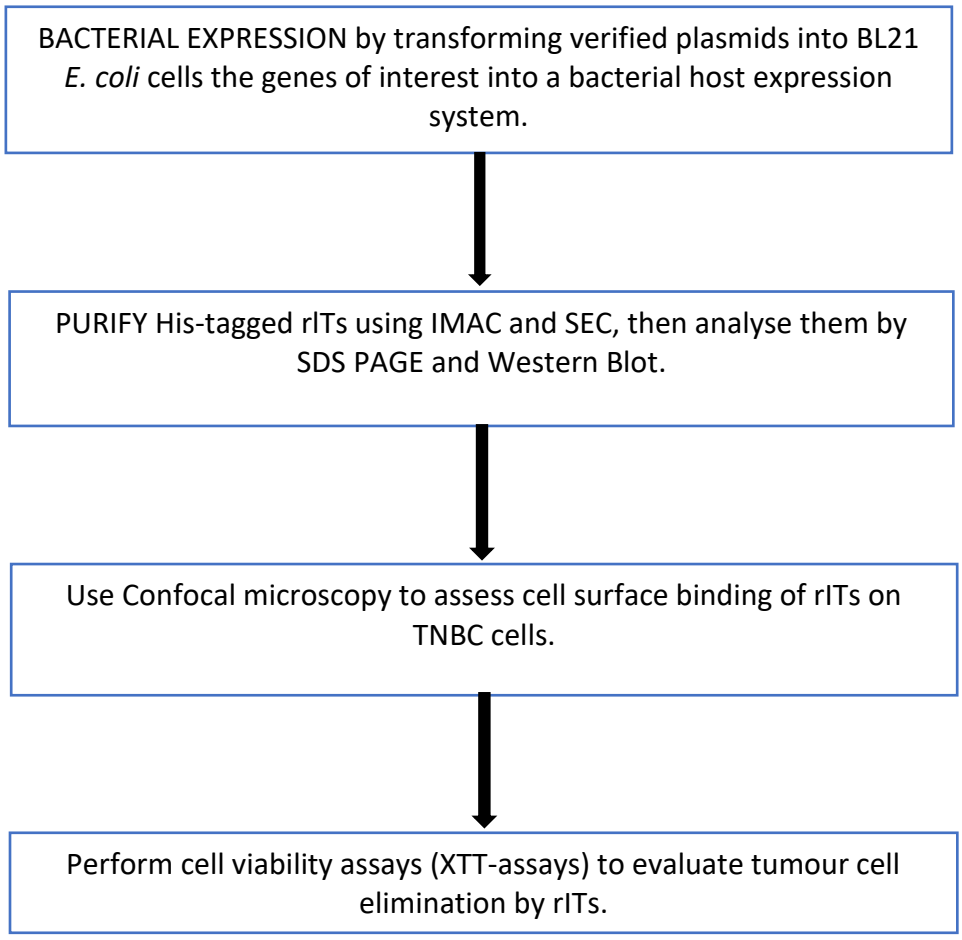

Figure 8: Study workflow. Showing a step-by-step summary of the work done to achieve the stated objectives. The first three steps summarise the process of recombinant protein production. The last three steps summarise protein characterization, to establish the functionality of the developed rITs for potential binding and cytotoxicity effect on TNBC cells.

CHAPTER 3: MATERIALS AND METHODS

This third chapter entails the materials and equipment used to establish methods, protocols, and standard operating procedures at the Medical Biotechnology and Immunotherapy Research Unit (MB&I). The methodology described is used by members of the MB&I and is thus representative of its background and know-how as documented by standard operation procedures, student theses and original publications.

3.1 Materials

3.1.1. Chemicals and Consumables Suppliers

The majority of the chemicals and consumables that were used in this study were bought from different companies, namely, Beckham Coulter (California, USA), Bio-Rad (California, USA), Gene script (Piscataway, USA), Inqaba Biotechnological Industries (Pretoria, South Africa), New England Biolabs (Massachusetts, USA), Sigma Aldrich (Missouri, USA), Qiagen (Hilden, Germany) and Thermofisher Scientific (Waltham, USA).

3.1.2 Solutions and Buffers

The stock solutions and buffers were prepared following the standard laboratory procedures or manufacturer's instructions using de-ionized water. Buffers were sterile filtered (using 0.45µm filters) and degassed. Heat-sensitive components such as antibiotics, kanamycin and Isopropyl β-d-1-thiogalactopyranoside (IPTG) were prepared as stock solutions and sterile filtered (0.22 µm) before being stored at -20°C. Titration of buffers was done by using 1M HCl (acid) or 10M NaOH (alkaline). The recipe for all buffers is summarized below (Table 3). Other solutions were autoclaved for 25 min at 121°C, for example, pre-made RPMI 1640 and DMEM media. RPMI and DMEM media were supplemented with 1% Penicillin, 10% Fetal Bovine Serum and Streptomycin.

Table 3: Buffers and Mediums

REAGENT	COMPOSITION	CONCENTRATION
Luria Bertani (LB) broth	Yeast extract Peptone NaCl	0.5% (w/v) 1% (w/v) 1%(w/v)
LB Agar	Yeast extract Peptone NaCl Agar	0.5%(w/v) 1% (w/v) 1% (w/v) 1.5%(w/v)
SOC	Peptone Yeast extract NaCl KCl $MgCl_2$ $MgSO_4$ Glucose	2% (w/v) 0.5% (w/v) 10mM 25mM 10mM 10mM 20mM
SDS PAGE gel (10%Separating gel)	Acrylamide/Bis-acrylamide (37/1) Tris-HCl (pH8.8) SDS TEMED APS	30% 1.5M, pH8.8 10% 10%
SDS PAGE gel (4% stacking gel)	Acrylamide/Bisacrylamide (37/1) Tris-HCl (pH 6.8) SDS TEMED APS	30% 0.5M, pH6.8 4% 10%
10x SDS Running buffer (pH 8.3)	Tris-Base Glycine SDS	250mM 1.92M 1% (w/v)
10x PBS (pH 7.4)	NaCl KCl Na_2HPO_4 KH_2PO_4	1.37M 27mM 81mM 15mM
10x TAE (pH7.5)	Tris Base Glacial acetic acid EDTA	0.4M 1.14% (v/v) 10mM
Terrific Broth (TB)	Peptone Yeast Extract NaCl	1.0% (w/v) 0.5% (w/v) 1% (w/v)
TBST	Tween 20 Tris NaCl	0.1% (w/v) 20mM 150mM

2.1.3 Equipment

Table 4 below has the list of equipment and the corresponding software used in this study.

Table 4: Equipment

EQUIPMENT	MANUFACTURER (MODEL)
BSLII Cabinet	ESCO Life technologies (Airstream AC2-458)
Centrifuge	Beckman coulter (Allegra X-30R)
Cell counter	Bio-rad (TC20)
Electrophoresis	Bio-rad (PowerPacTM HC)
Gel imager	Bio-rad (G Box Chemi XL)
Heating block	Eppendorf (Thermomixer Comfort)
Microscope	Bio-rad (Zoe)
Micro-centrifuge	LMS Co Ltd (MCF-2360)
pH meter	Dostmann Electronic (pH50+DHS)
Protein purification equipment	GE Healthcare (AKTA Avant)
Shaking incubator	Yinder Co Ltd (LM-510RD)
Sonicator	Qsonica L.L.C (Qsonica)
Spectrophotometer	Denovix (Denovix Ds-11)
SpeedVac drier	SP Scientific (miVAC DNA-23050-L00)
Tissue culture incubator	Nuaire (In-VitroCell
Vortex	LMS Co Ltd (VTX-3000L)
Weighing balance	Radwag (P5600.R2)
Western Blot	Bio-rad (Trans-Blot Cell)
Vortex	LMS Co Ltd (VTX-3000L)

3.1.4 Molecular cloning reagents

Restriction enzymes (*SfiI, NotI, BlpI and PvuII*), CutSmart® buffer, T4 DNA ligase and T4 ligase buffer were all purchased from New England Biolabs (USA). All reagents provided were used

according to the manufacturer's guidelines. Table 5 and Table 6 shows the commercial kits purchased and reagents used for molecular cloning work, respectively.

Table 5: Commercial kits used in the study.

KIT	MANUFACTURER (CATALOG NUMBER)
DNA sample loading dye	New England Biolabs, USA (7025)
QIAquick Gel Extraction kit	Qiagen, Germany (28704)
Zyppy Plasmid Miniprep kit	Zymo Research,USA(D4036)

The table below contains a list of solutions used during the molecular cloning experiments.

Table 6: Reagents used for Molecular cloning.

SOLUTION	COMPOSITION	CONCENTRATION
Solution I	Glucose Tris-HCl (pH8) EDTA (pH8)	50mM 25mM 10mM
Solution II	SDS NaOH	1% 0.2M
Solution III	Potassium Acetate Acetic acid	3M
Chloroform: isoamyl alcohol		24:1, v/v
Sodium Acetate		3M
Phenol/Chloroform		1:1, v/v
RNase A		10mg/mL

3.1.5 Bacterial Strains

Two bacterial strains were used in this study, DH5 alpha and BL21 (DE3) *E. coli*. The *E. coli* DH5 alpha strain was used for all intermediate cloning steps (transformation) and for the amplification

of plasmid DNA whilst the *E. coli* BL21(DE3) strain was used for the expression of recombinant fusion proteins. These two strains are described in the table below (Table 7) and they were all stored at -80°C until use.

Table 7: Bacteria strains purchased for cloning and protein expression.

STRAIN	GENOTYPE	PURPOSE	SOURCE
Escherichia coli (*E. coli*) DH5 alpha	*supE44 ΔlacU169 (F80 lacZΔM15) hsdR17 recA1 endA1gyrA96 thi-1 relA1*	Cloning of recombinant plasmids	New England Biolabs, USA
Escherichia coli (*E. coli*) BL21(DE3)	*F- ompT hsdSB (rB- mB-) gal dcm- lon-*	Expression of recombinant protein	New England Biolabs, USA

3.1.6 Cancer cell lines

The triple-negative breast cancer cell line (MD-MB-468) used for this study was provided through my supervisor, Professor Stefan Barth (University of Cape Town). Other cell lines that were used for control experiments include HL60 leukemia cell lines and MCF7 breast carcinoma cell lines. The table below shows the list of reagents used to prepare the cancer cell cultures.

Table 8: Cancer cell culture contents

REAGENT	COMPOSITION	CONCENTRATION	SOURCE
RPMI-1640	GlutaMAX Sodium pyruvate	2mM 3.7g/L	Gibco 61870

	Phenol red Fetal Bovine serum Penicillin Streptomycin	15.0 mg/L 10% v/v 100 I.U/mL 100µg/mL	
DMEM	GlutaMAX Sodium bicarbonate Phenol red Fetal Bovine serum Penicillin Streptomycin	2mM 3.7g/L 16.0 mg/L 10% v/v 100 I.U/mL 100µg/mL	Gibco 10566

3.1.7 Protein expression and purification reagents

Table 9 shows the list of reagents and buffers used during protein production and purification.

Table 9: reagents used for protein expression and purification.

BUFFER	COMPOSITION	CONCENTRATION
Compatible solutes	D-sorbitol Betaine monohydrate NaCl	500mM 40mM 4%
Binding buffer (pH 8)	Tris-HCl NaCl Imidazole Glycerol	100mM 300mM 150mM 10%
Equilibration Buffer (pH 8)	NaH_2PO_4 NaCl Imidazole	20mM 500mM 40mM
Elution Buffer (pH 8)	NaH_2PO_4 NaCl Imidazole	20mM 500mM 500mM

SEC buffer	PBS	1x

Table 10: Commercial reagents for protein characterization, functional analysis and cytotoxicity analysis

REAGENT/EQUIPMENT	SOURCE	CATALOGUE NUMBER
Aqua stain	Bulldog Bio, UK	AS001000
Colour Prestained Protein Standard Broad Range	New England Biolabs, UK	P7719S
PVDF transfer membrane	Roche, CH	03010040001
1-step TMB-Blotting Substrate Solution	Thermo-fisher Scientific, USA	34018
His-Tag primary antibody	Anatech analytical technology, ZA	CST2365S
Goat-anti-rabbit-IgG horadish peroxidase (HRP)	Bio-Rad, USA	1706515
Anti-His PE antibody	R&D systems, USA	IC050P
Mowiol®	Merk,USA	475904
Anti-Fade (Propyl-gallate)	Sigma Alridch,USA	P3130
Cell Proliferation Kit II (XTT)	Roche, CH	52751200

3.2 METHODS

3.2.1 *In silico* plasmid design and cloning.

With this readily available information such as antibody sequences, species of origin such as human or mouse, epitope recognition within an antigen, and with the application of recombinant DNA (rDNA) technology, mAb against target antigen was developed in a short time. Knowing the antibody sequences that identify the target antigen was imperative for the development of scFvs. Suresh Madheswaran used “Google Patents” and DEPATISnet online public repositories to identify the antibody sequences of interest and generated SNAP-based recombinant plasmids that I used as sources of the scFv DNA sequences of interest. SnapGene® software (v.5.0.8, GSL Biotech LLC, USA) was used to design the open reading frame (ORF) encoding the rITs for

expression in the pMT vector. The pMT prokaryotic expression vector has been optimized for bacterial periplasmic expression of rITs. The pMT-SNAP plasmids containing the scFv sequences of interest, flanked with *Sfi*I and *Not*I restriction sites, were provided by Professor Stefan Barth (MB&I). The pMT-SNAP vectors allowed for the excision of the scFv portion and compatible insertion of these portions into the pMT-ETA backbone. The pMT-ETA vector is also flanked with *Not*I and *Blp*I restriction sites which allowed for the excision of the ETA portion and compatible insertion of the dETA portions, to generate pMT-dETA recombinant plasmid versions. The resultant constructs are expressed within the periplasm of (*E. coli*, BL21 cells) using osmotic stress induction protocol, in the presence of compatible solutes. The pMT-ETA and pMT-dETA plasmids have been engineered to contain a pelB leader sequence that allows the exportation of the produced recombinant proteins periplasm. The bacterial expression vector also comprises of the scFv and upstream of the scFv is the N-terminal pelB peptide signal/leader sequence that directs the fusion protein to the bacterial periplasm, where the sequence is removed by signal peptidase, followed by (in order, N → C) the two recommended alanine (AA) residues, a poly(10x)-histidine tag, or His-tag233 and an enterokinase cleavage site (DDDDK), which allows digestive cleavage of the fusion protein for optional removal of the N-terminal elements (Table 12)**.**

Table 12: Elements of the pMT bacterial expression vector and their functions.

FEATURE	**FUNCTION**
pelB leader sequence	signal sequence for transportation of the recombinant protein to the periplasmic space
N-terminal poly-histidine tag (10X His-tag)	Essential for protein enrichment with the IMAC for protein purification and to detect the protein by western blot analysis.
Enterokinase cleavage (EKS)	Responsible for the separation of the recombinant protein from the 10X His-tag
C-terminus (ETA/dETA)	Is a deletion mutant of Pseudomonas Exotoxin A and its deimmunised version responsible for tumour cell killing

Kanamycin resistance gene (KanR)	Confers resistance to kanamycin to allow for the selection of transforme cells containing the plasmid of interest.
Lac operator (lacI)	Inhibits the transcription of lac genes
Lac promoter	Responsible for the transcription of the lac operon

3.2.2 Molecular cloning techniques

Plasmids that were successfully ligated to the targeting genes were transformed into DH5 alpha *Escherichia coli* (*E. coli*) cells and thereafter, recombinant plasmid DNA was isolated and purified. The source of a plasmid containing ETA backbone DNA and the plasmids with the desired ORFs were cultured in (50mg/mL) of Luria-Bertani (LB) broth prepared with (50mg/mL) kanamycin in a sterile glass flask. These were all incubated overnight at 37°C on a shaker.

3.2.2.1 Transformation of competent bacterial cells

Commercially available NEB® 5-alpha *E. coli* calcium-competent cells (Catalogue number: C2987I, New England Biolabs, USA), were thawed on ice[186]. The 50µL of competent cells were incubated with 1µg of plasmid DNA for 30 minutes on ice. The cells were heat-shocked for 60 seconds at 42 °C. The heat shock disrupts the bacterial membrane, rulting in the formation of pores that allow DNA entry [186]. The cells were treated with 950µL of room temperature Super Optimal Broth with Catabolite Repression (SOC). Each tube was mixed thoroughly and incubated at 37 °C for 60 minutes. All tubes were spun down to pellet the cells, 900µL of the supernatant was discarded and the cells were resuspended in the remaining 100µL and streaked on an kanamycin-supplemented LB agar plate. The streaked plates were incubated overnight at 37 °C. The next day, single colonies were selected from each plate and inoculated in 50mL of LB Broth, supplemented with kanamycin (200ng/µL). The cultures were incubated overnight on a shaking incubator at 37 °C.

3.2.2.2 Plasmid DNA Isolation by the Phenol-chloroform extraction method

The phenol-chloroform extraction method is a technique for large-scale plasmid DNA extraction and purification[186]. Glycerol stocks of the cultures were first prepared in a 1:1 ratio with 50% glycerol and subsequently stored at -80°C. 50mL of overnight transformed DH5-alpha (*E. coli*) cultures were extracted by centrifugation at 4 000 rcf. The supernatant was carefully discarded, and the pellet was resuspended in 1mL Lysis Solution I [50mM Glucose, 25mM Tris-HCl (pH8) and 10mM EDTA (pH8)] which is used to lyse the cells. The glucose raises the osmotic pressure in the extracellular environment of cells, enhancing cellular lysis[187]. EDTA assists in the prevention of genomic DNA degradation by chelating Mg2+, an essential cofactor of DNases[188]. Tris-HCL is a stabilizing buffer that maintains the optimal pH necessary for DNA isolation[189].

The DNA was denatured by the addition of 2mL of an alkaline Lysis Solution II (1% SDS and 0.2M NaOH) that raptures bacterial cells[190] and incubated on ice for 5 min. The circular DNA was renatured after adding 1.5 mL of Lysis Solution III (Potassium Acetate (3M) and Acetic acid)[190]. The contents of the vector tube were centrifuged at 13 000 rpm for 10 min to separate the supernatant containing the plasmid DNA from the pellet containing the cellular debris and denatured DNA. The supernatant was isolated in a new set of microcentrifuge tubes, and 10 mg/mL RNase A was added and incubated at 42°C for 30 min to eliminate RNA contaminants. The plasmid DNA was precipitated by the addition of 30% (v/v) isopropanol and incubated for 10 min at room temperature. To separate the protein from the DNA, 300 mM sodium acetate and 700 µL phenol-chloroform (1:1; v/v) were added and vortexed. The sample was centrifuged at 13 000 rpm for 10 min, and the aqueous phase (top layer) containing the DNA was isolated. 300 µL of chloroform: isoamyl alcohol (24:1; v/v) was added to the recovered DNA and mixed by inversion, followed by centrifugation at 13 000 rpm for 10 min. The aqueous phase was once again recovered, and the DNA was allowed to precipitate at -20°C for 30 min after the addition of 100% ethanol. The plasmid DNA was pelleted by centrifugation at 13 000 rpm for 30 min and rinsed with 70% cold ethanol. The pellet was allowed to dry at room temperature before its resuspension in nuclease-free water and DNA was quantified by the DS-11 spectrophotometer (DeNovix).

3.2.2.3 Mini preparation of plasmid DNA

The Zyppy™ Miniprep Kit (Catalogue number: D4019, Zymo Research, USA) was used for the small-scale isolation of plasmid DNA from *E.coli* cells, according to the manufacturer's protocol. One change was made to the manufacturer's instructions: prewarmed distilled H_2O(50°C) was used to elute the DNA instead of Zyppy™ Elution Buffer. The DNA was quantified by spectrometry and

stored at 4°C.

3.2.2.4 Restriction endonuclease reactions

Restriction digestion reactions with appropriate endonuclease enzymes from NEB were performed to cleave the plasmid constructs to generate insert and backbone fragments with compatible DNA ends. A mixture of reagents was set up consisting of enzyme, buffer, restriction enzymes, water, and 2ug of DNA(Table 13). The scFv insert fragment was excised out of the pMT-SNAP vector, and the ETA-containing backbone from the pMT-anti-H22(scFv)-ETA construct, using *Not*I and *Sfi*I restriction enzymes. The restriction endonuclease reaction was set up in 1.5mL microcentrifuge tubes. Table 13 indicates the volume of each reagent added to the reaction mixture. For each reaction mixture, *Sfi*I was incubated at 50°C for 3 hours followed by adding *Not*I and incubating at 37°C overnight.

Table 13: Reaction parameters for restriction endonuclease reactions.

COMPONENT	**QUANTITY**
Plasmid DNA	2µg
Cut Smart Buffer®	5µl
Restriction Enzyme	2µl
Nuclease free water	Topped up to 50µl

3.2.2.5 Agarose Gel Electrophoresis (AGE) DNA Extraction

Agarose gel electrophoresis was used to resolve the fragments of DNA after endonuclease digestion. 1.2% (w/v) agarose gels were prepared according to the manufacturer's protocol by dissolving 1.2g agarose in 1x TAE buffer solution (Table 3). The mixture was boiled till the agarose was completely dissolved and slightly cooled, thereafter 10ML SYBR™ safe DNA gel stain (Thermo Fisher Scientific, SA) was added (1:10000 dilution) and the gel was poured into the prepared casting apparatus and allowed to set. The solid gel was placed into a BioRad flat buffer tank and fully submerged in 1x TAE Buffer. DNA samples were stained with 6X Purple Gel Loading Dye (New England BioLabs®, USA) in a 1:10 ratio and 20µL of stained DNA samples were loaded onto the gel. 10µL each of the Gene ruler 100bp Plus and Quick-Load 1000bp DNA ladder (New England BioLabs®, USA) were added to aid in the determination of DNA band sizes. The buffer tank was connected via positive and negative terminals to the Bio- Rad PowerPac which was set to a voltage of 100V for the Mini Sub-Cell. The gel was allowed to run for 90 minutes and thereafter visualized on the Dark Reader Trans illuminator (Clare Chemical Research, USA) at 509nm.

3.2.2.6 Isolation of restriction digestion products

The QIAquick Gel Extraction Kit (Catalogue number: 28704, Qiagen, Germany) was used for the retrieval of the DNA from the agarose gel, according to the manufacturer's instructions. The DNA bands were visualized with a UV gel documentation system and band sizes matching the theoretical sizes of the insert and backbone were excised and purified. The DNA was eluted with nuclease-free water and quantified using the DeNovix spectrophotometer.

3.2.2.7 Ligation and Transformation

DNA ligation is the process of joining two linear DNA fragments through the formation of a covalent phosphodiester bond between the 3' hydroxyl group of one fragment and the 5' phosphate group of the other fragment, catalyzed by the enzyme DNA ligase[191]. In molecular cloning, ligation is performed to incorporate insert DNA into a vector backbone. Ligation of the purified insert fragments and pMT-ETA backbone DNA was achieved by using T4 DNA ligase (Table 4) and incubated at 16°C overnight according to the manufacturer's instructions. The DNA

concentrations recorded were used to determine the ratio of vector to insert needed for the ligation reaction. The ratios of vector to insert used in the reaction were calculated using the New England Biolabs calculator (https://nebiocalculator.neb.com/#!/ligation). The length of the insert DNA and the length and concentration of the backbone (vector) DNA were entered into the online calculator which then determined the concentration of insert DNA required for a range of vector: insert ratios. The ligation reactions were set up in 1.5mL microfuge tubes on ice (Table 14). A control with bacteria only was also set up. The ligation reactions were incubated at 16°C O/N, as this is optimal for sticky end ligation. After this step, each ligation reaction was heat-inactivated at 65°C for 10 minutes. Each ligation mixture (containing recombinant clones) was chilled on ice and 5µL was transformed into 50µL DH5α competent cells as mentioned previously. The ratios selected were 1:0 (control), 1:1 and able.

Table 14: DNA ligation reaction parameters

COMPONENT	QUANTITY
T4 DNA Ligase buffer	2µl
Vector DNA (backbone)	50ng
Insert DNA (1:1 and 1:3)	Required amount
T4 DNA Ligase	1µl
Nuclease free water	Topped up to 20µl

3.2.2.8 Restriction Mapping

The previously described restriction digestion protocol was followed for the restriction mapping of the generated recombinant plasmid vectors using the *Pvu*II restriction enzyme.

Table 15: Restriction mapping reaction parameters

COMPONENT	QUANTITY
Plasmid DNA	1µg
Cut Smart Buffer®	5µl

PvuII Restriction Enzyme	1µl
Nuclease free water	Topped up to 20µl

3.2.2.9 Sequence analysis

The culture volume of 0.5 mL from the identified positive colonies was inoculated in 50 mL LB broth supplemented with (50mg/mL) kanamycin and incubated at 37°C overnight on a shaker. DNA was extracted from these cultures using the phenol-chloroform method described in section 3.2.2.1. The DNA was then sent for Sanger sequencing analysis at Inqaba Biotec (South Africa). Sequencing data were analyzed using SnapGene software and aligned to the designed ORF as reference sequences.

3.2.3 Recombinant Protein Expression

3.2.3.1 Periplasmic Bacterial Expression

Positive clones were cultured in LB broth and supplemented to a final concentration of50g/mL Kanamycin overnight at 37^{o}C at 180rpm. Recombinant DNA plasmids were isolated from the overnight cultures using the Zippy kit (New England Biolabs, # ZR D4019). The bacterial strain BL21 (DE3) *E. coli* cells (Table 7) was used as the bacterial host expression system. The isolated DNA plasmids were transformed into BL21 *E. coli* cells and incubated on an agar plate supplemented with Kanamycin (50mg/mL) at 37^{o}C overnight. A 50mL starter culture consisting of terrific broth supplemented with Kanamycin (50mg/mL) and a single colony from the agar plate was incubated at 37°C at 180rpm overnight. The starter culture was used to inoculate a 500mL culture. The culture was incubated at 26°C at 180 rpm and the OD600 was measured every hour until the OD600 of the cultures reached 1.6. Once the OD600 reached 1.6, compatible solutes (500mM D-sorbitol, 40mM Betaine monohydrate and 4% NaCl) were added to the culture and incubated for 30 minutes at 180rpm. The cultures were induced with 1mM IPTG and incubated for 16 hours. After 16 hours of incubation, the cells were harvested by centrifugation at 4000g at 4^{o}C for 40 minutes. The pellets were collected and weighed. They were homogenated using a pestle and motar. Binding buffer (100mM Tris-HCl, 300mM NaCl, 150mM imidazole and 10% glycerol) was added to the pellet in a ratio of 2:1 (buffer to pellet) and was resuspended and

lysed via sonication at the following parameters: 15 seconds on, 15 seconds off at 30% amplitude for 4 minutes. The lysed cells were centrifuged at 24 000g for 30 minutes. The supernatant was collected and filtered using a 0.45-micron syringe filter. The supernatant was purified using IMAC purification.. The homogenized pellet was centrifuged at 24 000g for 30 minutes. The supernatant was collected and labelled as an insoluble fraction.

3.2.4 Protein purification and characterization.

3.2.4.1 Immobilised metal affinity chromatography (IMAC)

The ÄKTA Avant system (GE Healthcare, USA) was used for immobilized metal ion affinity chromatography (IMAC), to purify expressed recombinant proteins containing a short poly-histidine affinity tag. IMAC purification relies on the strong interaction of the high-affinity transitional metal ion, Co2+, immobilized on a matrix with a negatively charged 10x histidine chain. This strong interaction keeps the recombinant protein bound to the matrix during washing steps, allowing for the release of unbound proteins. The purified protein is recovered during an elution step using a column buffer with a high concentration of imidazole. The ÄKTA Avant system elutes fractions from the column which potentially contain the recombinant protein. In parallel to this, an elution profile is generated which records the absorbance profile (UV= 280nm) of the matrix. Pronounced peaks in the absorbance profile are indicative of the presence of protein. All of the peak-containing fractions were visualized on a 10% SDS gel to detect the presence of protein in each fraction.

3.2.4.2 Amicon Filteration

Thereafter, the protein-containing fractions were pooled and concentrated with a 10 kDa Amicon® Ultra-15 Centrifugal Filter Unit (Sigma-Aldrich, USA). A maximum of 15mL pooled fraction was spun in Amicon filter columns each at a time, at 4225 rcf for 30 minutes. The flow through was discarded and the spin repeated until all the pooled sample was concentrated and ~500µL was retained. For the final spin, buffer exchange was carried out by adding sterile phosphate buffered saline (PBS) (pH 7.4) into the filter and concentrated to a volume of ~500µL.

The pH and salinity of PBS, when compared to that of the elution buffer, are more optimal for correct protein folding and this helps to prevent protein aggregation, thus maintaining protein integrity. The buffer exchange also removes traces of imidazole. The concentrated protein solution was quantified using spectrometry (Denovix™ Spectrophotometer, A280nm) and all protein samples were stored at -20^{o}C.

3.2.4.3 Sodium dodecyl sulphate polyacrylamide gel electrophoresis (SDS-PAGE) analysis

SDS-PAGE was used to detect the presence and determine the integrity of the purified rITs after IMAC enrichment. This technique employs the use of electrophoresis to separate proteins based on their size under reducing conditions.[192] The theoretical molecular weight of each rITs was calculated using the conversion calculator available at https://www.aatbio.com/tools/calculate-peptide-and-protein-molecular-weight-mw. A sample loading dye was added by mixing β-mercaptoethanol with 4x Laemmli sample buffer (Bio-Rad Laboratories, USA) in a 1:9 ratio, and 5µL of the sample buffer was added to 15µL of sample and thereafter incubated at 95^{o}C for 10 minutes. A 10% SDS gel was made, and protein samples were loaded to run at 100V for 20 minutes, followed by 150V for 70 minutes. Next, the gel was incubated with Acqua Stain (Bulldog Bio, USA), following the manufacturer's instructions, to allow for the visualization of protein bands. The Gel Doc XR+ (Gel Doc™ XR System) was used for image capture.

3.2.4.4 Immunoblot analysis (Western Blot)

Immunoblot analysis was used to determine the functionality of the N-terminal of recombinant proteins, where the 10x His tag is located. It was also used to identify which of the additional bands present on the SDS polyacrylamide gels were cleaved or degraded recombinant proteins. Two gels were prepared, one for the immunoblot and another one was stained with AcquaStain to allow for a comparison between the immunoblot and the denaturing polyacrylamide gel.

Protein samples (20 µg) were prepared for SDS-PAGE which was performed in duplicate. The concentrated fractions were collected and mixed with 4x Laemmli Sample Buffer (Bio-rad, USA, #161747) before being denatured at 95^{o}C for 10 minutes. The proteins were run on a 10% SDS

gel, once completed the separated proteins were transferred onto a PVDF (25V for 30 minutes). Before the transfer, the membrane was activated by incubating it in methanol for 1 minute, followed by distilled water for 1 minute. This process was repeated three times before incubating the membrane in 1x transfer buffer. Following the transfer, the membrane was blocked with fat-free milk for 1 hour followed by incubation with anti-His primary rabbit antibody (Cell Signalling Technology) diluted in fat-free milk (1:1000) at 4°C overnight overnight at 4^{o}C. The following day the membrane was washed with 1x TBST for 5 minutes, which was repeated three times. The membrane was then incubated with goat anti-rabbit horseradish peroxidase antibody for an hour at room temperature. The membrane was washed three times with 1x TBST before being visualized using a 1-step TMB-Blotting Substrate Solution (ThermoFisher, #34018).

3.3 *In vitro* functional assays

3.3.1 Culturing of cancer cell lines

The triple-negative breast cancer cell line (MDA-MB-468) was selected as the target antigens-positive cell line and cultured in Dulbecco's Modified Eagle Medium (DMEM) media supplemented with 10% (v/v) fetal bovine serum (FBS) (Gibco) and 1% PenStrep (ThermoFisher scientific). H22(scFv)-ETA was provided from another MB&I student. Its treatment on MDA-MB-468 cells was used as a control because the cell line does not express the H22 antigen. The antigen-negative cell lines identified as controls were HL60 and MCF7 leukemia and breast carcinoma cell lines respectively. The HL60 cell line served as an antigen-negative control for LGR5 and 15EpCAM, whilst MCF7 served as an antigen-negative control for CD90. Both of the negative control cell lines were cultured in RPMI-1640 supplemented with 10% FBS, 100 U/mL penicillin and 100 ug/mL streptomycin. All cell cultures were incubated at 37^{o}C and 95% humidity with 5% CO_2. Cells were passaged twice a week and counted using a T20 cell counter (Bio-Rad, USA). The tumour cells were passaged at 90% confluency. The adherent tumour cells required trypsinization to subculture them. This was achieved by removing all traces of FBS-supplemented media from the cell culture flasks by rinsing the cells twice with 1x PBS. The 1x Trypsin-EDTA (Sigma) was added to the flasks until the cells were morphologically round and nearly lifted. The Trypsin-EDTA was removed and inactivated with the addition of FBS-supplemented media, and

the cells were resuspended by aspiration. The cultures were passaged by retaining 5% of the cells in fresh media.

3.3.2 Binding analysis using confocal microscopy.

3.3.2.1 Labelling recombinant proteins with Anti-His PE antibody

Specific rITs binding was visualised with confocal microscopy. The recombinant proteins were conjugated to Anti-His PE for downstream imaging experiments. The purified protein fractions were pooled and concentrated using a 50kDa Amicon® Ultra-15 centrifugal filter (Sigma, USA, UFC901008). The concentrated proteins(20µg) were conjugated to Anti-His PE antibody (R&D systems, IC050P) in the presence of DTT(5mM). The reaction was incubated at 37^{o}C for 1 hour in the dark.

3.3.2.2 Preparation of tumour cells and recombinant fusion proteins labelled with Anti-His PE

1x10^{5} of the TNBC tumour cells were seeded on a coverslip and incubated overnight at 37^{o}C and 95% humidity with 5% CO_2 overnight. After 24 hours, the seeded cells were incubated with Hoechst nuclear stain (1:5000) and 1mL of unsupplemented RPMI/DMEM media, for 30 minutes at 37^{o}C and 95% humidity with 5% CO_2. The cells were washed thrice with sterile 1x PBS. They were incubated with the Anti-His PE labelled recombinant proteins and unsupplemented media for 1 hour at 37^{o}C and 95% humidity with 5% CO_2. The cells were washed three times with 1xPBS. They were then fixed by incubating in 4% Paraformaldehyde (PFA) at room temperature. Following the incubation, the cover slide was mounted on a slide and viewed using the LSM 880 Airysan confocal microscope (Zeiss) at 40x magnification and images were captured for further analysis. These imaging experiments were done to confirm the cell surface binding of the recombinant proteins on the TNBC tumour cell line.

3.3.3 Cell viability assay (XTT)

The XTT cell viability assay (Cell proliferation kit II; Roche, CH) was used to evaluate the cytotoxicity of the rITs on the tumour cells. In this assay the tetrazolium salt, XTT, is cleaved in

the presence of phenazine, thereby producing a soluble formazan salt by metabolically active cells. This reduction reaction results in a colour change, from yellow to orange and this can be detected by a spectrophotometer[193]. The results were analyzed by measuring the absorbance of the XTT reagent at 450nm as the measurement filter and 650mn as the reference filter on a spectrophotometer (iMark™ Absorbance reader, Bio-Rad, USA). All experiments performed had five technical replicates. The absorbance readings were normalized in comparison to the control (untreated and Zeocin) and the results represented as a percentage of cell viability. GraphPad Prism v.9.0 software was used to calculate the concentration of rIT that would achieve 50% cell death (IC_{50}). The same cell line and controls used in the binding studies were also used for the cytotoxicity experiments. HL60 leukemia cells were used to assess the nonspecific killing effect of LGR5 and EpCAM rITs whilst MCF7 breast carcinoma cells were used to assess the nonspecific killing of CD90. H22-ETA was used as the negative control since the H22 antigen is not expressed in the TNBC MDA-MB-468 cell line.

CHAPTER 4: RESULTS

The lack of available targeted therapies for TNBC in addition to its aggressive and heterogeneous nature means that novel therapeutic options are desperately needed. The relationship between CD90, LGR5 and EpCAM, and TNBC survival suggests that these are potential targets for antibody-based therapeutic schemes. Therefore, six novel rITs were generated (anti-CD90(scFv)-ETA, anti-LGR5(scFv)-ETA, anti-EpCAM(scFv)-ETA, anti-CD90(scFv)-dETA, anti-LGR5(scFv)-dETA, and anti-EpCAM(scFv)-dETA) to evaluate their potential in selectively targeting antigen positive TNBC cells and delivering therapeutic probes. The rITs were successfully expressed in the periplasmic space of BL21 (DE3) *E. coli* cells using the osmotic stress protocol as described in section 3.2.3. The expressed rITs were purified using IMAC and Size Exclusion (section 3.2.4). Therefore, this section of the study reports on the findings of the study, describing the design and development of these rITs, their functional characterization and *in vitro* assessments.

4.1 *In silico* design of bacterial vectors

The process of designing a recombinant immunotoxin typically began with selecting appropriate target antibodies. Suresh Madeswaran (Ph.D.) used publicly available patent sequences targeting LGR5, CD90 and EpCAM, from their respective patent files, US9,175,089B2, WO2017/214050A1 and US2015/0017230A1 respectively (Table 11). The sequences generated were pasted into Ig Blast (https://www.ncbi.nlm.nih.gov/igblast/) to access the FR and CDR regions as well as to further ascertain the existence of the VH and VL chains of each scFv. This was followed by codon optimization using the IDT codon optimization tool (https://eu.idtdna.com/pages/tools/codon-optimization-tool). Anti-CD90(scFv), anti-EpCAM(scFv) and anti-LGR5(scFv) genes were modified to introduce restriction endonuclease cleavage sites to allow for incorporation into a suitable bacterial protein expression vector using SnapGene® software (v.5.0.8, GSL Biotech LLC, USA) as outlined in section 3.2.1. These genes of interest were provided by Suresh Madheswaran in the form of SNAP-based recombinant DNA plasmids. The plasmids containing the scFvs of interest (pMT-anti-LGR5(scFv)-SNAP, pMT-anti-CD90(scFv)-SNAP and pMT-anti-15EpCAM(scFv)-SNAP) were individually excised, and each of which was inserted into the backbone derived from pMT–

anti-H22(scFv)-ETA to generate pMT-anti-CD90-ETA, pMT-anti-LGR5-ETA, and pMT-anti-15EpCAM-ETA respectively (section 4.1.1). The dETA gene was obtained from the pUC57 plasmid containing dETA, designed with *Not*I and *Blp*I restriction sites flanking the dETA gene (Figure 10). *Not*I and *Blp*I restriction sites are also present in pMT-anti-H22(scFv)-ETA. The software, SNAP-GENE® (v.5.0.8, GSL Biotech LLC, USA) was used to simulate the replacement of the ETA C-terminus with dETA C-terminus (Section 4.1.2). The molecular weights of the recombinant proteins were theoretically calculated using Expasy (https://web.expasy.org/translate/), an online translation tool.

Table 11: Patent files for the selected target antigens and the corresponding antibodies

CELL SURFACE ANTIGEN	scFv	REFERENCE
EpCAM	OCAb9-1	US20150017230A1
LGR5	YW353	US 9175089 B2
CD90	h5-Thy1	WO 2017214050 A1

These markers are reported to be differentially overexpressed in different cancers including TNBC hence they were chosen for this study.

4.1.1 *In silico* cloning of ETA-based rITs

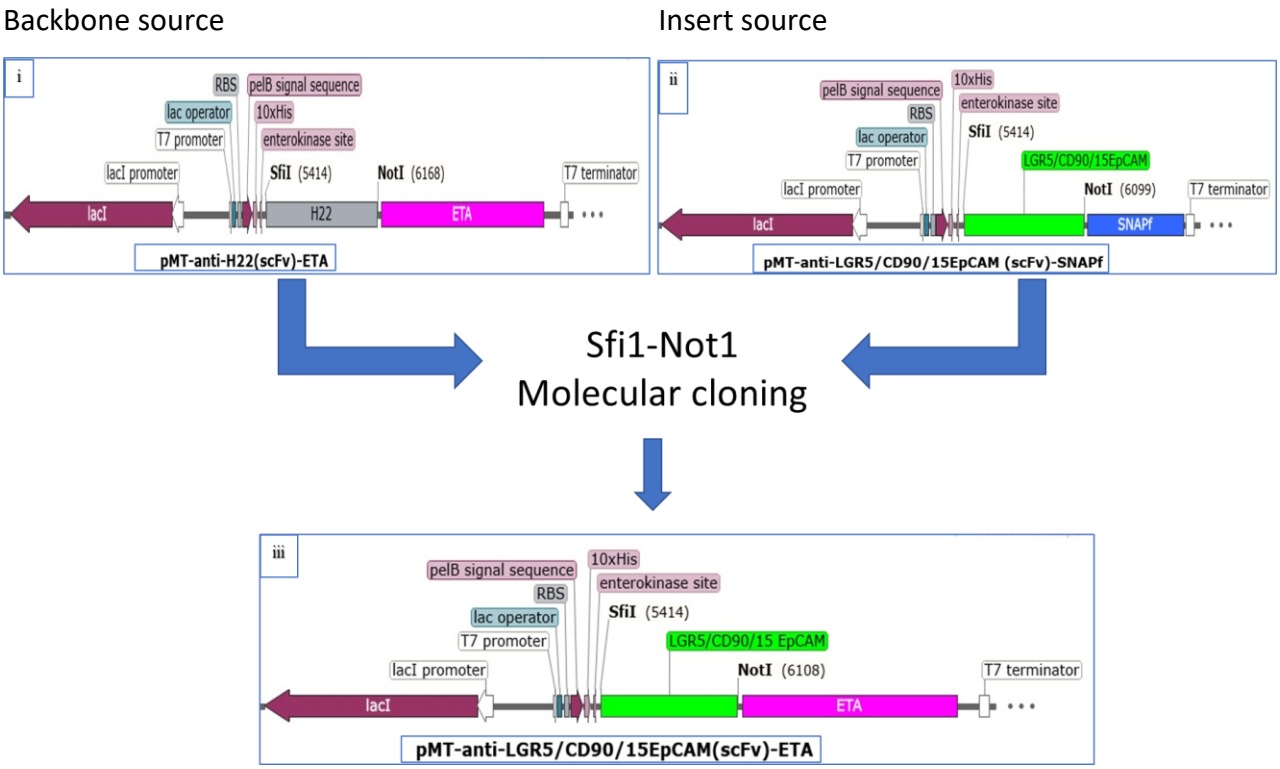

Figure 9. Schematic representation of the *In silico* open reading frames (ORFs) of the bacterial expression vectors for the generation of ETA-based rITs. (i) pMT-anti-H22(scFv)-ETA (ii) pMT-anti-LGR5/CD90/15EpCAM(scFv)-SNAPf (iii) pMT-anti-LGR5/CD90/15EpCAM(scFv)-ETA. The *Not*I and *Sfi*I restriction sites used during the molecular cloning process into the bacterial expression vector are indicated, along with the respective scFvs and other important components of the construct. The designed ORFs of the pMT-vector of periplasmic expression contain all necessary components for downstream cloning, expression and purification experiments (Table 12).

4.1.2 *In silico* design of plasmids coding for dETA-based rITs

The pMT-anti-H22(scFv)-ETA plasmid was further modified to develop a dETA-containing backbone. This was used to generate the corresponding dETA plasmid versions targeting the same CSRs (CD9O, LGR5 and EpCAM). The pMT-anti-H22(scFv)-ETA was flanked on the *Not1* and *BlpI* restriction sites to allow for the excision and replacement of wild-type ETA with dETA RG7787 (R456T)-R490A respectively, forming pMT-anti-H22(scFv)-dETA as illustrated by Figure 10. Similar to the wt ETA-

based simulation, the dETA-based plasmids were also generated by flanking anti-H22(scFv) on the pMT-anti-H22(scFv)-dETA using *Sfi*I and *Not*I and individually inserting with the genes of interest (anti-LGR5(scFv), anti-CD90(scFv) and anti-15EpCAM(scFv)) to form the three corresponding dETA plasmids pMT-anti-LGR5(scFv)-dETA, anti-CD90(scFv)-dETA and anti-15EpCAM(scFv)-dETA as described in section 3.2.2.4. These plasmids also contain the same features and functions as described for the ETA-based rITs (Table 12). The major difference between the two is on the C-terminus, where the dETA toxin domain contains point mutations at positions: R427A, R456T, D463A, R467A, R505A and R538A.

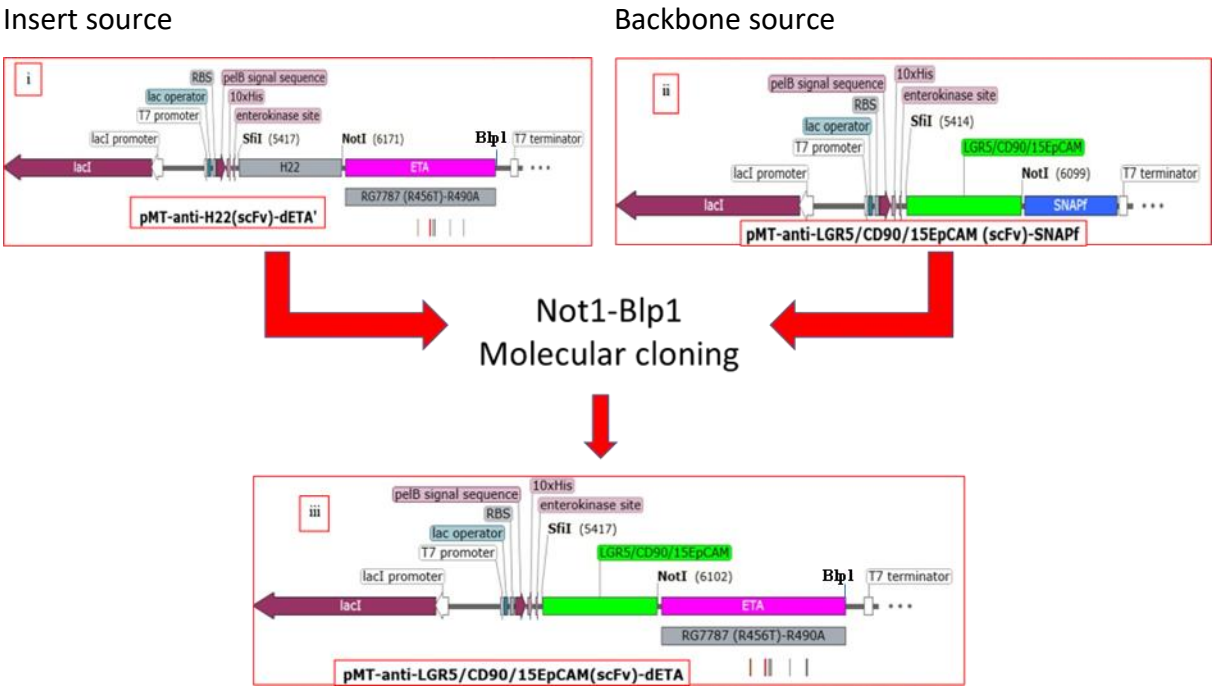

Figure 10. Schematic representation of the *in silico* open reading frames (ORFs) of the bacterial expression vectors for the generation of dETA-based rITs. (i) pMT-anti-H22(scFv)-ETA (ii) pMT-anti-LGR5/CD90/15EpCAM(scFv)-SNAPf (iii) pMT-anti-LGR5/CD90/15EpCAM(scFv)-dETA

A total of six new recombinant plasmids encoding for three ETA-based and three corresponding dETA-based rITs targeting LGR5, CD90 and 15EpCAM were developed. The newly generated *in silico* plasmid maps are shown in Figure 11.

ETA and dETA-based bacterial expression plasmid Maps generated using Snapgene® v3.2.1

(A)(i)

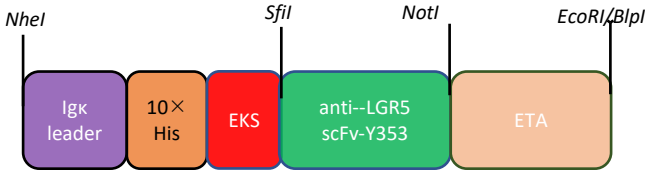

(ii)

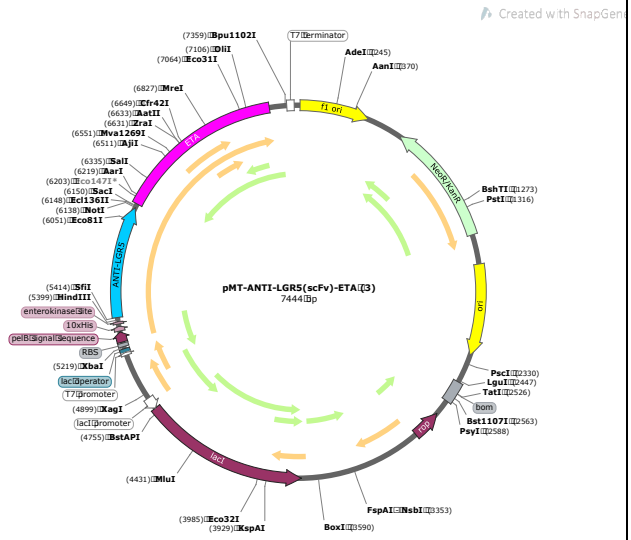

(B)(i)

EcoRI/BlpI

(ii)

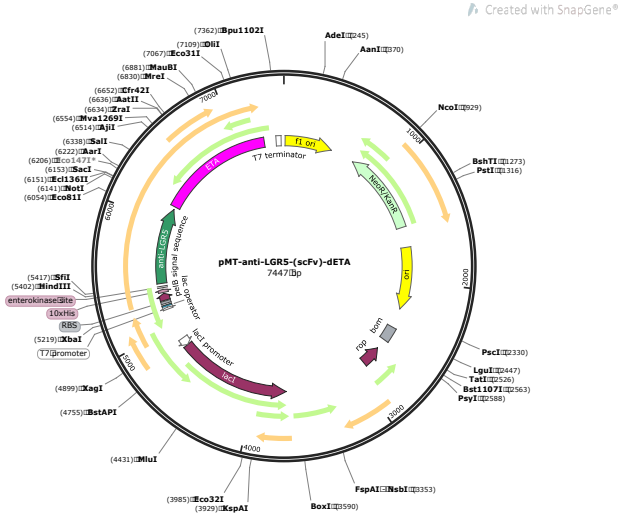

(C)(i) *EcoRI/BlpI*	**(ii)** 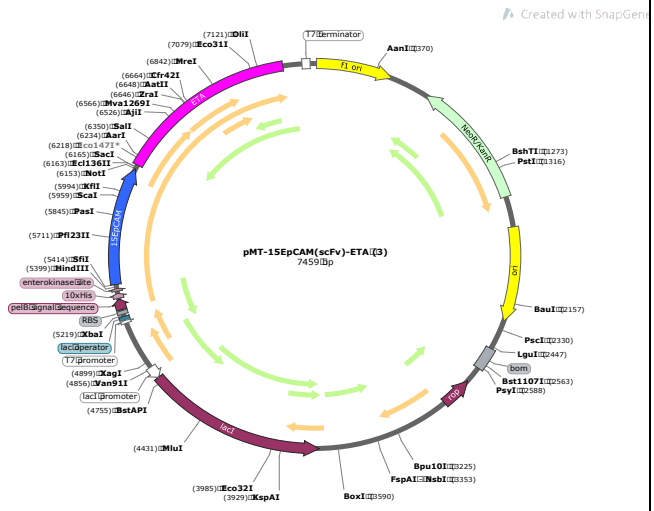
(D)(i) *EcoRI/BlpI*	**(ii)** 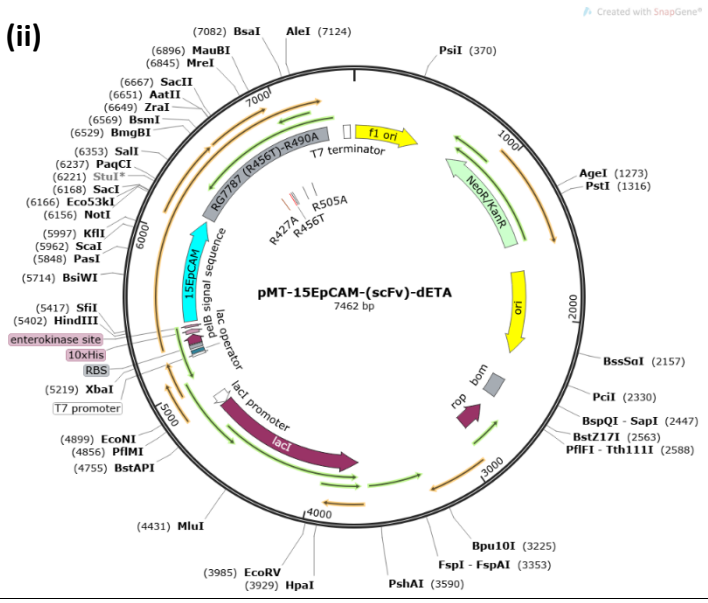

(E)(i)

EcoRI/BlpI

(ii)

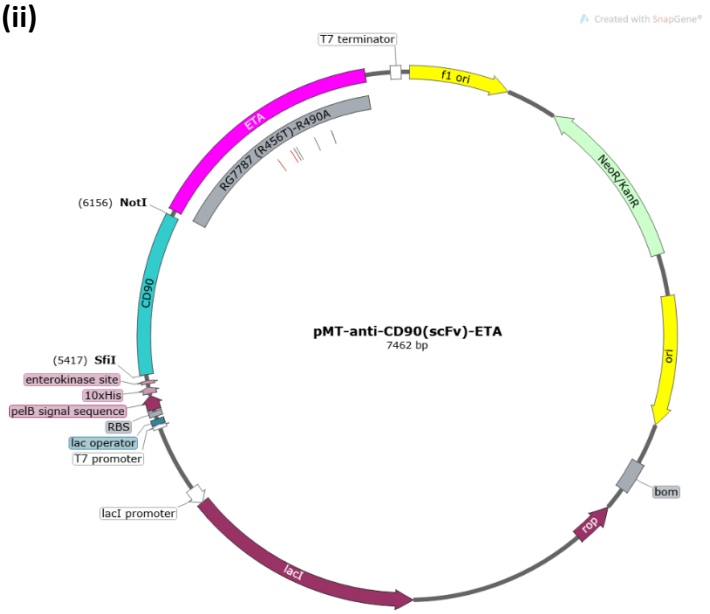

(F)(i)

EcoRI/BlpI

(ii)

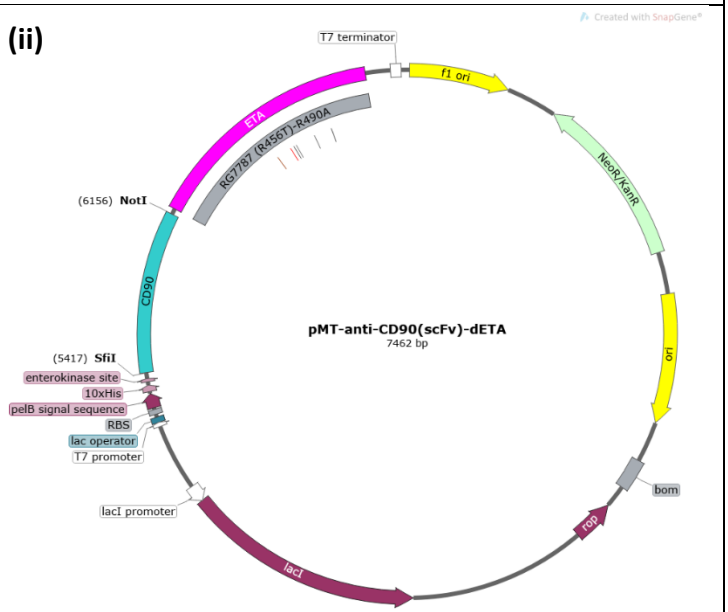

Figure 11. Schematic representation of open reading frames (ORFs) for bacterial expression vectors for the generation of rITs. A. pMT-anti-LGR5 (ScFv)-ETA, **B.** pMT-anti-LGR5 (ScFv)-dETA, **C.** pMT-anti-15EpCAM (ScFv)-ETA, **D.** pMT-anti-15EpCAM (ScFv)-dETA, **E.** pMT-anti-CD90 (ScFv)-ETA, **F.** pMT-anti-CD90 (ScFv)-dETA.

4.2 Molecular cloning results

In silico cloning mirrored molecular cloning. The results generated in this section are in accordance with the predicted *in silico* cloning simulations.

4.2.1 Molecular cloning of ETA-based rIT encoding plasmids

The DNA plasmids, pMT-ant-LGR5(scFv)-SNAP, pMT-ant-CD90(scFv)-SNAP and pMT-ant-EpCAM(scFv)-SNAP, pUC57-dETA and the backbone pMT–anti-H22(scFv)-ETA were individually transformed into *E. coli* (Dh5-alpha) competent cells and prepared for bulk DNA isolation by phenol-chloroform extraction (section 3.2.2.2). The vector backbone (Figure 12) was generated by flanking the anti-H22(scFv) from pMT–anti-H22-ETA using *Sfi1* and *Not1* restriction endonucleases (Section 3.2.2.4). These restriction endonucleases produce sticky ends for replacement with the different constructs included in this study (Figure 13). The ETA backbone simulation was expected at 6720 bp minus the anti-H22(scFv) as depicted by the fragments after digestion as visualized on an agarose gel (Figure 12).

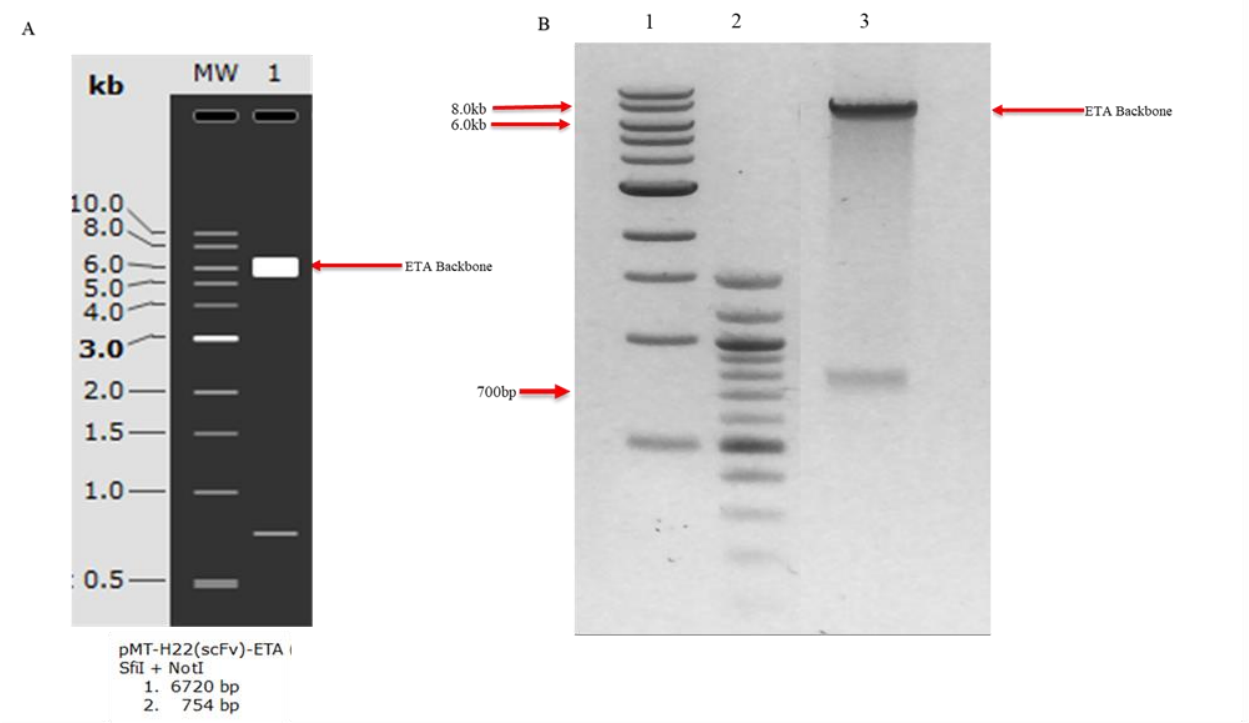

Figure 12: Restriction double digestion of pMT-anti-H22-ETA (A) Simulated double digestion product of pMT-anti-H22(scFv)-ETA. Lane Mw represents the simulated marker and Lane 1- represents the simulated double-digested product of pMT-anti-H22(scFv)-ETA. (B) Double-digested product of pMT-H22-ETA(B). Lane 1 – contains a 1Kb marker, lane 2- contains a 100bp marker and lane 3 contains the double digestion product of pMT-anti-H22(scFv)-ETA.

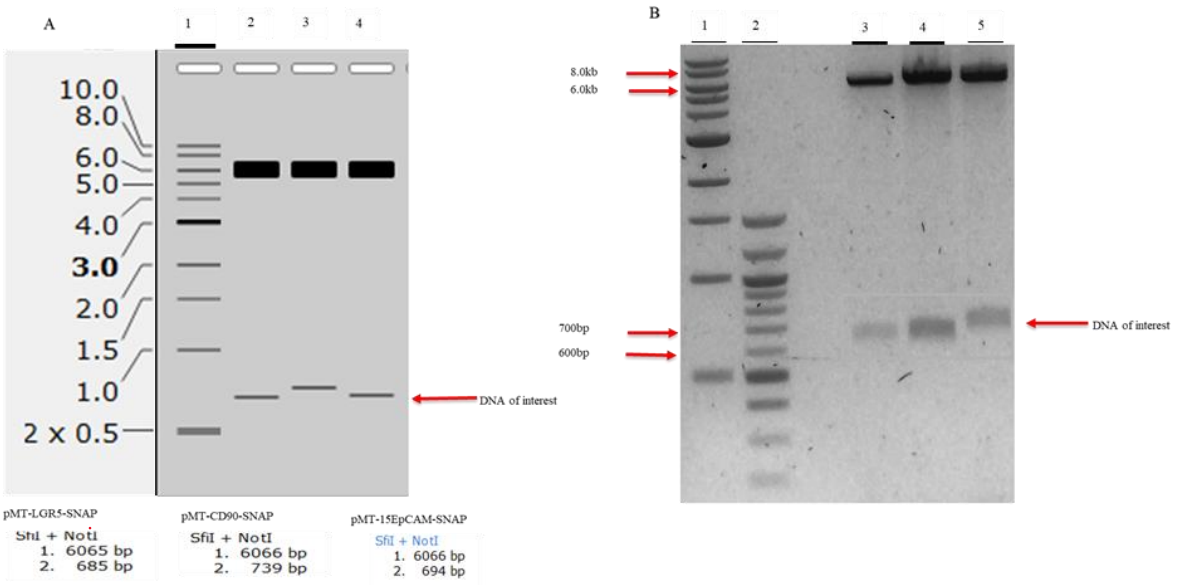

Figure 13. Restriction double digestion of desired scFvs (A) Simulated double digested of pMT-anti-LGR5(scFv)-SNAPf, pMT-anti-CD90(scFv)-SNAPf, and pMT-anti-15EpCAM(scFv)-SNAP. Lane 1 contains the marker, Lane 2 contains simulated double-digested product of pMT-anti-LGR5(scFv)-SNAPf, Lane 3 contains simulated double-digested product of pMT-anti-CD90(scFv)-SNAPf and Lane 4 contains simulated double digested product of pMT-anti-15EpCAM(scFv)-SNAPf. (B) Double digest product of pMT-anti-LGR5(scFv)-SNAPf, pMT-anti-15EpCAM(scFv)-SNAPf and pMT-anti-CD90(scFv)-SNAPf. Lane 1 contains a 1Kb marker, lane 2 contains a 100bp marker, lane 3 contains the double digest product of pMT-anti-LGR5(scFv)-SNAPf, lane 4 contains the double digest product of pMT-anti-15EpCAM(scFv)-SNAPf and lane 5 contains the double digest product of pMT-anti-CD90(scFv)-SNAPf.

Based on the simulated agarose gel, the expected band sizes of the various scFv genes are theoretically predicted. Anti-LGR5(scFv),anti-CD90(scFv) and anti-15EpCAM(scFv) generated a band of 685bp, 739bp and 694bp respectively. The double digest results successfully match the simulated results as all the double digest reactions produced bands between the 600bp and

700bp marker. These results indicate successful restriction digestion, as outlined in section 3.2.2.4. The fragment-containing gel sections were excised, purified and quantified for downstream processing.

4.2.2 T4 DNA ligation of anti-LGR5(scFv), anti-CD90(scFv), anti-EpCAM(scFv) and pMT-ETA

After purification and quantification of the excised DNA backbone and inserts of interest, the pMT-ETA backbone was ligated individually to anti-CD90(scFv), anti-LGR5(scFv), anti-EpCAM(scFv) as described in section 3.2.2.7. The insert and backbone DNA were ligated using T4 ligase at vector to insert ratios, 1:1 and 1:3, whilst the control experiment was 1:0. These ligation products were transformed into DH5 alpha *E. coli* cells (section 3.2.2.7). Untransformed cells were used as a control to ensure a successful transformation reaction. For the control plates, the unsupplemented plate had growth whilst the untransformed cell on supplemented plates (Kanamycin 50mg/mL) had no colonies. On the 1:0 plate, there were 10 colonies, whereas the 1:1 and 1:3 plates both had >300 colonies. The 1:3 ratio plate had 6 colonies selected and cultured in 3mL of LB broth supplemented with kanamycin (50mg/mL). The plasmids were isolated using a zippy plasmid miniprep. Isolated DNA clones exhibiting appropriate endonuclease restriction profiles were sent to Inqaba Biotech company (Pretoria, South Africa) for Sanger sequencing, to confirm successful molecular cloning (section 3.2.2.9). The positive ligation products were transformed into BL21 *E. coli* cells for protein expression as described in section 3.2.3.1.

4.2.3 Molecular cloning of dETA-based rITs.

The developed pMT-anti-H22(scFv)-ETA plasmid was further modified to generate a dETA-based backbone plasmid (Figure 10). The H22 (scFv)-ETA was flanked on the *Not1* and *BlpI* restriction sites to remove wild-type ETA and insert dETA. Therefore, the dETA-based plasmids were generated by inserting the anti-LGR5(scFv), anti-CD90(scFv) and anti-15EpCAM(scFv) into the pMT-dETA plasmid to form the three corresponding dETA plasmids pMT-anti-LGR5(scFv)-dETA, anti-CD90(scFv)-dETA and anti-15EpCAM(scFv)-dETA.

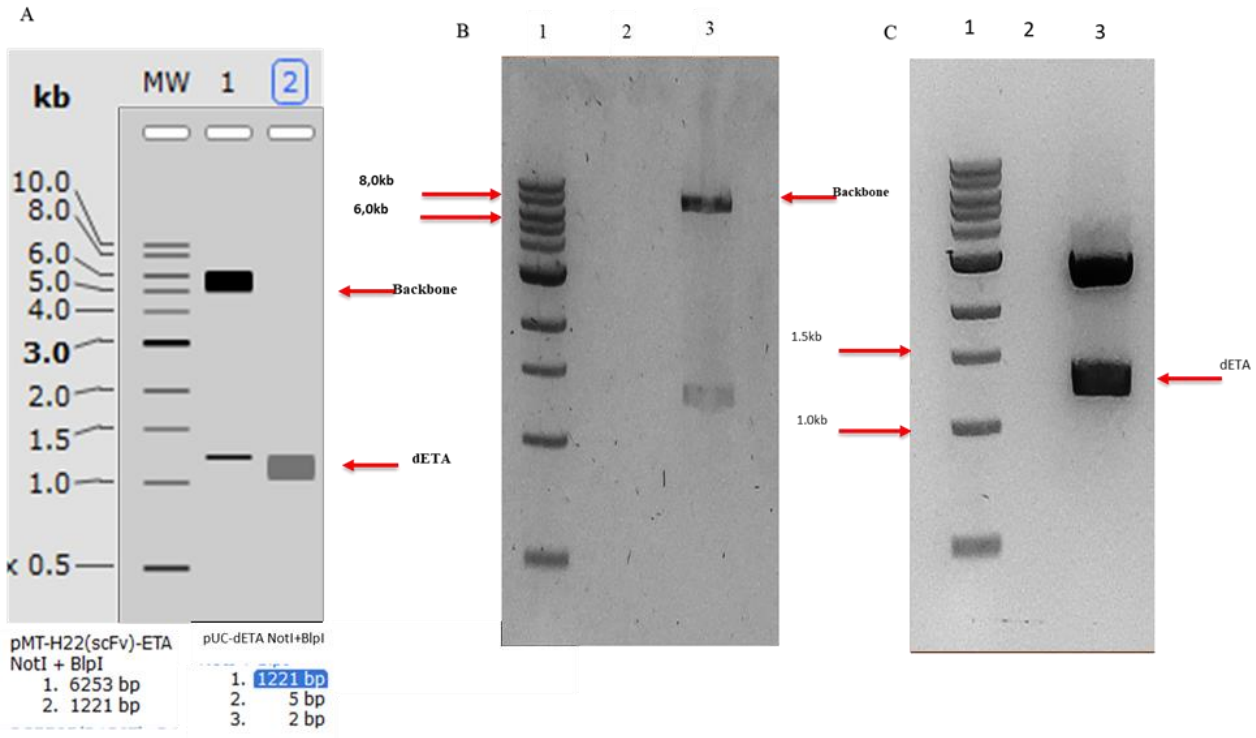

Figure 14: Molecular cloning of dETA-based bacterial expression plasmids (A) Simulation of the double digest of pMT-anti-H22(scFv)-ETA and pUC57-dETA. Mw represents the simulated marker. Lane 1 represents the simulated double digestion product of pMT-anti-H22(scFv)-ETA and Lane 2 represents the expected size of the dETA gene and double-digested product of pUC57-dETA. Lane 1 contains a 1Kb marker, lane 2 is blank and lane 3 contains the *NotI* and *BlpI* double digest product. (B) Double digestion product of pMT-anti-H22(scFv)-ETA. Lane 1 contains a 1Kb marker, lane 2 is blank and lane 3 contains the *NotI* and *BlpI* double digest product. (C) Double digestion product of pUC57-dETA. Lane 1 contains a 1Kb marker, lane 2 is blank and lane 3 contains the double digest product of *NotI* and *BlpI.*

The bands of interest were identical to the Wildtype and were matching the sizes that were suggested by the simulation. The successful cloning of dETA-based plasmids vectors was done by Sanger sequencing at Inqaba Biotech company (Pretoria, South Africa) to confirm successful molecular cloning (section 3.2.2.9). The bands of interest were excised from the agarose gel and ligated and transformed into DH5alpha *E. coli* cells and followed similar procedures as in sections 4.2.1 and 4.2.2. Positive clones were isolated, transformed into BL21 *E. coli* and used for protein expression.

4.3 Characterization of rIT proteins

4.3.1 Protein expression & characterization of ETA-based rITs.

The plasmids were successfully transformed into BL21 *E. coli* cells for periplasmic protein expression using the protocol described in section 3.2.3.1. The confirmed clones (pMT-anti-LGR5(scFv)-ETA, pMT-anti-CD90(scFv)-ETA and pMT-anti-15EpCAM(scFv)-ETA) were transformed into BL21 *E. coli*. The transformed BL21 *E. coli* containing recombinant plasmids of interest were cultured to perform periplasmic protein expression under osmotic stress as detailed in section 3.2.3.1. The cells were harvested and resuspended before being lysed via sonication. The supernatant was harvested and filtered before undergoing IMAC purification (section 3.2.4.1). The IMAC fractions were analyzed on a 10% SDS PAGE. The online molecular weight calculator (https://www.bioinformatics.org/sms/prot_mw.htmL), was used to calculate the molecular weights of the rITs. All the rITs had a molecular weight of approximately 72kDa.

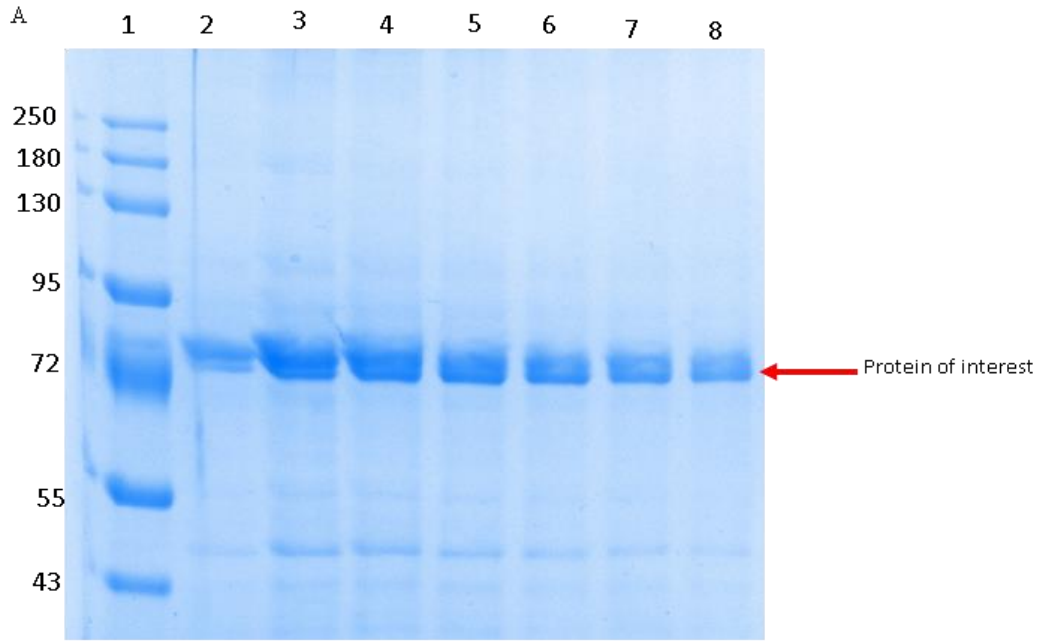

Figure 15 A: IMAC fractions of purified pMT-anti-LGR5(scFv)-ETA. Lane 1 contains protein ladder and lanes 2-8 contain eluted fractions from IMAC purification.

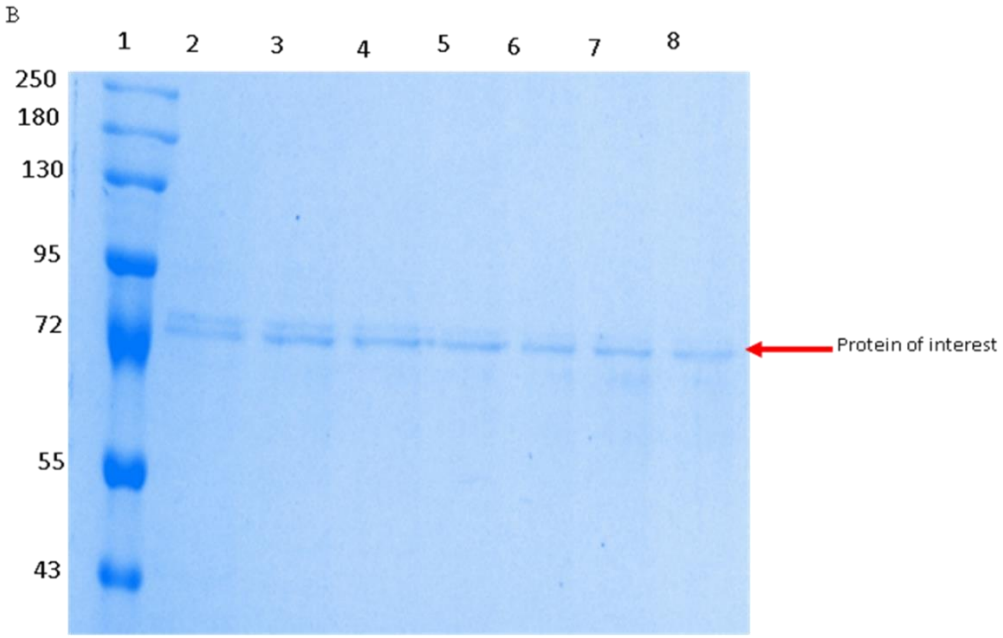

Figure 15 B: IMAC fractions of purified pMT-anti-CD90(scFv)-ETA. Lane 1 contains the protein ladder and lanes 2-8 contain the eluted fractions from IMAC purification.

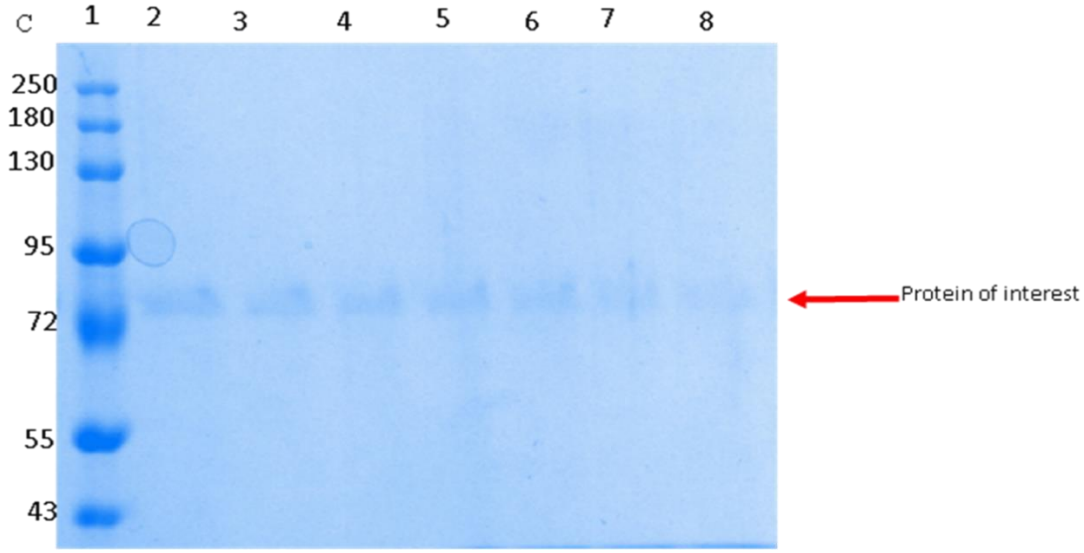

Figure 15 C: IMAC fractions of purified pMT-anti-15EpCAM(scFv)-ETA. Lane 1 contains the protein ladder and lanes 2-8 contain the eluted fractions from IMAC purification.

4.3.1.1 SDS PAGE and Immunoblotting of ETA-based rITs.

The protein purification was successful as the SDS PAGE analysis indicates the presence of the proteins of interest at 72kDa (section 3.2.3.4). The fractions were pooled and concentrated using a 50kDa Amicon® Ultra-15 centrifugal filter (Sigma, USA, UFC901008). The concentrated fractions were used for SEC. The SEC fractions were concentrated and analyzed on a 10% SDS PAGE and Western blot as outlined in sections 3.2.4.2 and 3.2.4.3 respectively. The concentrated and purified protein ran on a 10% SDS gel, and it was transferred onto a PVDF membrane for Western blot analysis as described in section 3.2.4.3. The immunoblot (Figure 16B) confirmed the identity of the rITs by detecting the N-terminal 6-Histidine tag.

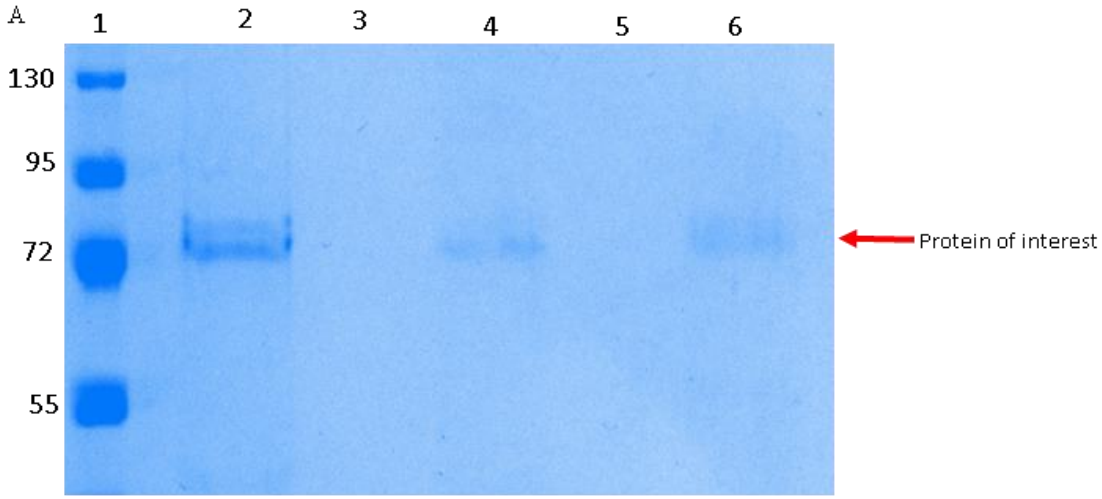

Figure 16 A: SDS PAGE of purified ETA-based rITs. Lane 1 contains the protein ladder, lane 2 contains pMT-anti-LGR5(scFv)-ETA, lane 4 contains pMT-anti-CD90(scFv)-ETA and lane 6 contains pMT-anti-15EpCAM(scFv)-ET

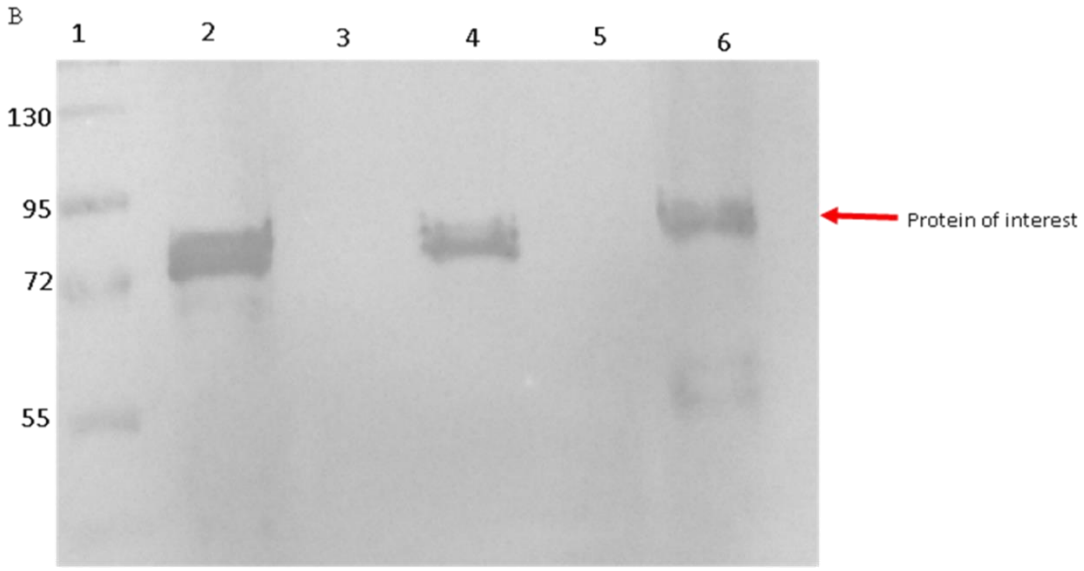

Figure 16 B: Western Blot of purified ETA-based rITs. Lane 1 contains the protein ladder, lane 2 contains pMT-anti-LGR5(scFv)-ETA, lane 4 contains pMT-anti-CD90(scFv)-ETA and pMT-anti-15EpCAM(scFv)-ETA. The SEC was successful as the protein of interest was present at 72kDa (red arrow) in the SDS PAGE and Western Blot.

4.3.2 Protein expression & characterization of dETA-based rITs.

This was achieved by following similar steps as outlined in the above section (4.3.1). The dETA-containing plasmids were successfully transformed into BL21 *E. coli* cells for periplasmic protein expression. The confirmed clones (pMT-anti-LGR5(scFv)-dETA, pMT-anti-CD90(scFv)-dETA and pMT-anti-15EpCAM(scFv)-dETA) were transformed into BL21 *E. coli*. The transformed BL21 *E. coli* containing recombinant plasmids of interest were cultured to perform bacterial protein expression under osmotic stress as detailed in section 3.2.3.1. The cells were harvested and resuspended before being lysed via sonication. The supernatant was harvested and filtered before undergoing IMAC purification. The IMAC fractions were analyzed on a 10% SDS PAGE. The molecular weights of the rITs were calculated using a Protein Molecular weight calculator (https://www.bioinformatics.org/sms/prot_mw.htmL). All the rITs had a molecular weight of approximately 72kDa.

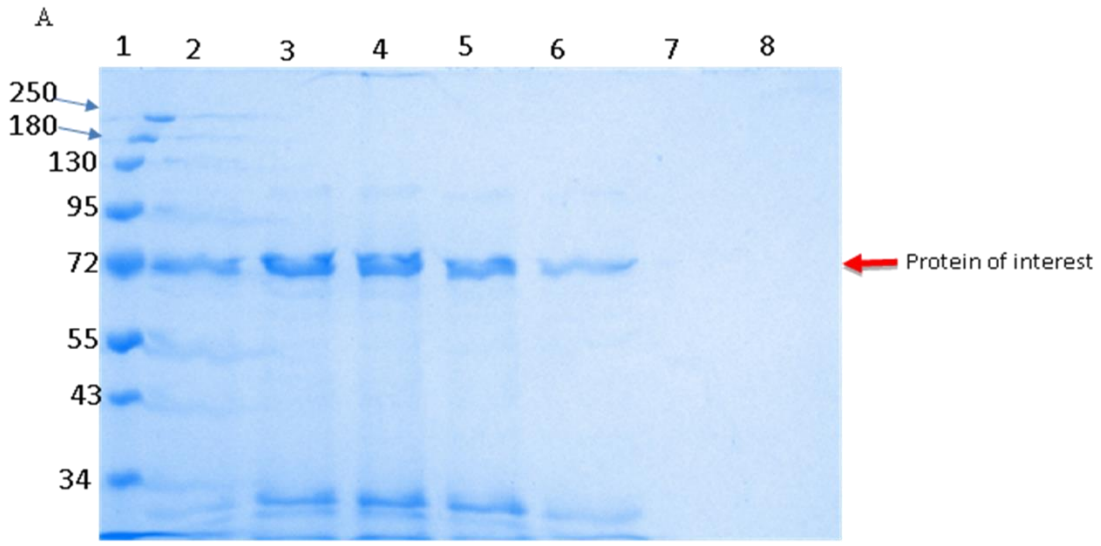

Figure 17 A: IMAC fractions of purified pMT-anti-LGR5(scFv)-dETA. Lane 1 contains the protein ladder and lanes 2-8 contain the eluted fractions from IMAC purification.

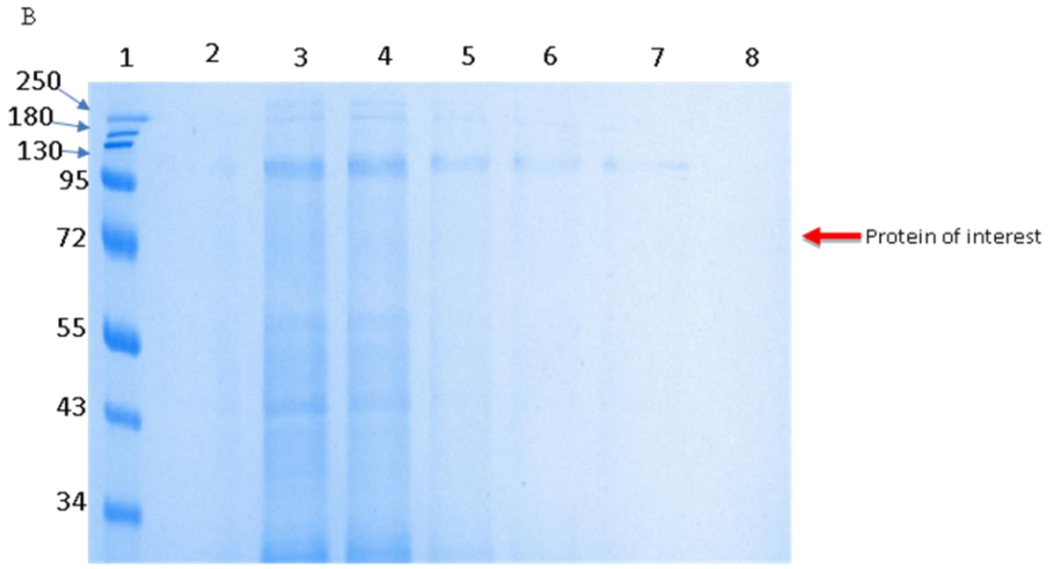

Figure 17 B: IMAC fractions of purified pMT-anti-CD90(scFv)-dETA. Lane 1 contains the protein ladder and lanes 2-8 contain the eluted fractions from IMAC purification.

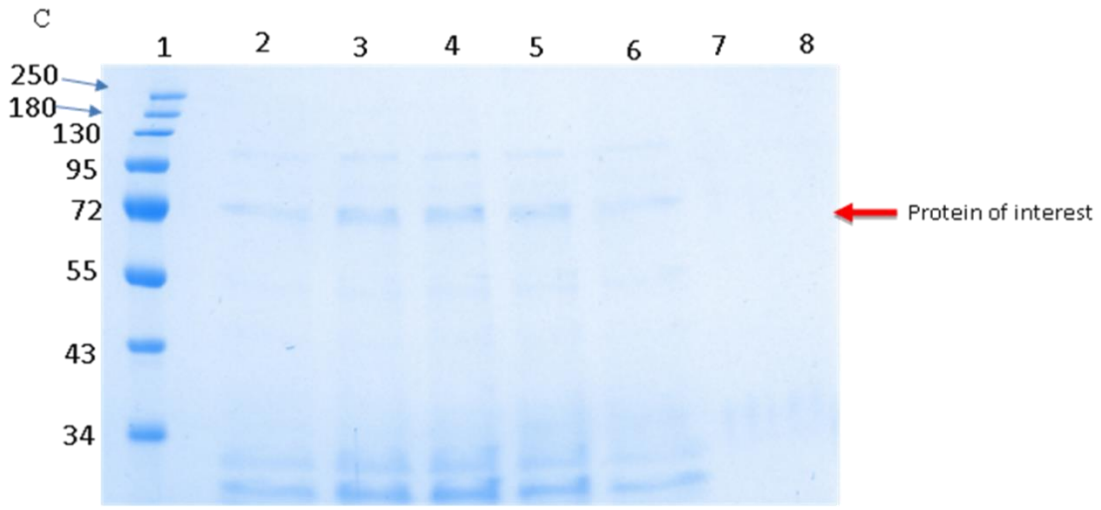

Figure 17 C: IMAC fractions of purified pMT-anti-15EpCAM(scFv)-dETA. Lane 1 contains the protein ladder and lanes 2-8 contain the eluted fractions from IMAC purifications.

4.3.2.1 SDS PAGE and Immunoblotting of dETA-based rITs.

The protein purification was successful as the SDS PAGE analysis indicates the presence of the proteins of interest at 72kDa.The "cleanest" fractions were selected and concentrated using a 50kDa Amicon® Ultra-15 centrifugal filter (Sigma, USA, UFC901008). The concentrated fractions were used for SEC. The SEC fractions were concentrated and analyzed on a 10% SDS PAGE and Western blot.

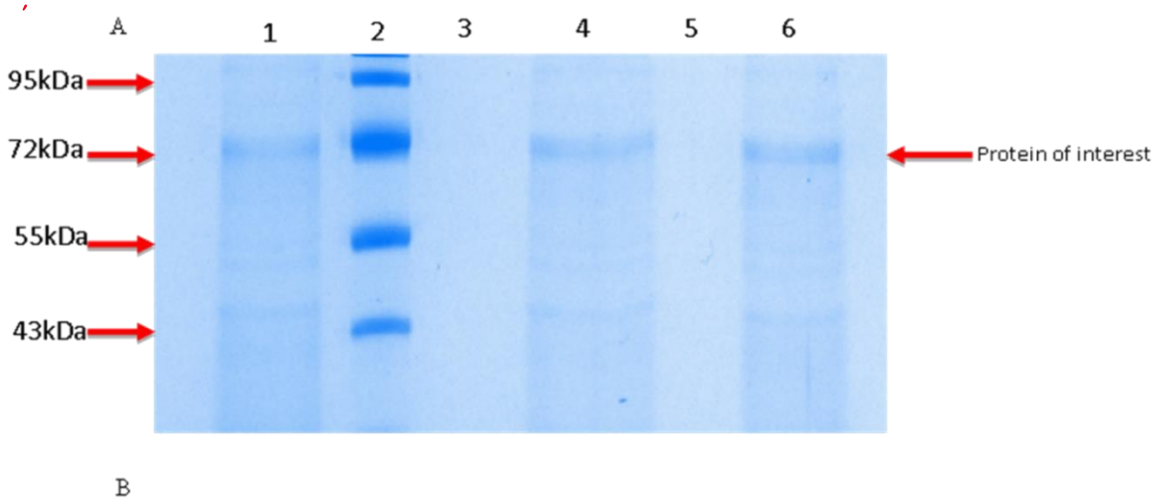

Figure 18 A: SDS PAGE of dETA rITs post IMAC and SEC(A). Lane 1 contains anti-LGR5-dETA, lane 2 contains the protein ladder, lanes 3 and 5 are blank, lane 4 contains anti-CD90(scFv)-dETA and lane 6 contains anti-15EpCAM(scFv)-dETA.

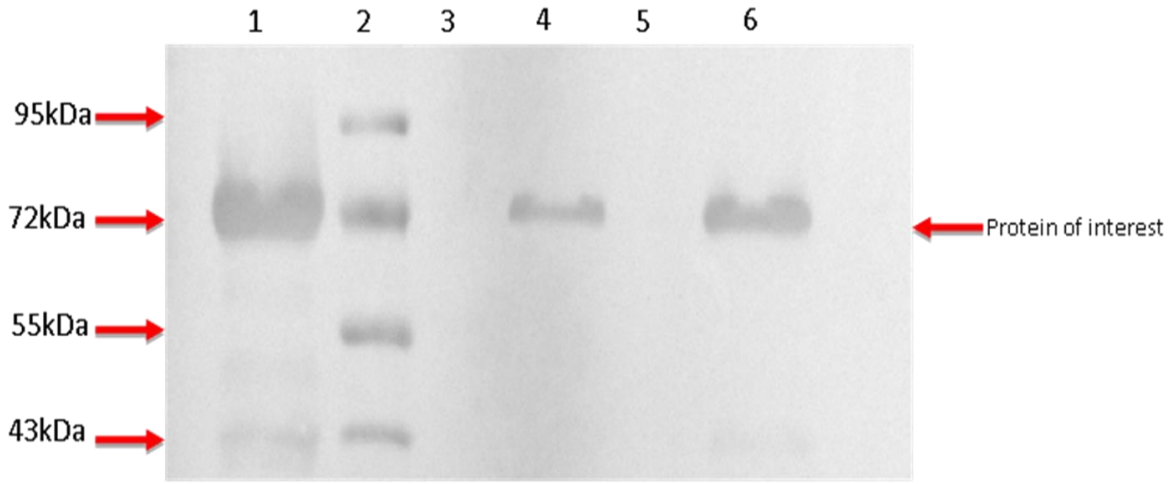

Figure 18 B: Western blots of dETA rITs Post IMAC and SEC (B). Lane 1 contains anti-LGR5-dETA, lane 2 contains the protein ladder, lanes 3 and 5 are blank, lane 4 contains anti-CD90(scFv)-dETA and lane 6 contains anti-15EpCAM(scFv)-dETA.

The dETA-based rITs were successfully purified using the combination of IMAC and SEC. This was indicated by both the SDS PAGE and Western blot described in sections 3.2.4.2 and 3.2.4.3 respectively. The SDS PAGE indicated the presence of a 72kDa protein as the band corresponded with the 72kDa marker on the protein ladder (Figure 18A). The western blot (Figure 18B) confirmed the identity of the rITs by detecting the N-terminal 6-Histidine tag.

4.4 Cell surface binding analysis

These purified rITs were used for binding studies using confocal microscopy as outlined in section 3.3.2. Cells were incubated with Hoechst (1:5000 dilution) at 37^{o}C for 30 minutes to stain the nuclei (blue). They were incubated with anti-His-PE labelled rITs at 37^{o}C for 30 minutes. The cells were washed 3 times with 1x PBS, followed by incubation in 4% PFA at room temperature for 20 minutes to fix the cells to the coverslip. The coverslip was then mounted on a microscope slide before being viewed under a Zeiss confocal scanner microscope (LSM880) at 20µm (Figure 19).

(A) **Anti-LGR5(scFv)-ETA binding to MDA-MB-468 cells**

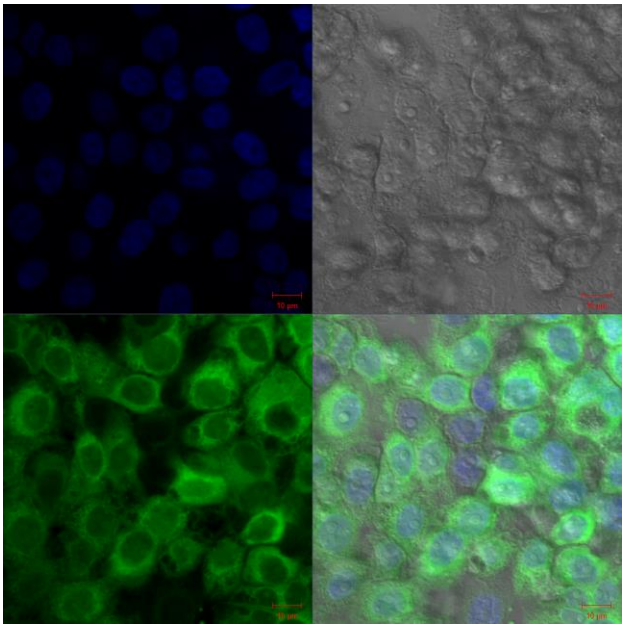

(B) **Anti-LGR5(scFv)-ETA showing no binding to HL60 cells**

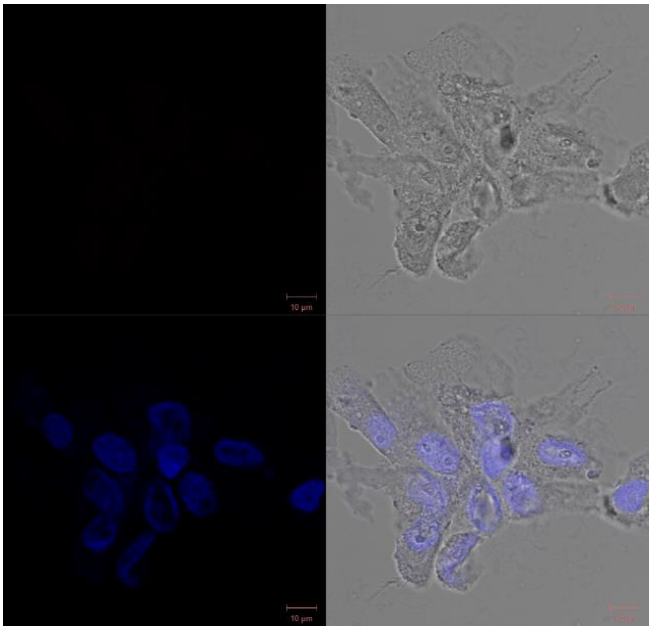

(C) Anti-CD90(scFv)-ETA binding to MDA-MB-468 cells

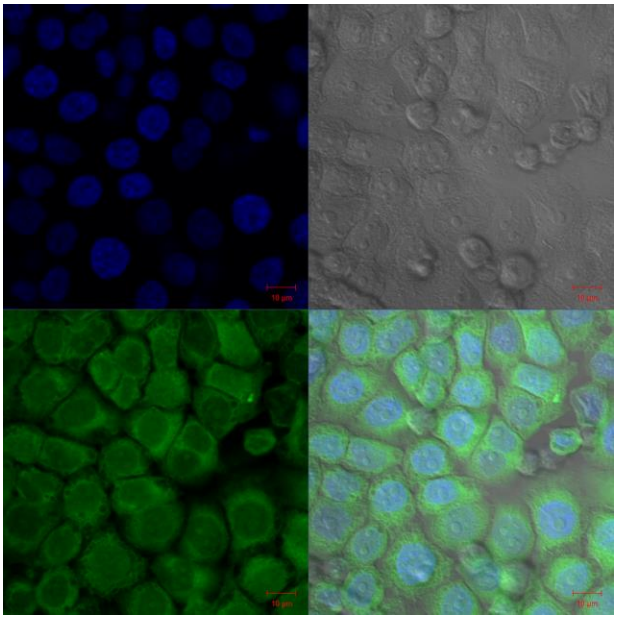

(D) Anti-CD90(scFv)-ETA showing no binding to MCF7 cells

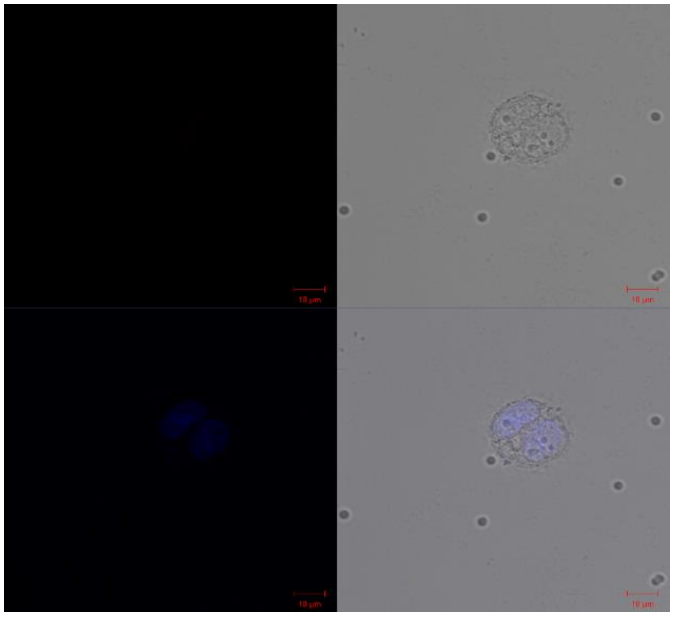

(E) **Anti-EpCAM(scFv)-ETA binding to MDA-MB-468 cells** (F) **Anti-EpCAM(scFv)-ETA showing no binding to HL60 cells**

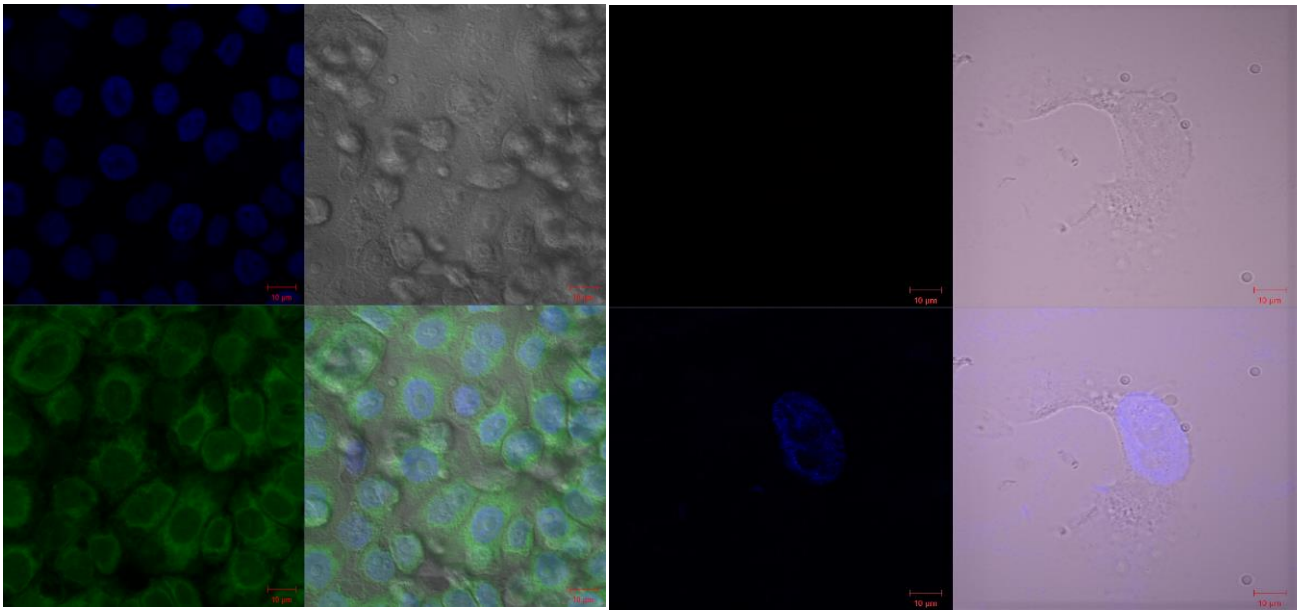

(G) **Anti-H22(scFv)-ETA binding to MDA-MB-468 cells**

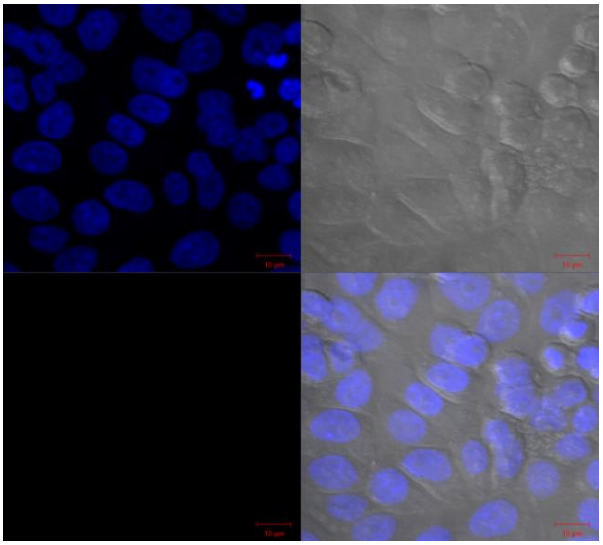

Figure 19: Confocal microscopy demonstrating surface binding of rITs on MDA-MB-468 cells (A) Anti-LGR5(scFv)-ETA binding to MDA-MB-468 cells. (B) Anti-LGR5(scFv)-ETA showing no binding to HL60 cells. (C) Anti-CD90(scFv)-ETA binding to MDA-MB-468 cells. (D) Anti-CD90(scFv)-ETA showing no binding to MCF7 cells. (E) Anti-EpCAM(scFv)-ETA binding to MDA-MB-468 cells. (F) Anti-EpCAM(scFv)-ETA showing no binding to HL60 cells. (G) Anti-H22(scFv)-ETA binding to MDA-MB-468 cells. Cells were incubated with Hoechst (1:5000 dilution) at 37^{o}C for 30 minutes to stain the nuclei (blue). The cells were incubated with rITs labelled with anti-His-PE antibody at 37^{o}C for 30 minutes. They were washed 3 times with 1x PBS, followed by being incubated with 4% PFA at room

temperature for 20 minutes to fix the cells to the coverslip. The coverslips were then mounted on a microscope slide before being viewed under a Zeiss confocal scanner microscope (LSM88) at 20µm.

4.5. Cytotoxicity analysis of rITs

Once it was shown that the rITs successfully bind selectively, to the TNBC MDA-MB-468 antigen-positive tumour cells, their tumour cell-killing potential was investigated. The tumour cell lines were treated with each of the rITs, and XTT cell viability assays (section 3.3.3) were used to determine the cytotoxicity relative to the untreated (100%) and 0% cell viability controls. Using serially diluted rITs, dose-dependent reduction in MDA-MB-468 cell viability treated with the rITs was observed and this enabled the calculation of the IC_{50} values shown in Figure 20. There was no dose-dependent reduction of the antigen-negative cells used as a control for all three rITs.

A

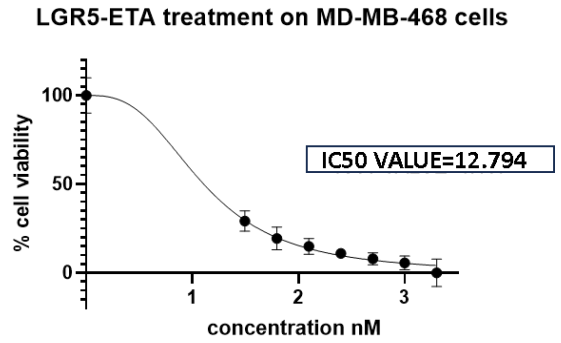

B

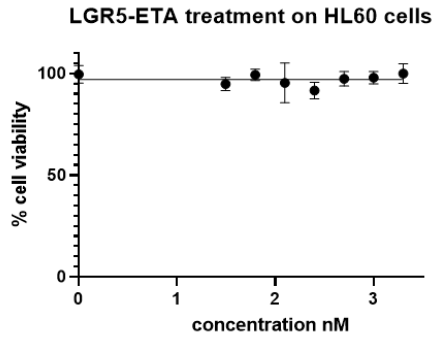

C

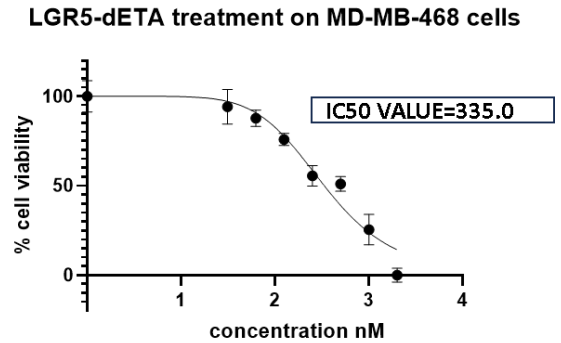

D

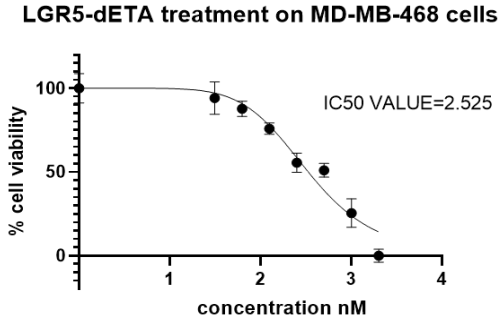

E

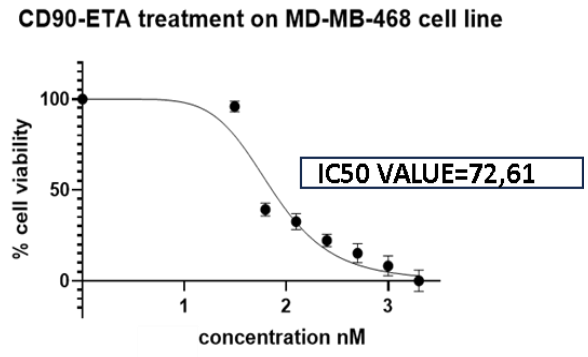
CD90-ETA treatment on MD-MB-468 cell line
% cell viability
100
50
0
1
2
3
concentration nM
IC50 VALUE=72,61

F

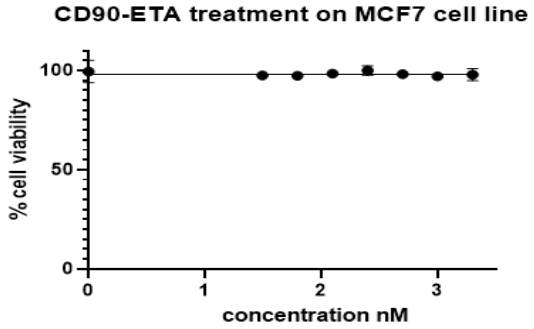
CD90-ETA treatment on MCF7 cell line
% cell viability
100
50
0
0
1
2
3
concentration nM

G

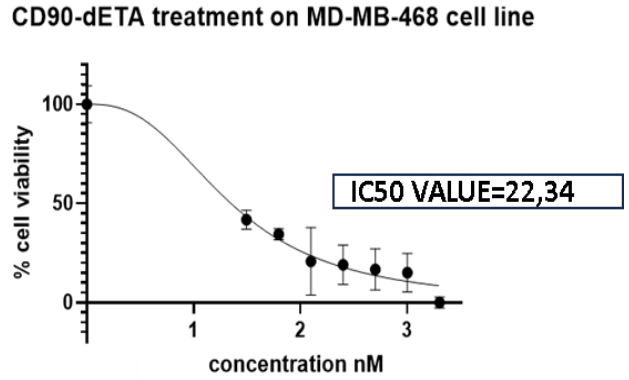
CD90-dETA treatment on MD-MB-468 cell line
% cell viability
100
50
0
1
2
3
concentration nM
IC50 VALUE=22,34

H

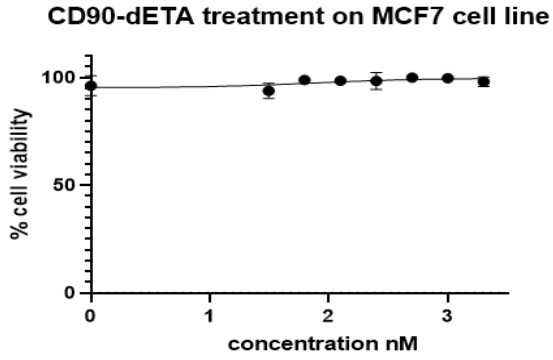
CD90-dETA treatment on MCF7 cell line
% cell viability
100
50
0
0
1
2
3
concentration nM

I

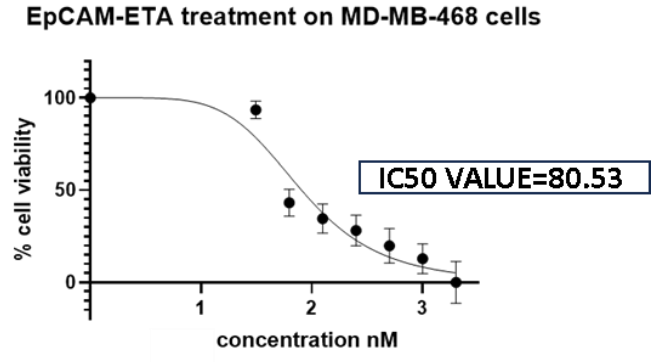
EpCAM-ETA treatment on MD-MB-468 cells
% cell viability
100
50
0
1
2
3
concentration nM
IC50 VALUE=80.53

J

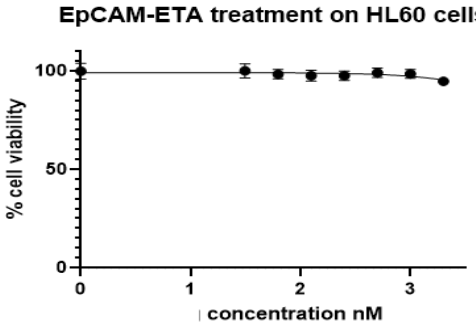
EpCAM-ETA treatment on HL60 cells
% cell viability
100
50
0
0
1
2
3
concentration nM

K L

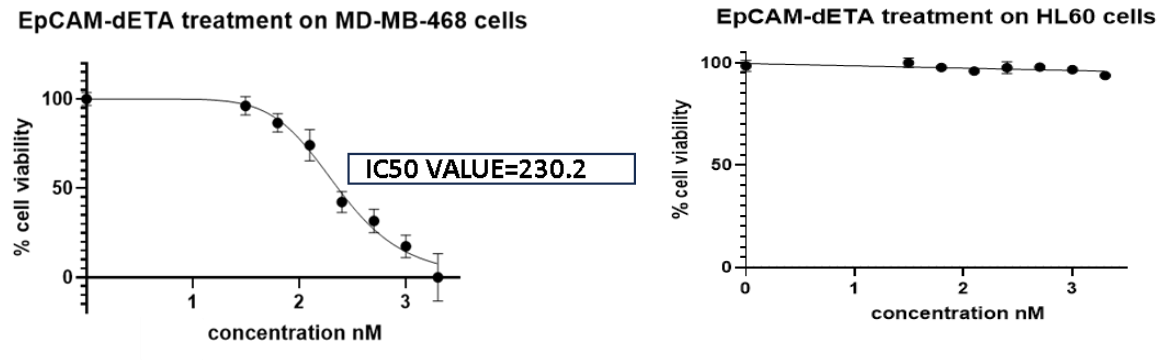

Figure 20. Dose-response curves depicting the cytotoxicity of rITs. The cytotoxicity effect of the rITs was assessed using an XTT cell viability assay. The cells were treated with 7-fold serially diluted concentrations of rITs followed by running XTT cell viability assays. Controls were untreated (negative control) and cells were treated with zeocin(100µg/mL) (positive control). The HL60 cell lines were used as an antigen-negative control for LGR5 and EpCAM rITs. The MCF7 cell line was used as an antigen-negative control for the CD90 rIT. The negative control for the MDA-MB-468 cell line used in this study was anti-H22(scFv)-ETA.

After confirming the strong binding cell surface binding of the rITs to TNBC cells *in vitro*, by confocal analysis, the cell killing potential of these rITs was also investigated using the XTT cell viability assay (Cell proliferation kit II; Roche, CH) as described in section 3.3.3. The rITs were used to evaluate their cytotoxicity on the tumour cells. All rITs developed showed a dose-dependent response against the MDA-MB-468 tumour cells, aligning with the results of the binding studies. The results were analyzed by measuring the absorbance of the XTT reagent at 450nm as the measurement filter and 650mn as the reference filter on a spectrophotometer (iMark™ Absorbance reader, Bio-Rad, USA). GraphPad Prism v.9.0 software was used to calculate the concentration of rIT that would achieve 50% cell death (IC_{50}). The ETA-based rITs demonstrated higher potent dose-dependent cytotoxicity against the MB-MB-468 cells except for anti-CD90(scFv)-dETA which demonstrated more cytotoxicity than its wt ETA version. To assess the non-specific tumour cell killing, all antigen-negative controls were not affected by the rITs, showing the absence of nonspecific cytotoxicity caused by the rITs. For ETA-based rITs, Anti-LGR5-ETA demonstrated the most potent dose response, followed by anti-15EpCAM-ETA and

anti-CD90-ETA successively. This indicates that the LGR5, EpCAM and CD90 receptors are not only overexpressed in TNBC cell lines but also easily assessable for the rITs.

Table 16: Dose-dependent response of TNBC (MD-MB-468) cell lines to ETA and dETA-based recombinant immunotoxins (rITs)

CONSTRUCT	CELL LINE	ANTIGEN EXPRESSED			ETA (IC_{50})	dETA (IC_{50})
		LGR5	EpCAM	CD90		
Anti-LGR5(scfv)	MD-MB-468	Positive+	Positive+	Positive+	12.794nM	335.0nM
	HL60	Negative-	Negative-	Positive+	N/A	N/A
Anti-15EpCAM(scfv)	MD-MB-468	Positive+	Positive+	Positive+	80.53nM	230.2nM
	HL60	Negative-	Negative-	Positive+	N/A	N/A
Anti-CD90(scfv)	MD-MB-468	Positive+	Positive+	Positive+	72.61nM	22.34nM
	MCF7	Positive+	Positive+	Negative-	N/A	N/A
Anti-H22(scfv)	MD-MB-468	Positive+	Positive+	Positive+	N/A	N/A

Anti-CD90-dETA demonstrated a higher cytotoxicity than its wt ETA version towards the TNBC MB-MD-468 cell line as shown by the IC_{50} values 22.34nM and 72.61nM respectively. For the rITs targeting LGR5, the wt version anti-LGR5-ETA exhibited higher toxicity on the TNBC MB-MD-468 cell line compared to its deimmunized version anti-LGR5-dETA as highlighted by the respective IC_{50} values of 12.794nM and 335.0nM. Similarly, the same phenomenon was also demonstrated by the IC_{50} values of anti-15EpCAM-ETA and anti-15EpCAM-dETA, 80.53nM and 230.2nM respectively. Among the three targeted CSRs, LGR5 targeting rITs exhibited the highest toxicity on the TNBC MDA-MB-468 cell line. This may indicate that the EpCAM and CD90 receptors on the MDA-MB-468 cell surface may be less accessible for the rITs in comparison to the LGR5 receptor. This is observed by the difference in their IC_{50} values as highlighted in Table 12. For the antigen-

negative controls, the HL60 cell line expresses the CD90 biomarker but does not express the EpCAM and LGR5 CSRs. The cell viability of the HL60 cells was not affected by the anti-15EpCAM-ETA and anti-LGR5-ETA rITs, indicating that the rITs do not kill nonspecifically. The same can be observed with CD90-ETA on the MCF7 cell line, as 15EpCAM and LGR5 are expressed but not CD90. The cell viability of the MCF7 cells was not affected by CD90-ETA. For the negative rIT control, the cell viability of the TNBC MDA-MB-468 cell line was not affected by anti-H22-ETA.

CHAPTER 5: DISCUSSION

5.1 TNBC: Problem statement

According to the World Health Organization (WHO), breast cancer is the most common cancer worldwide and is the leading cause of cancer deaths in women[1]. TNBC is one of the most aggressive and clinically challenging subtypes of breast cancer, which is mainly characterized by a high risk of metastasis, poor prognosis, low survival rates and tumours that show negative expression of ER, PR, and HER2 receptors[77], [66]. Globally, TNBC accounts for 10-20% of all occurring breast cancers[67], but strangely, in the African continent, the incidence rates are higher at about 30%[194]. TNBC has a greater morbidity and mortality that has an unexplainable inclination to young females of African ancestry [77], [195], [196].

Triple-negative breast cancer (TNBC) is difficult to manage due to the lack of targeted therapeutic alternatives[197]. This is a result of the absence of hormone receptors ER, PR and HER2. This limitation leads to overall low survival rates and poor prognosis for TNBC patients[197]. For the longest time, there hasn't been any proven effective agent that targets a defining vulnerability in triple-negative breast cancer, until the first ADC (Sacituzumab govitecan) was recently approved by the FDA for TNBC in 2021[198]. Consequently, there is high dependence on traditional treatment methods like chemotherapy with taxanes and anthracyclines which are the current mainstay treatment for TNBC patients. However, chemotherapy has limitations such as short disease-free survival due to a higher risk of relapse which reduces its clinical effectiveness[197]. In addition, recurring local or distal TNBC tumours are particularly resistant to chemotherapeutic strategies [199].

TNBC has six distinct subtypes that possess multiple unique gene expression profiles and ontologies that have highlighted the acute diversity and heterogeneity of this disease[75]. This underscores the importance of focusing global research efforts on identifying reliable prognostic factors or markers that can accurately stratify TNBC patients into high and low-risk categories based on their predicted differential response to targeted agents[73]. Therefore, TNBC tumours

have vast molecular diversity and relying on singular traditional treatment modalities for disease management is not likely to yield effective results.

5.2. Precision medicine for TNBC

In order to circumvent the challenges associated with high molecular diversity of TNBC tumours, the precision medicine approach has gained popularity as a promising approach for identifying patients best benefiting from certain treatments. Traditional treatment modalities utilize singular treatment strategies for the management of TNBC and they are usually unsuccessful[200], [201]. To effectively manage TNBC, a precision medicine approach is necessary, which involves analyzing the molecular diversity of tumours to identify specific characteristics that can predict how a particular patient will respond to different therapies. This personalized approach has shown promising results in improving patient outcomes and reducing treatment-related side effects[202], [203]. Therefore, characterizing the heterogeneity of TNBC tumours and tailoring treatments to individual patients has the greatest potential for enhancing prognosis and disease-free survival.

To categorize tumours and identify relevant biomarkers, TNBC patients undergo histological, immunohistochemical, and gene expression analyses on biopsied tumour samples[204]. These biomarkers, which may be prognostic, therapeutic, or predictive of treatment response, are used to stratify patients based on the presence or absence of these biomarkers[205]. Personalized treatment plans can then be developed based on this stratification, utilizing a combination of conventional and targeted therapies for optimal treatment response, resulting in improved prognosis and survival rates[205].

The higher prevalence and poorer prognosis of TNBC in African countries have long been attributed to poor healthcare infrastructure and inadequate screening methods[206]. Although the reason behind the tendency of TNBCs inclination in occurring in women of African ancestry is unknown, recent research, however, suggests that there may also be an ancestral risk factor at play[206]. A multinational study, analyzing gene expression in an African-enriched cohort identified 613 genes associated with African descent and included over 2000 genes correlated to

regional African ancestry[194]. The study revealed distinct immunological profiles in TNBC tumours of patients with African ancestry[194]. These findings indicate that a patient's ancestral background can affect the molecular diversity of TNBC tumours, and incorporating this information into the development of novel diagnostic and treatment approaches could significantly improve disease outcomes, as implied in this master's project.

Owing to the extensive research underway in clinical trials, there are only two targeted therapies that have been approved by the FDA for clinical treatment of TNBC. These two are pembrolizumab (an immune checkpoint inhibitor mAb) [207] and sacituzumab govitecan (an ADC)[198]. These two drugs have shown the great potential of a personalized approach to TNBC treatment. However, based on a patient's ancestral background, the heterogeneity of TNBC tumours still pose a challenge as some TNBC patients cannot benefit from these drugs. It is unlikely that a single targeted strategy can be sufficient to effectively treat the disease[194]. This is mainly because different patients have different ancestries, as their molecular tumour and tumor-associated immunologic profiles can be influenced by their ancestry[194]. Therefore, a multi-targeted approach that includes a variety of treatment modalities will likely be necessary to successfully manage TNBC on a global scale.

It is therefore imperative to identify new diagnostic and therapeutic biomarkers for the development of TNBC-targeted therapies in clinical settings across different populations[208], [209]. Biomarkers could be utilized to diagnose and categorize patients based on their anticipated disease progression and their response to targeted and standard treatment approaches[210]. This information would enable clinicians to make informed decisions regarding the most effective management and treatment strategies for each patient, leading to better prognosis and improved disease-free survival rates.

5.3. Recombinant Immunotoxins as immunotherapeutic agents: a targeted approach

Different antibody-based therapies are being explored for TNBC treatment as alternative treatment options compared to traditional treatment modalities. These include antibody-drug conjugates (ADCs), immune checkpoint inhibitors (ICIs) and recombinant immunotoxins

(rITs)[211][212]. Passive immunotherapy offered by these treatment regimens has been modified to address the limitations of traditional non-targeted therapies, for instance, off-target side effects[88]. One of the current mainstay treatment options for TNBC is conventional chemotherapy, which functions by eliminating rapidly multiplying cells[213]. However, there are off-target side effects associated with the latter, including systemic toxicity as it is non-specific and highly toxic to even healthy dividing cells[214]. The off-target side effect associated with systemic cytotoxicity can be addressed by the use of targeted drug delivery methods, for example, rITs. These are known to improve the patient's quality of life.

Immunotoxins (ITs) are protein molecules formed by a combination of an antibody or antibody fragment (targeting moiety) and a cytotoxic component (toxin)[143]. The targeting moiety (ligand) is responsible for the selective identification of the target cell population by recognizing a specific antigen on the surface of the targeted cells [146]. Unlike the first and second generations, the 3rd generation of immunotoxins aims at addressing the challenges faced by recombinant proteins formed from full mAbs[155]. The major drawback of the full antibody-based recombinant proteins is the poor penetration potential into tumour masses, due to a relatively larger size of the full mAb[215]. This drawback can be overcome with scFv-based recombinant proteins. These are relatively small in size, easy and cheaper to produce in large quantities whilst maintaining the binding specificity of a full mAb[215]. Due to their relatively smaller size, scFv-based recombinant immunotoxins can easily penetrate tumour masses and be cleared from circulation as they lack an Fc region[212].

Identifying an appropriate target for a rIT is critical for its therapeutic efficacy. The cell surface receptors CD90[112], EpCAM[184] and LGR5[216]) used in this study are all differentially upregulated in various cancer types and evidence suggests that their upregulation is associated with TNBC occurrence in different ways. Studies have shown the role of these CSRs in signalling pathways that are key for the initiation and progression of TNBC as detailed in subsections (1.7.1, 1.7.2 and 1.7.3). These three biomarkers are attractive potential immunotherapeutic targets for TNBC since they are reported to be overexpressed in the majority of TNBC patients[112], [184], [178]. In this study, I developed and explored these antibody-based rITs targeting CD90, EpCAM

and LGR5-positive TNBC cell lines. However, these rITs comprised of the scFv constructs of interest, genetically fused to a bacterial toxin that is responsible for cell killing of CD90, EpCAM and LGR5 positive TNBC cell lines.

For this study, Pseudomonas exotoxin A (ETA) was a preferred bacterial toxin to consider for the synthesis of immunotoxins, due to its high potency, expression and purification yields (section 4.3), ease of cloning (section 4.2) and low non-specific toxicity[166]. It is a potent virulence factor secreted by the gram-negative bacteria *Pseudomonas aeruginosa,* that can be used as an anti-cancer agent[148], [156]. There are several *Pseudomonas exotoxin* A (ETA)-based rITs that have been studied in clinical trials and have yielded promising results. The majority of them have been developed using a truncated form of (PE) called PE38 [165]. Moxetumomab pasudotox (Lumoxiti) is an example of a rIT based on PE38, which has the domain Ia and part of domain Ib missing, in contrast to the native PE[166].

Despite the promising clinical trials results that ETA brings as an alternative therapeutic, there are limitations with the use of these ETA-based rITs. The major drawback faced by ETA-based rITs in clinical trials is the enhancement of immunogenicity in patients[166]. When administered to patients, the toxin component of rITs derived from bacterial, non-human sources can elicit an immune response that produces human anti-toxin-neutralizing antibodies[170]. According to Wayne *et a.*,2017, most patients who were treated with immunotoxins for solid tumours developed anti-toxin antibodies after 1 or 2 cycles of immunotoxin treatment. Owing to the extreme cytotoxicity of PE-based rITs (demonstrated in section 4.5), dosage and concentration should be well monitored as high concentrations may lead to side effects, such as vascular leak syndrome[171]. This immune reaction can prevent repeated dosing of the rIT, which can limit its effectiveness in treating the targeted disease. For immunotoxins to be effective, multiple cycles of treatment need to be administered especially in patients who develop an immune response, therefore the immunogenicity needs to be addressed[217]. In an attempt to address this issue, we introduced point mutations at various positions within the ETA domain (section 4.1.2). However, the clinical trials assessment and comparison of the immunogenicity between these de-immunized immunotoxins and the original wild type have to be analyzed in future work and cannot be done in such a master's project.

5.4. Expression of rITs

5.4.1 Protein expression using bacterial periplasmic osmotic stress protocol.

In this study, all six recombinant immunotoxins (anti-LGR5(scFv)-ETA, anti-CD90(scFv)-ETA, anti-EpCAM(scFv)-ETA, anti-LGR5(scFv)-dETA, anti-CD90(scFv)-dETA and anti-EpCAM(scFv)-dETA) were effectively expressed (Figures 16 and 18) in a bacterial host expression system (BL21 *E. coli* cells). This method of protein expression was designed to enable the synthesis of difficult to produce recombinant proteins, including immunotoxins, within the periplasmic space of *E. coli* bacteria as shown by the SDS PAGE and Western blot results sections 4.3.1 and 4.3.2. This was achieved by subjecting the *E. coli* cells to osmotic stress conditions in the presence of compatible solutes. These compatible solutes use a stress response to induce the production of heat shock proteins/molecular chaperones by creating a stabilizing periplasmic microenvironment at high salt concentrations. Adding compatible solutes to shaking cultures enables bacterial growth within the described osmotic stress conditions as used in this study (section 3.2.3.1). This protocol was established in 2000 by Prof. Dr. Dr. Stefan Barth, who led the research at the University of Cologne in Germany[218]. The results generated in this study showed the expression of full-length recombinant immunotoxins using SDS PAGE and Western blot (sections 4.3.1.1 and 4.3.2.1). These findings showing the recovery of functional proteins using the bacterial periplasmic osmotic stress expression protocol are similar to a report by Nachreiner et al. [219].

There are different factors to consider when choosing a bacterial host expression system for producing recombinant proteins. The *E. coli* host expression system has since been used and preferred due to its cost-effectiveness. Extensive genetic research spanning several decades has provided a wealth of knowledge and tools for manipulating and engineering the organism making it an attractive option for recombinant protein expression[220].

In this study, the *BL21(DE3) E. coli* strain was employed for the expression of recombinant immunotoxins (rITs). It possesses specific genetic alterations in the Lon protease and OmpT protease genes, resulting in defects in these enzymes[221]. The expression system comprises a

region known as the Lac operon, which consists of a Lac promoter preceding an operon, along with the LacI repressor encoded by a specific gene[222]. Activation of the lac operon is achieved by the addition of IPTG (section 3.1.2), which binds to the active LacI repressor, leading to its dissociation from the operator site[223], [224]. Additionally, this strain harbours a DE3 lysogen that carries the T7 RNA polymerase gene under the control of a LacUV5 promoter. The recombinant protein, utilizing the *Pel*B signal sequence, is directed to the periplasmic space of *E. coli*[223] (Table 12).

E. coli can adapt to osmotic pressure by accumulating organic compounds called osmolytes, as evidenced by their ability to thrive in terrestrial environments, meninges, intestinal and urinary tracts of mammals[225]. Osmolytes, such as betaine and sorbitol, play a crucial role in improving protein solubility and stability by facilitating protein refolding and preventing protein aggregation[226], [225]. Betaine, specifically, is known to modulate the free energy of the denatured state, favourably shifting the equilibrium towards the native state of the recombinant protein[226].

The concept of periplasmic protein expression has also been used and confirmed by other researchers who highlight the advantages of this approach[227]. In the periplasm, disulfide bonds can form in recombinant proteins, promoting proper protein folding, and this compartment also contains fewer protease enzymes than the cytoplasm[220], [228]. Varying concentrations of salts, peptone, and yeast extract can enhance the yield of recombinant proteins[227]. Therefore, by harnessing *E. coli*'s ability to adapt to osmotic stress, utilizing osmolytes, and taking advantage of the periplasmic environment, researchers have demonstrated an effective approach for producing rITs and other recombinant proteins. These recombinant proteins have improved solubility, stability, and proper folding[218], as illustrated by full-length rITs generated in this study (Figures 16 and 18). A higher sorbitol concentration in the media can effectively suppress protein aggregation in the periplasmic space during protein production[229]. This is because the increased osmotic pressure stabilizes the native structure of the protein. Several factors have a significant impact on protein expression and solubility, including the post-induction temperature, optical density (OD) of the culture, and duration of the induction[230].

A lower induction temperature is generally beneficial for recombinant protein production[231], [224], hence an induction temperature of 26°C was used in this study. This is because it triggers an energy conservation response that reduces the central carbon metabolism, resulting in a slower growth rate[224]. The expression of recombinant proteins imposes a metabolic burden on the host, leading to the accumulation of target proteins in insoluble aggregates called inclusion bodies[229]. Aggregation reactions are favored at higher temperatures due to the temperature-dependent nature of hydrophobic interactions between amino acids[231]. By lowering the induction temperature, protein aggregation can be minimized [232]. The optical density of the culture is also an important factor to consider, as cultures with high cell densities may not be ideal for protein production. At high cell densities, metabolic activity decreases due to various factors such as nutrient limitations, acetate production, reduced availability of dissolved oxygen, and elevated carbon dioxide levels, which ultimately impede recombinant gene expression[233]. Moreover, high temperatures can increase the likelihood of plasmid loss due to the faster growth rate[224].

The duration of the induction is crucial as well, as prolonged incubation can lead to protein aggregation. Many studies have adopted a standard induction duration of 16 hours. However, for certain proteins, an extended induction period at a low temperature may be beneficial[231]. Barth *et al*. (2000) demonstrated that by extending the induction duration, they were able to accumulate 95% functional proteins, compared to standard conditions where less than 10% functional protein was obtained[218]. In contrast, Mukherjee *et al.*,2004 showed that *E. coli* cells could secrete 90% of a recombinant single-chain antibody fragment (scFv) fused to a *Pel*B signal sequence[234]. SDS-PAGE analysis confirmed the high level of recombinant protein expression in their study. Based on the results of these studies, it further supports the notion that the periplasmic space of *E. coli* is an optimal location for recombinant protein production when selecting a bacterial expression system[218], [234]. However, it should be noted that the purification of proteins from the periplasmic space remains challenging[235].

5.4.2 Protein purification

Several unanticipated challenges were faced during this process. Achieving the highest yield of the target protein requires a balanced approach to purification, considering parameters such as purification speed, recovery rate, capacity, and resolution [88]. In this study, adjustments to these parameters were necessary as the initial purification attempts did not yield satisfactory amounts of the target recombinant proteins. For this study, immobilized metal affinity chromatography (IMAC) purification was used as a first step into purification. IMAC depends on the interaction between a transition metal ion (e.g., Co2+, Ni2+, Cu2+, and Zn2+) immobilized on a matrix and a specific amino acid side chain[236]. These specific amino acids can be genetically fused to the target protein, resulting in the expression of a "tag" on the protein. Various affinity tags, such as the Histidine tag (His-tag), Arg-tag, glutathione S-transferase (GST) tag, and Strep-tag II, are available for this purpose[237]. In this study, a His-tag was employed for target protein purification due to its advantages over other affinity tags. Firstly, the His-tag can be easily added to the protein of interest, typically at the N- or C-terminus during genetic engineering. His tags are commonly preferred due to their small size and minimal disruption to the function of the target protein compared to other affinity tags[237]. Histidine exhibits the strongest interaction with the immobilized metal matrices, as the electron donor groups on the histidine imidazole ring readily coordinate with the immobilized transition metal[238], [236]. Additionally, a poly-His-tag can be eluted under mild conditions from the IMAC resin, allowing the target protein to retain its biological function[236]. However, the His-tag affinity system has certain disadvantages, such as the nonspecific binding of proteins to the IMAC column[236]. In some cases, alternative affinity tag systems have demonstrated higher degrees of enrichment for the tagged protein compared to poly-His-tag systems. For instance, biotinylated-accepting domain affinity tags have been shown to provide a higher yield of the target protein than poly-His-tag affinity tags[239], [240]. Overcoming this challenge was a significant difficulty in this study, but certain parameters were modified to achieve the best possible yield.

During the purification process, impurities with similar properties to the target protein can hinder the yield of the purified target protein. Using the poly-His-tag affinity tag for purification presents

a particular concern, as some cellular proteins contain two or more adjacent histidine residues, which can bind to the IMAC matrix and coelute with the target protein, resulting in contamination of the final product[238], [241]. This could be the cause of unwanted bands that were observed in Figures 15 and 17, post-IMAC purification. Studies suggest that the inclusion of 10 mM 2-mercaptoethanol in the loading, washing, or elution buffer may help address these issues[236].

In this study, adjustments were made to parameters such as purification speed, recovery rate, capacity, and resolution to improve the yield of the target protein.

Another factor that may contribute to the coelution of non-specific proteins is nonspecific hydrophobic interactions with the IMAC matrix. To mitigate this, low levels of non-ionic detergents like Triton X-100 or Tween 20 can be added to the buffers to reduce the interactions of non-specific proteins without affecting the binding of the target protein to the IMAC matrix[242]. Additionally, the addition of salt (500mM NaCl), glycerol (20%), or low levels of ethanol (20%) can help minimize the binding of hydrophobic non-specific proteins to the IMAC matrix[241]. Including low concentrations of imidazole (20mM to 50mM) in the binding or wash buffer is also recommended to reduce the coelution of non-specific proteins with the target protein. However, in this study, the use of the non-ionic detergent Triton X-100 did not produce the desired results[241]. The combination that resulted in the highest purity consisted of a binding buffer containing 300mM NaCl, 10% glycerol, 100mM Tris-HCl, and 150mM imidazole, along with a wash buffer comprising 20mM $NaPO_3$, 500mM NaCl, and 40mM imidazole[243]. The higher concentration of imidazole in the binding buffer, compared to other studies, was necessary due to the elevated levels of contaminating proteins. It was observed that when the imidazole concentration exceeded 150mM, the target protein failed to bind to the IMAC matrix[244]. Thus, the inclusion of 150 mM imidazole in the binding buffer significantly reduced the presence of non-specific proteins during the purification process.

The choice of metal used in IMAC is crucial as different metals possess varying binding capacities with His-tag proteins. The poly-His-tag on the target protein can specifically bind to the metal chelates present in the IMAC matrix, enabling the capture of the target protein from the cell

lysate[245]. However, IMAC resins generally have lower binding capacities compared to other chromatography resins, leading to the need for additional chromatography steps to complete the purification process[246]. Studies have demonstrated that using IMAC agarose beads with a larger diameter can yield a higher quantity of the target protein during chromatography[246]. In this study, a 5mL IMAC column was utilized to provide maximum surface area for the target protein to bind to the matrix.

An investigation on the effect of charging the resin with different metal ions, including Ni2+, Co2+, Zn2+, Cu2+, Mg2+, Mn2+, and Fe2+ showed that resins charged with Ni2+, Co2+, Zn2+, or Cu2+ exhibited a higher binding capacity at 10% breakthrough compared to pre-charged Ni2+ resin. Conversely, resins charged with Mg2+, Mn2+, and Fe2+ demonstrated lower binding capacities in comparison to those charged with Ni2+, Co2+, Zn2+, and Cu2+. The breakthrough profiles were examined on IMAC 6 Sepharose columns in their study[246].

The Co2+ was selected as the metal for IMAC in this particular study, despite its weak binding to tagged proteins. This may appear counterintuitive; however, the rationale behind using Co2+ is to reduce the presence of contaminating proteins. The target protein carries a poly-Histidine-tag consisting of 10 histidine residues, which increases the likelihood of binding to the Co2+ resin compared to nonspecific proteins. Co2+ is sometimes used as an alternative to Ni2+ since Ni2+ exhibits a strong binding affinity to histidine-bearing proteins[247]. In contrast, the literature suggests that Cu2+ is commonly employed for purifying untagged proteins. Cu2+ has a robust binding capability with a wide range of proteins, which would be detrimental when the objective is to isolate a specific protein from a mixture of proteins[236]. The accessibility of the His tag to the IMAC resin can be hindered by the folding of the protein, resulting in the occlusion of the tag[236]. This is one of the many hurdles faced during protein purification that can however be addressed by carrying out the purification under denaturing conditions.

The selection of a suitable purification strategy for a target protein depends primarily on its physiochemical properties and the desired level of purification[236]. In this study, IMAC was chosen as the initial purification step due to its effectiveness in purifying target proteins from

crude cell lysate[248]. Following IMAC purification, additional chromatography techniques such as ion exchange or size exclusion can be employed for further purification[241]. Compared to other affinity-based protein purification methods, the use of IMAC offers a rapid and cost-effective approach. The IMAC purification procedure followed the protocol described by Barth et al. (2000) [218]. The cell lysate was prepared in a buffer at pH 8 and carefully loaded onto the IMAC column, allowing sufficient time for the target protein to strongly chelate to the metal within the column. The slightly basic pH was chosen to inhibit protease activity and maintain protonation of the histidine residues for optimal binding. To remove weakly bound non-specific proteins, the column was washed with a wash buffer containing imidazole (10-50mM), which increased the stringency of the wash. Alternatively, a lower pH buffer could be used for washing to remove non-specific protein binding. The addition of agents like 2-mercaptoethanol in the wash buffer could aid in the removal of non-specific proteins. The target protein could be eluted either by lowering the pH inside the column to disrupt the interaction between histidine and the metal or by using imidazole as a competitive eluent for the bound poly-His-tag protein. Based on these principles, the IMAC purification procedure was designed, maintaining an alkaline pH of 8 for all buffers, washing with imidazole to remove non-specific protein binding, and eluting the target protein using a high concentration of imidazole (500mM). As a final polishing step, size exclusion chromatography was employed to eliminate any remaining contaminants from target recombinant immunotoxins.

5.5. Functional activity of rITs in antigen-positive TNBC cancer cell lines

5.5.1. Binding analysis Anti-His PE-labeled recombinant immunotoxins on a TNBC cell line

Breast cancer management relies heavily on early screening and detection and accurate diagnosis is crucial for determining prognosis and delivering optimal therapy, especially for aggressive types like triple-negative breast cancers (TNBCs).)[39][249]. Traditionally, TNBC diagnosis involves immunohistochemistry (IHC) to assess hormone receptors (ER, PR) and HER2 status[40]. However, clinical practice often combines morphological imaging and IHC. TNBCs present a challenge in imaging due to their limited reports on imaging features. Mammography is the most common screening test that enables a quite early detection of breast cancers. However, it is

insufficient for diagnosing TNBCs, and ultrasound (an alternative) also shows higher sensitivity but lacks enduring diagnostic potential and may encounter benign features in TNBC lesions. Both ultrasound and mammography have limitations in visualizing intratumoral characteristics like necrosis and fibrosis, which are common in TNBCs.

While gene-expression profiling has transformed our understanding of breast cancer, its practical benefits in the clinical setting are limited. However, molecular breast cancer markers, such as ER, PR, HER2, cytokeratin 5/6, and EGFR status, can be used to classify TNBC subtypes based on prognosis and response to specific treatments[250]. Molecular biomarkers for TNBC have the potential to expedite the development of effective therapies and improve patient outcomes[251]. Given the complex nature of TNBC, a combination of targeted approaches will likely be necessary to make significant progress in treating this aggressive disease.

Consequently, through the generation of rITs targeting CD90, LGR5 and EpCAM, this study has a long-term potential to contribute to molecular biomarker-based TNBC patient selection. Upon successful expression of these full-length recombinant immunotoxins, as confirmed by SDS-PAGE and Western blot analysis (Figures 16 and 18), they were assessed for TNBC (MDA-MB-468) cell surface binding analysis by confocal microscopy. In this analysis, approximately 20 µg of each of the three ETA-based rITs was labelled with Anti-His PE antibody. Anti-His PE is an antibody conjugated to the fluorochrome Phycoerythrin (PE) that specifically recognizes and binds to a Poly Histidine (6X or 10X) tag [241].

The purified His-tagged rIT were independently incubated with anti-His PE antibody to recognize and bind specifically to their 10X His tag on their N-terminus. This combination forms a stable complex between the His tag and the anti-His PE antibody, allowing for the detection and quantification of the rITs bound to the TNBC cells [241], as demonstrated by the results in Figure 19. The bound anti-His PE antibody emits fluorescence when excited by the appropriate laser wavelength, which can be detected by confocal microscopy. This fluorescence signal is used to determine the presence and abundance of the His-tagged rIT on the surface of the cells [241], [242]. It was used to label MDA-MB-468 cells, a TNBC cell line that expresses the CD90, EpCAM and LGR5 cell surface receptors (CSRs).

The behaviour of cancer cell lines in culture determines the most suitable method for binding analysis. For example, cells that grow in suspension and adherent cells can be viewed by flow cytometry and confocal microscopy respectively.

Confocal microscopy has proven to be a useful tool for visualizing interactions between antibodies and their target receptors[252], as illustrated in the findings of this study (Figure 19). It is particularly effective for analyzing sub-cellular features in uniform samples but has limitations when it comes to detecting weak fluorescent signals or analyzing large numbers of cells in heterogeneous samples[253]. To enhance the sensitivity of confocal microscopy, one can spend more time imaging a single cell, but this may lead to photobleaching in areas outside the focal plane and compromise the image quality[254]. It is crucial in a confocal microscopy experiment to choose the correct technique, objective, fluorophores, mounting medium, and optical components to achieve the best images[253]. An alternative method for assessing the surface binding of the rITs is flow cytometry. This is mostly recommended when the cancer cell lines are growing in suspension.

Flow cytometry prioritizes high acquisition rates and fluorescence sensitivity over imaging capabilities, providing numerical measurements of fluorescence intensity for each detected cell based on forward and side scatter signals[255]. The forward scatter reflects cell size, while the side scatter indicates cell granularity[256]. The key advantage of flow cytometry in contrast to confocal microscopy is its ability to rapidly analyze large cell populations, allowing for high-throughput analysis of cell morphology and multichannel fluorescence imaging on a single-cell level[257]. In contrast to confocal microscopy, which focuses on a limited subset of cells, flow cytometry offers a suitable alternative for the comprehensive analysis of heterogeneous cell populations.

In this study MDA-MB-468 TNBC cell lines were utilized to evaluate the binding capacity of the rITs, yielding successful results. Interestingly, the accumulation of the rITs on the cancer cells showed that the potential for internalization of the rITs (Figure 19). However, future investigations should incorporate additional cell lines such as MD-MB-23. Researchers using the

precision medicine approach for cancer are eagerly searching for more realistic, cost-effective, and timely tumour models to aid drug development and precision oncology[258]. Ultimately, the focus should shift towards utilizing patient-derived samples, as cell lines do not fully imitate the diverse nature of human tumours. Established cell lines are derived from specific subsets of tumours that can grow under laboratory conditions, which introduces limitations due to the lack of *in vitro* adaptation and potential disparities between experimental and clinical outcomes[259]. Two alternatives to cell lines are patient-derived tumour xenografts (PDTX) and genetically engineered mouse tumour (GEMT) models[258]. These alternatives offer advantages over cell lines as they maintain the characteristics of the original tumour, including tumour heterogeneity and complexity. Despite these limitations, cell lines are however easy to use and cost effective especially for *in vitro* proof of concept studies like this. In addition, they are also providing a pure population of cells, allowing for reproducibility of the results[260]. While the application of cell validation techniques goes beyond the mandate of this master's thesis, it is hypothesized that a better understanding of receptor dynamics within tumour cells (and the consequences thereof) might be contributory to future TNBC therapeutic predictions.

5.5.2. Cytotoxicity analysis

Recombinant immunotoxins are targeted anticancer therapeutics that use bacterial toxins to selectively kill cancer cells[143]. These have faced challenges in their development for solid tumor malignancies due to issues related to immune response and limited effectiveness[261]. Advancements in protein engineering techniques have led to the creation of a new generation of immunotoxin molecules with reduced immunogenicity and lower non-specific toxicity[170], as partially supported by the findings of this master's project. The development of these improved immunotoxins has reignited enthusiasm in the field, offering a potentially valuable addition to the arsenal of targeted therapies.

Upon confirmation of binding of the developed rITs to the TNBC MD-MB-468 cancer cells (Figure 19), cytotoxicity analysis was performed on the same TNBC cell line (MDA-MB-468). To evaluate the cytotoxicity of the rITs, an XTT colorimetric assay was employed. This assay measures the

metabolic activity of cells by assessing a biochemical marker. Specifically, the XTT assay gauges cell proliferation by monitoring the reduction of tetrazolium salt XTT, leading to the formation of orange-colored formazan compounds. The intensity of the orange formazan color can be quantified using a spectrophotometer. The IC50 values revealed that the MDA-MB-468 cell line demonstrated greater sensitivity to wt ETA-based rITs compared to dETA-based rITs, except for the case of CD90 targeting rITs. This suggests that the mutations present in the toxin domain influence the enzymatic activity of the dETA-based rITs. However, the case of CD90 indicates that the deimmunized ETA may have restored the enzymatic activity ETA, subject to further investigation. This study investigated the cell-killing potential of three wild-type ETA-based rITs against three corresponding deimmunized versions, dETA-base rITs.

In a study by Hassan *et al*., a PE38-based rIT called SS1P was developed and tested in a phase 1 clinical trial for targeting the mesothelin receptor[172]. However, limited therapeutic effects were observed as 90% of patients developed neutralizing antibodies against the bacterial toxin after one treatment cycle[172]. This induction of immunogenicity in patients was the major drawback of this rIT. Other epitopes and protease cleavage sites that decreased the effectiveness of intracellular processing were abolished when the majority of domain II was deleted. With equivalent *in vitro* activity to PE38, less reactivity with human antisera, and less nonspecific toxicity in rodent models in vivo, this new-generation PE (PE24) enables the safe administration of 5- to 10-fold higher dosages.

In conjunction with Roche, a novel mesothelin-targeted rIT known as RG7787 was created using the PE24 platform, targeting TNBC and gastric cancers [215]. Alewene *et al* (2015) evaluated the SS1P rIT, as well as its PE24 derivatives, SS1-LR (wild-type) and RG7787 (dETA), on mesothelin-expressing cell lines of triple-negative breast cancer (TNBC) and gastric cancer. In TNBC cell lines HCC70 and SUM149, HCC70 cells exhibited higher sensitivity to SS1-LR (IC50 19.6 pM) compared to RG7787 (IC50 45.2 pM). Similarly, the SUM149 cell line demonstrated the same trend, with SS1-LR (IC50 30.2 pM) being more effective than RG7787 (IC50 64.8 pM). These results indicated that the deimmunized PE24 (RG7787) was less active than wild-type PE24 (SS1-LR). Notably, despite SUM149 cells overexpressing mesothelin to a greater extent than HCC70 cells, HCC70 cells exhibited a more potent response. In the case of gastric cancer cell lines, three out of four

cell lines showed higher sensitivity to SS1P than RG7787. Among the MKN7, MKN28, MKN45, and MKN74 cell lines, MKN45 cells were more sensitive to RG7787 (IC50 6.8 pM) compared to SS1P (IC50 37.1 pM), while the other cell lines demonstrated greater sensitivity to SS1P. SS1P achieved IC50 values ranging from 5.5 pM to 37.1 pM, while RG7787 showed IC50 values ranging from 75.6 pM to >1200 pM. These findings demonstrated that RG7787 did not consistently exhibit similar or improved enzymatic activity compared to its wild-type counterpart. Although RG7787 was found to have a longer half-life and less immunogenicity, it also showed reduced enzymatic activity and cytotoxicity compared to its wild type.

In consequence, our research group, in collaboration with Professor Paolo Carloni used high supercomputer simulations to identify potential mutations on RG7787 within the B cell epitopes (R427A, R456A, D463A, R467A, R490A, R505A and R538A), including one that activates the enzyme (R490A). The computer simulations proposed R456T and R456C as possible point mutations that could restore the wild-type enzymatic activity of wt ETA while retaining the reduced immunogenicity. The R456T-containing dETA was investigated in this master's project.

The wt ETA was successfully fused with three scFv constructs that target EpCAM, CD90, and LGR5 individually. Each of these constructs was then fused to the dETA(R456T). A total of six recombinant immunotoxins were developed in this study. The plasmids encoding for the expression of the desired rITs were successfully cloned into a pMT expression vector. They were successfully expressed in the periplasm of *E.coli* BL21 (DE3) and purified by IMAC and SEC as illustrated in section 4. Two ETA-based rITs targeting LGR5 and EpCAM demonstrated a strong targeted cell-killing effect on TNBC (MDA-MB-468) cells compared to their corresponding dETA-based rITs. The opposite phenomenon was observed in the CD90 targeting rITs, where the dETA version exhibited more cell-killing potential than the wt ETA version. The differences between the published RG7787 variants and wt were around 2-fold less effective for constructs targeting mesothelin[262], and similarly less effective for the EpCAM and LGR5 (Figure 20) targeting constructs used in this study. In the case of LGR5 and EpCAM, (Figure 20 I-L) targeting rITs, the difference shown was 27-fold and 3-fold difference noted for the published RG7787. Another MSc student's preliminary results demonstrated a less than 2-fold difference for the dETA-based constructs targeting CD90, EpCAM and LGR5, on a cervical cancer Caski cell line confirming a

trend of the constructs to demonstrate partially recovered enzymatic activity in comparison to the original RG7787 mutant.

In the case of CD90 (Figure 20 E-H), the targeting rITs demonstrated the opposite phenomenon as the results support the hypothesis generated from computer simulations regarding the R456T mutant. However, this was different from the findings of Marc, who compared cytotoxicity of these similar rITs targeting CD90, on cervical cancer cell line (CasKi). This difference may have been caused by differential upregulation of CSRs by different pathophysiological mechanisms that might lead to different responses to treatment between different CD90 positive tumours. In contrast to the published RG7787 variants and wt ETA version, the RG7787 version was >2-fold less effective for constructs targeting mesothelin, unlikethe constructs targeting CD90 that demonstrated approximately 3-fold improvement of the dETA version as compared to the wt ETA version. This might indicate an improved enzymatic activity of the R456T mutation compared to the original dETA version which would need to be confirmed on further cervical cancer cell lines [262]. Although the majority of the dETA-based rITs were not as potent towards the target TNBC cells, the results suggest that both ETA-based and dETA-based rITs are capable of targeted cell killing. Further investigations using different TNBC cell lines should be conducted to determine if the dETA-based rITs exhibit similar or enhanced cytotoxic activity compared to the ETA-based rITs. Additionally, future studies should involve mouse models to evaluate the immunogenicity of both ETA-based and dETA-based rITs.

CHAPTER 6: CONCLUSION

The tri modality therapy (Chemotherapy, surgery, and radiation) is the primary method of breast cancer treatment in modern day medicine[263]. However, adverse side effects of these treatments have been reported, leading researchers to question their true benefits in cancer management. These treatment methods therapies often cause significant damage to not only

cancer cells but also normal cells, including immune cells. As a result, patients experience cumulative detrimental effects that hinder their recovery and contribute to overall debilitation. To alleviate the undesirable consequences of traditional therapies, molecular-targeted cancer therapies have been developed. One such approach is armed antibody therapy, which has been devised to specifically target cancer cells, for example, rITs. However, the success rate of these targeted therapies has been limited thus far.

This study was able to generate and characterize an antibody protein format, rITs, that can be used for therapeutic and supported by companion diagnosis in TNBC and other cancers. During the study, successful cloning of anti-CD90(scFv)-ETA and anti-CD90(scFv)-dETA was achieved. These two cloned recombinant immunotoxins (rITs) were successfully expressed in the periplasm of *E. coli* BL21 using osmotic stress, in the presence of compatible solutes. The study demonstrated the potential of the *E. coli* BL21 periplasmic space as a suitable environment for generating complex and difficult to produce recombinant proteins, thanks to its nonreducing nature. Moreover, the periplasmically expressed full-length rITs were successfully purified using a combination of immobilized metal affinity chromatography (IMAC) and size exclusion chromatography (SEC). The purified rIT, anti-CD90-ETA, was labelled with anti-His PE and used for confocal imaging analysis and exhibited strong binding affinity to the MDA-MB-468 TNBC cell line. Cytotoxicity studies were conducted upon positive binding results. In contrast, both anti-CD90-ETA and anti-CD90-dETA rITs demonstrated potent cytotoxic effects against the MDA-MB-468 TNBC cell line. After the successful establishment of all these methods using CD90 targeting ETA and dETA-based rITs, similar methods and applications were used to successfully demonstrate the activity of additional ETA and dETA-based rITs targeting LGR5 and EpCAM CSRs. Interestingly, CD90-dETA demonstrated higher cytotoxicity than CD90-ETA, supporting the hypothesis that the point mutations introduced by MB&I in collaboration with Professor Paolo Carloni may potentially restore the enzymatic activity of the dETA-version. However, the LGR5 and EpCAM targeting ETA-based rITs showed a different phenomenon, exhibiting higher cytotoxicity than their corresponding dETA versions. This could be attributed to the functions of these CSRs on the signalling pathways for the survival of the cancer cells. Presumably, CD90 plays

a key role in the survival of TNBC cancer cells than LGR5 and EpCAM does. These results were also used to further enhance the understanding of this therapeutic approach for TNBC.

Future studies should incorporate more TNBC cell lines to further evaluate the binding capability and potency against TNBC patient tissue samples. Assessing the immunogenicity of ETA-based and dETA-based rITs in *ex vivo* patient derived models (previously Pseudomonas aeruginosa infected) would provide valuable insights for the clinical development of these rITs. In the context of TNBC, the primary objective should be preventing relapse in patients. Consequently, the results of this thesis demonstrate that this treatment modality may serve as a viable alternative for patients in advanced stages of TNBC.

In conclusion, the findings in this work also show rITs' potential for clinical application. Firstly, when labelled with Anti-His PE, the rITs exhibited specific binding activity *in vitro*, showing their potential for TNBC immunodiagnostic use. Secondly, the ability of ETA and dETA toxins to specifically kill TNBC antigen-positive tumour cells was shown, indicating targeted therapeutic potential. The rITs investigated in this study will be used in targeted therapy practice in the future to reach TNBC tumours.

CHAPTER 7: REFERENCES

[1] "the-global-breast-cancer-initiative-flyer-june-2022 (1)".

[2] "Global Cancer Observatory." https://gco.iarc.fr/causes/ (accessed Jan. 11, 2023).

[3] D. Kashyap *et al.*, "Global Increase in Breast Cancer Incidence: Risk Factors and Preventive Measures," *Biomed Res Int*, vol. 2022, pp. 1–16, Apr. 2022, doi: 10.1155/2022/9605439.

[4] O. M. Ginsburg, “Breast and cervical cancer control in low and middle-income countries: Human rights meet sound health policy,” *J Cancer Policy*, vol. 1, no. 3–4, pp. e35–e41, Sep. 2013, doi: 10.1016/j.jcpo.2013.07.002.
[5] “Breast cancer | Definition, Causes, Symptoms, & Treatment | Britannica.” https://www.britannica.com/science/breast-cancer (accessed Dec. 15, 2022).
[6] C. Katsura, I. Ogunmwonyi, H. K. Kankam, and S. Saha, “Breast cancer: presentation, investigation and management,” *Br J Hosp Med*, vol. 83, no. 2, pp. 1–7, Feb. 2022, doi: 10.12968/hmed.2021.0459.
[7] A. Sudhakar, “History of Cancer, Ancient and Modern Treatment Methods,” *J Cancer Sci Ther*, vol. 01, no. 02, pp. i–iv, 2009, doi: 10.4172/1948-5956.100000e2.
[8] “Types of Breast Cancer.” https://www.breastcancer.org/types?gclid=Cj0KCQiAn4SeBhCwARIsANeF9DIHIkksijVKQC2VrPetmZ2KH-oecZ7iylKjXVxX8zDkQ4pvK1iA_MgaAoqfEALw_wcB (accessed Jan. 13, 2023).
[9] L. M. Gannon, M. B. Cotter, and C. M. Quinn, “The classification of invasive carcinoma of the breast,” *Expert Rev Anticancer Ther*, vol. 13, no. 8, pp. 941–954, Aug. 2013, doi: 10.1586/14737140.2013.820577.
[10] R. J. Lee, L. A. Vallow, S. A. McLaughlin, K. S. Tzou, S. L. Hines, and J. L. Peterson, “Ductal Carcinoma In Situ of the Breast,” *Int J Surg Oncol*, vol. 2012, pp. 1–12, 2012, doi: 10.1155/2012/123549.
[11] “What Is Breast Cancer? | CDC.” https://www.cdc.gov/cancer/breast/basic_info/what-is-breast-cancer.htm (accessed Jan. 10, 2023).
[12] J. Sariego, “Breast Cancer in the Young Patient,” *Am Surg*, vol. 76, no. 12, pp. 1397–1400, Dec. 2010, doi: 10.1177/000313481007601226.
[13] B. Weigelt and J. S. Reis-Filho, “Histological and molecular types of breast cancer: is there a unifying taxonomy?,” *Nat Rev Clin Oncol*, vol. 6, no. 12, pp. 718–730, Dec. 2009, doi: 10.1038/nrclinonc.2009.166.
[14] “Breast Anatomy - StoryMD.” https://storymd.com/journal/mrkdbaduzw-breast-anatomy/page/nprlvtberle-breast-anatomy (accessed Jan. 12, 2023).
[15] A. Javed and A. Lteif, “Development of the Human Breast,” *Semin Plast Surg*, vol. 27, no. 01, pp. 005–012, May 2013, doi: 10.1055/s-0033-1343989.
[16] A. Javed and A. Lteif, “Development of the Human Breast,” *Semin Plast Surg*, vol. 27, no. 01, pp. 005–012, May 2013, doi: 10.1055/s-0033-1343989.
[17] C. I. Li, D. J. Uribe, and J. R. Daling, “Clinical characteristics of different histologic types of breast cancer,” *Br J Cancer*, vol. 93, no. 9, pp. 1046–1052, Oct. 2005, doi: 10.1038/sj.bjc.6602787.
[18] M. Ahuja *et al.*, “Primary breast sarcoma: A case series.,” *Indian J Pathol Microbiol*, vol. 65, no. 1, pp. 152–156, 2022, doi: 10.4103/IJPM.IJPM_1315_20.
[19] G. Lissidini *et al.*, “Malignant phyllodes tumor of the breast: a systematic review,” *Pathologica*, vol. 114, no. 2, pp. 111–120, Apr. 2022, doi: 10.32074/1591-951X-754.
[20] “23.5: Breasts - Biology LibreTexts.” https://bio.libretexts.org/Bookshelves/Human_Biology/Book%3A_Human_Anatomy_Lab/23%3A_The_Reproductive_System_(Female)/23.05%3A_Breasts (accessed Jan. 13, 2023).
[21] H. R. Brewer, M. E. Jones, M. J. Schoemaker, A. Ashworth, and A. J. Swerdlow, “Family history and risk of breast cancer: an analysis accounting for family structure,” *Breast*

Cancer Res Treat, vol. 165, no. 1, pp. 193–200, Aug. 2017, doi: 10.1007/s10549-017-4325-2.

[22] B. A. J. Ponder, "Genetic predisposition to breast cancer," *The Breast*, vol. 6, no. 5, p. 323, Oct. 1997, doi: 10.1016/S0960-9776(97)90052-7.

[23] Y. Feng *et al.*, "Breast cancer development and progression: Risk factors, cancer stem cells, signaling pathways, genomics, and molecular pathogenesis," *Genes Dis*, vol. 5, no. 2, pp. 77–106, Jun. 2018, doi: 10.1016/j.gendis.2018.05.001.

[24] T. B. Pearlstein, G. A. Bachmann, H. A. Zacur, and K. A. Yonkers, "Treatment of premenstrual dysphoric disorder with a new drospirenone-containing oral contraceptive formulation," *Contraception*, vol. 72, no. 6, pp. 414–421, Dec. 2005, doi: 10.1016/j.contraception.2005.08.021.

[25] Y.-S. Sun *et al.*, "Risk Factors and Preventions of Breast Cancer," *Int J Biol Sci*, vol. 13, no. 11, pp. 1387–1397, 2017, doi: 10.7150/ijbs.21635.

[26] C.-X. Deng, "BRCA1: cell cycle checkpoint, genetic instability, DNA damage response and cancer evolution," *Nucleic Acids Res*, vol. 34, no. 5, pp. 1416–1426, Mar. 2006, doi: 10.1093/nar/gkl010.

[27] H. Sánchez *et al.*, "Architectural plasticity of human BRCA2–RAD51 complexes in DNA break repair," *Nucleic Acids Res*, vol. 45, no. 8, pp. 4507–4518, May 2017, doi: 10.1093/nar/gkx084.

[28] N. Petrucelli, M. B. Daly, and T. Pal, "BRCA1- and BRCA2-Associated Hereditary Breast and Ovarian Cancer," *GeneReviews®*, May 2022, Accessed: Jan. 15, 2023. [Online]. Available: https://www.ncbi.nlm.nih.gov/books/NBK1247/

[29] B. N. Peshkin, M. L. Alabek, and C. Isaacs, "BRCA1/2 MUTATIONS AND TRIPLE NEGATIVE BREAST CANCERS," *Breast Dis*, vol. 32, no. 0, pp. 25–33, 2010, doi: 10.3233/BD-2010-0306.

[30] M. Galiè, "RAS as Supporting Actor in Breast Cancer," *Front Oncol*, vol. 9, Nov. 2019, doi: 10.3389/fonc.2019.01199.

[31] M. M. Moasser, "The oncogene HER2; Its signaling and transforming functions and its role in human cancer pathogenesis," *Oncogene*, vol. 26, no. 45, p. 6469, Oct. 2007, doi: 10.1038/SJ.ONC.1210477.

[32] A. E. Karnoub *et al.*, "Mesenchymal stem cells within tumour stroma promote breast cancer metastasis," *Nature*, vol. 449, no. 7162, pp. 557–563, Oct. 2007, doi: 10.1038/nature06188.

[33] A. L. Siu, "Screening for Breast Cancer: U.S. Preventive Services Task Force Recommendation Statement," *Ann Intern Med*, vol. 164, no. 4, pp. 279–296, Feb. 2016, doi: 10.7326/M15-2886.

[34] C. M. Ronckers, C. A. Erdmann, and C. E. Land, "Radiation and breast cancer: a review of current evidence," *Breast Cancer Research*, vol. 7, no. 1, p. 21, Jan. 2005, doi: 10.1186/BCR970.

[35] M. Awatef, G. Olfa, M. Kacem, L. Sami, H. Makram, and B. A. Slim, "Association between body mass index and risk of breast cancer in Tunisian women," *Ann Saudi Med*, vol. 31, no. 4, p. 393, Jul. 2011, doi: 10.4103/0256-4947.83211.

[36] J. A. McDonald, A. Goyal, and M. B. Terry, "Alcohol Intake and Breast Cancer Risk: Weighing the Overall Evidence," *Curr Breast Cancer Rep*, vol. 5, no. 3, pp. 208–221, Sep. 2013, doi: 10.1007/S12609-013-0114-Z.

[37] J. H. Park, J. H. Moon, H. J. Kim, M. H. Kong, and Y. H. Oh, "Sedentary Lifestyle: Overview of Updated Evidence of Potential Health Risks," *Korean J Fam Med*, vol. 41, no. 6, p. 365, Nov. 2020, doi: 10.4082/KJFM.20.0165.
[38] R. A. Smith, S. W. Duffy, R. Gabe, L. Tabar, A. M. F. Yen, and T. H. H. Chen, "The randomized trials of breast cancer screening: what have we learned?," *Radiol Clin North Am*, vol. 42, no. 5, pp. 793–806, Sep. 2004, doi: 10.1016/J.RCL.2004.06.014.
[39] C. Coleman, "Early Detection and Screening for Breast Cancer," *Semin Oncol Nurs*, vol. 33, no. 2, pp. 141–155, May 2017, doi: 10.1016/J.SONCN.2017.02.009.
[40] M. G. O'Rourke and P. J. Day, "The diagnosis of breast cancer," *Medical Journal of Australia*, vol. 153, no. 6, pp. 364–364, Sep. 1990, doi: 10.5694/j.1326-5377.1990.tb136967.x.
[41] "Accreditation | American College of Radiology." https://www.acr.org/Clinical-Resources/Accreditation (accessed Jan. 17, 2023).
[42] R. Shah, "Pathogenesis, prevention, diagnosis and treatment of breast cancer," *World J Clin Oncol*, vol. 5, no. 3, p. 283, 2014, doi: 10.5306/wjco.v5.i3.283.
[43] M. A. Roubidoux, J. E. Bailey, L. A. Wray, and M. A. Helvie, "Invasive Cancers Detected after Breast Cancer Screening Yielded a Negative Result: Relationship of Mammographic Density to Tumor Prognostic Factors," *Radiology*, vol. 230, no. 1, pp. 42–48, Jan. 2004, doi: 10.1148/radiol.2301020589.
[44] G. Lip, N. Zakharova, S. Duffy, M. Gillan, and F. Gilbert, "Breast density as a predictor of breast cancer risk," *Breast Cancer Research*, vol. 12, no. S3, p. P1, Oct. 2010, doi: 10.1186/bcr2654.
[45] S. M. McKinney *et al.*, "International evaluation of an AI system for breast cancer screening," *Nature*, vol. 577, no. 7788, pp. 89–94, Jan. 2020, doi: 10.1038/s41586-019-1799-6.
[46] K. M. Kelly, J. Dean, W. S. Comulada, and S. J. Lee, "Breast cancer detection using automated whole breast ultrasound and mammography in radiographically dense breasts," *Eur Radiol*, vol. 20, no. 3, pp. 734–742, Mar. 2010, doi: 10.1007/S00330-009-1588-Y.
[47] A. E. Giuliano, S. B. Edge, and G. N. Hortobagyi, "Eighth Edition of the AJCC Cancer Staging Manual: Breast Cancer," *Ann Surg Oncol*, vol. 25, no. 7, pp. 1783–1785, Jul. 2018, doi: 10.1245/S10434-018-6486-6/TABLES/2.
[48] G. Cserni, E. Chmielik, B. Cserni, and T. Tot, "The new TNM-based staging of breast cancer," *Virchows Archiv*, vol. 472, no. 5, pp. 697–703, May 2018, doi: 10.1007/s00428-018-2301-9.
[49] L. Caplan, "Delay in breast cancer: Implications for stage at diagnosis and survival," *Front Public Health*, vol. 2, no. JUL, p. 87, Jul. 2014, doi: 10.3389/FPUBH.2014.00087/BIBTEX.
[50] S. E. Singletary and F. L. Greene, "Revision of breast cancer staging: The 6th edition of theTNM classification," *Semin Surg Oncol*, vol. 21, no. 1, pp. 53–59, 2003, doi: 10.1002/ssu.10021.
[51] "Breast Cancer Tumor Size and Stage." https://www.verywellhealth.com/know-your-breast-tumor-size-4114640 (accessed Jun. 30, 2023).
[52] N. W. Wilkinson, A. Shahryarinejad, J. S. Winston, N. Watroba, and S. B. Edge, "Concordance with Breast Cancer Pathology Reporting Practice Guidelines," *J Am Coll Surg*, vol. 196, no. 1, pp. 38–43, Jan. 2003, doi: 10.1016/S1072-7515(02)01627-7.

[53] M. Solanki and D. Visscher, “Pathology of breast cancer in the last half century,” *Hum Pathol*, vol. 95, pp. 137–148, Jan. 2020, doi: 10.1016/j.humpath.2019.09.007.
[54] J. Li, Z. Chen, K. Su, and J. Zeng, “Clinicopathological classification and traditional prognostic indicators of breast cancer.,” *Int J Clin Exp Pathol*, vol. 8, no. 7, pp. 8500–5, 2015.
[55] “Bloom-Richardson Grading System.” https://www.datadictionary.nhs.uk/nhs_business_definitions/bloom-richardson_grading_system.html (accessed Jan. 18, 2023).
[56] T. O. Nielsen *et al.*, “Immunohistochemical and clinical characterization of the basal-like subtype of invasive breast carcinoma,” *Clinical Cancer Research*, vol. 10, no. 16, pp. 5367–5374, Aug. 2004, doi: 10.1158/1078-0432.CCR-04-0220.
[57] F. M. Blows *et al.*, “Subtyping of Breast Cancer by Immunohistochemistry to Investigate a Relationship between Subtype and Short and Long Term Survival: A Collaborative Analysis of Data for 10,159 Cases from 12 Studies”, doi: 10.1371/journal.pmed.1000279.
[58] C. Sotiriou *et al.*, “Breast cancer classification and prognosis based on gene expression profiles from a population-based study,” *Proc Natl Acad Sci U S A*, vol. 100, no. 18, p. 10393, Sep. 2003, doi: 10.1073/PNAS.1732912100.
[59] J. Li, Z. Chen, K. Su, and J. Zeng, “Clinicopathological classification and traditional prognostic indicators of breast cancer.,” *Int J Clin Exp Pathol*, vol. 8, no. 7, pp. 8500–5, 2015.
[60] J. J. Gao and S. M. Swain, “Luminal A Breast Cancer and Molecular Assays: A Review,” *Oncologist*, vol. 23, no. 5, p. 556, May 2018, doi: 10.1634/THEONCOLOGIST.2017-0535.
[61] A. Goldhirsch *et al.*, “Personalizing the treatment of women with early breast cancer: highlights of the St Gallen International Expert Consensus on the Primary Therapy of Early Breast Cancer 2013,” *Ann Oncol*, vol. 24, no. 9, pp. 2206–2223, Sep. 2013, doi: 10.1093/ANNONC/MDT303.
[62] F. Schettini *et al.*, “HER2-enriched subtype and pathological complete response in HER2-positive breast cancer: a systematic review and meta-analysis,” *Cancer Treat Rev*, vol. 84, p. 101965, Mar. 2020, doi: 10.1016/J.CTRV.2020.101965.
[63] P. Eroles, A. Bosch, J. Alejandro Pérez-Fidalgo, and A. Lluch, “Molecular biology in breast cancer: Intrinsic subtypes and signaling pathways,” *Cancer Treat Rev*, vol. 38, no. 6, pp. 698–707, Oct. 2012, doi: 10.1016/j.ctrv.2011.11.005.
[64] Y. Bando *et al.*, “Triple-negative breast cancer and basal-like subtype : Pathology and targeted therapy,” *The Journal of Medical Investigation*, vol. 68, no. 3.4, pp. 213–219, 2021, doi: 10.2152/jmi.68.213.
[65] E. A. Rakha, J. S. Reis-Filho, and I. O. Ellis, “Basal-Like Breast Cancer: A Critical Review,” *Journal of Clinical Oncology*, vol. 26, no. 15, pp. 2568–2581, May 2008, doi: 10.1200/JCO.2007.13.1748.
[66] C. M. Perou, “Molecular Stratification of Triple-Negative Breast Cancers,” *Oncologist*, vol. 16, no. S1, pp. 61–70, Jan. 2011, doi: 10.1634/theoncologist.2011-S1-61.
[67] P. Kumar and R. Aggarwal, “An overview of triple-negative breast cancer,” *Archives of Gynecology and Obstetrics 2015 293:2*, vol. 293, no. 2, pp. 247–269, Sep. 2015, doi: 10.1007/S00404-015-3859-Y.
[68] E. Montagna *et al.*, “Breast cancer subtypes and outcome after local and regional relapse,” *Annals of Oncology*, vol. 23, no. 2, pp. 324–331, Feb. 2012, doi: 10.1093/annonc/mdr129.

[69] W. D. Foulkes, I. E. Smith, and J. S. Reis-Filho, “Triple-Negative Breast Cancer,” *New England Journal of Medicine*, vol. 363, no. 20, pp. 1938–1948, Nov. 2010, doi: 10.1056/NEJMra1001389.

[70] G. J. Morris *et al.*, “Differences in breast carcinoma characteristics in newly diagnosed African–American and Caucasian patients,” *Cancer*, vol. 110, no. 4, pp. 876–884, Aug. 2007, doi: 10.1002/cncr.22836.

[71] K. R. Bauer, M. Brown, R. D. Cress, C. A. Parise, and V. Caggiano, “Descriptive analysis of estrogen receptor (ER)-negative, progesterone receptor (PR)-negative, and HER2-negative invasive breast cancer, the so-called triple-negative phenotype,” *Cancer*, vol. 109, no. 9, pp. 1721–1728, May 2007, doi: 10.1002/cncr.22618.

[72] R. Dent *et al.*, “Triple-Negative Breast Cancer: Clinical Features and Patterns of Recurrence,” *Clinical Cancer Research*, vol. 13, no. 15, pp. 4429–4434, Aug. 2007, doi: 10.1158/1078-0432.CCR-06-3045.

[73] B. D. Lehmann *et al.*, “Identification of human triple-negative breast cancer subtypes and preclinical models for selection of targeted therapies,” *Journal of Clinical Investigation*, vol. 121, no. 7, pp. 2750–2767, Jul. 2011, doi: 10.1172/JCI45014.

[74] A. M. Badowska-Kozakiewicz and M. P. Budzik, “Immunohistochemical characteristics of basal-like breast cancer.,” *Contemp Oncol (Pozn)*, vol. 20, no. 6, pp. 436–443, 2016, doi: 10.5114/wo.2016.56938.

[75] B. D. Lehmann and J. A. Pietenpol, “Identification and use of biomarkers in treatment strategies for triple-negative breast cancer subtypes,” *J Pathol*, vol. 232, no. 2, pp. 142–150, Jan. 2014, doi: 10.1002/path.4280.

[76] M. D. Burstein *et al.*, “Comprehensive Genomic Analysis Identifies Novel Subtypes and Targets of Triple-Negative Breast Cancer,” *Clinical Cancer Research*, vol. 21, no. 7, pp. 1688–1698, Apr. 2015, doi: 10.1158/1078-0432.CCR-14-0432.

[77] C. K. Anders and L. A. Carey, “Biology, Metastatic Patterns, and Treatment of Patients with Triple-Negative Breast Cancer,” *Clin Breast Cancer*, vol. 9, pp. S73–S81, Jun. 2009, doi: 10.3816/CBC.2009.s.008.

[78] L. A. Carey *et al.*, “The Triple Negative Paradox: Primary Tumor Chemosensitivity of Breast Cancer Subtypes,” *Clinical Cancer Research*, vol. 13, no. 8, pp. 2329–2334, Apr. 2007, doi: 10.1158/1078-0432.CCR-06-1109.

[79] A. M. Gonzalez-Angulo *et al.*, “Incidence and Outcome of *BRCA* Mutations in Unselected Patients with Triple Receptor-Negative Breast Cancer,” *Clinical Cancer Research*, vol. 17, no. 5, pp. 1082–1089, Mar. 2011, doi: 10.1158/1078-0432.CCR-10-2560.

[80] T. Shah and S. Guraya, “Breast cancer screening programs: Review of merits, demerits, and recent recommendations practiced across the world,” *J Microsc Ultrastruct*, vol. 5, no. 2, p. 59, 2017, doi: 10.1016/j.jmau.2016.10.002.

[81] O. Ginsburg *et al.*, “Breast cancer early detection: A phased approach to implementation,” *Cancer*, vol. 126, no. S10, pp. 2379–2393, May 2020, doi: 10.1002/cncr.32887.

[82] “Breast Surgeon New York | Surgical Oncology New York | Dr. DeRisi.” https://nybreasthealth.com/news/the-importance-of-early-detection-for-triple-negative-breast-cancer (accessed Jun. 18, 2023).

[83] T. J. Eberlein, “Race, Breast Cancer Subtypes, and Survival in the Carolina Breast Cancer Study,” *Yearbook of Surgery*, vol. 2007, pp. 304–305, Jan. 2007, doi: 10.1016/S0090-3671(08)70227-1.
[84] M. Maqbool, F. Bekele, and G. Fekadu, “Treatment Strategies Against Triple-Negative Breast Cancer: An Updated Review,” *Breast Cancer: Targets and Therapy*, vol. Volume 14, pp. 15–24, Jan. 2022, doi: 10.2147/BCTT.S348060.
[85] C. Liedtke *et al.*, “Response to Neoadjuvant Therapy and Long-Term Survival in Patients With Triple-Negative Breast Cancer,” *Journal of Clinical Oncology*, vol. 26, no. 8, pp. 1275–1281, Mar. 2008, doi: 10.1200/JCO.2007.14.4147.
[86] K. R. Bauer, M. Brown, R. D. Cress, C. A. Parise, and V. Caggiano, “Descriptive analysis of estrogen receptor (ER)-negative, progesterone receptor (PR)-negative, and HER2-negative invasive breast cancer, the so-called triple-negative phenotype,” *Cancer*, vol. 109, no. 9, pp. 1721–1728, May 2007, doi: 10.1002/cncr.22618.
[87] R. Sharma *et al.*, “Mapping Cancer in Africa: A Comprehensive and Comparable Characterization of 34 Cancer Types Using Estimates From GLOBOCAN 2020,” *Front Public Health*, vol. 10, Apr. 2022, doi: 10.3389/fpubh.2022.839835.
[88] “Active Immunotherapy and Passive Immunotherapy.” https://www.beckman.com/support/faq/research/active-immunotherapy-and-passive-immunotherapy (accessed Jul. 18, 2023).
[89] L. Li, F. Zhang, Z. Liu, and Z. Fan, “Immunotherapy for Triple-Negative Breast Cancer: Combination Strategies to Improve Outcome,” *Cancers (Basel)*, vol. 15, no. 1, p. 321, Jan. 2023, doi: 10.3390/cancers15010321.
[90] X. Wang *et al.*, “Immunological therapy: A novel thriving area for triple-negative breast cancer treatment,” *Cancer Lett*, vol. 442, pp. 409–428, Feb. 2019, doi: 10.1016/j.canlet.2018.10.042.
[91] C. Lee Ventola, “Cancer Immunotherapy, Part 2: Efficacy, Safety, and Other Clinical Considerations,” *Pharmacy and Therapeutics*, vol. 42, no. 7, p. 452, Jul. 2017, Accessed: Apr. 12, 2023. [Online]. Available: /pmc/articles/PMC5481296/
[92] J. Cortes *et al.*, “Pembrolizumab plus Chemotherapy in Advanced Triple-Negative Breast Cancer,” *New England Journal of Medicine*, vol. 387, no. 3, pp. 217–226, Jul. 2022, doi: 10.1056/NEJMoa2202809.
[93] S. P. Kang *et al.*, “Pembrolizumab KEYNOTE-001: an adaptive study leading to accelerated approval for two indications and a companion diagnostic,” *Annals of Oncology*, vol. 28, no. 6, pp. 1388–1398, Jun. 2017, doi: 10.1093/annonc/mdx076.
[94] C. M. Mckertish and V. Kayser, “Advances and Limitations of Antibody Drug Conjugates for Cancer,” *Biomedicines*, vol. 9, no. 8, p. 872, Jul. 2021, doi: 10.3390/biomedicines9080872.
[95] A. Bardia *et al.*, “Sacituzumab Govitecan in Metastatic Triple-Negative Breast Cancer,” *New England Journal of Medicine*, vol. 384, no. 16, pp. 1529–1541, Apr. 2021, doi: 10.1056/NEJMoa2028485.
[96] L. A. Carey *et al.*, “Sacituzumab govitecan as second-line treatment for metastatic triple-negative breast cancer—phase 3 ASCENT study subanalysis,” *NPJ Breast Cancer*, vol. 8, no. 1, p. 72, Jun. 2022, doi: 10.1038/s41523-022-00439-5.

[97] X. Wang and C. Guda, “Integrative exploration of genomic profiles for triple negative breast cancer identifies potential drug targets,” *Medicine*, vol. 95, no. 30, p. e4321, Jul. 2016, doi: 10.1097/MD.0000000000004321.
[98] C. Criscitiello, “Tumor-Associated Antigens in Breast Cancer,” *Breast Care*, vol. 7, no. 4, pp. 262–266, 2012, doi: 10.1159/000342164.
[99] M. A. Firer and G. Gellerman, “Targeted drug delivery for cancer therapy: the other side of antibodies,” *J Hematol Oncol*, vol. 5, no. 1, p. 70, Dec. 2012, doi: 10.1186/1756-8722-5-70.
[100] P. Yuan *et al.*, “Chondroitin sulfate proteoglycan 4 functions as the cellular receptor for Clostridium difficile toxin B,” *Cell Res*, vol. 25, no. 2, pp. 157–168, Feb. 2015, doi: 10.1038/cr.2014.169.
[101] S. Park *et al.*, “Unlike LGR4, LGR5 potentiates Wnt–β-catenin signaling without sequestering E3 ligases,” *Sci Signal*, vol. 13, no. 660, Dec. 2020, doi: 10.1126/scisignal.aaz4051.
[102] M.-F. Hou, P.-M. Chen, and P.-Y. Chu, “LGR5 overexpression confers poor relapse-free survival in breast cancer patients,” *BMC Cancer*, vol. 18, no. 1, p. 219, Dec. 2018, doi: 10.1186/s12885-018-4018-1.
[103] R. G. Morgan, E. Mortensson, and A. C. Williams, “Targeting LGR5 in Colorectal Cancer: Therapeutic gold or too plastic?,” *Br J Cancer*, vol. 118, no. 11, pp. 1410–1418, May 2018, doi: 10.1038/S41416-018-0118-6.
[104] B. Z. Stanger, “Cellular Homeostasis and Repair in the Mammalian Liver,” *Annu Rev Physiol*, vol. 77, p. 179, Feb. 2015, doi: 10.1146/ANNUREV-PHYSIOL-021113-170255.
[105] S. Xiao and L. Zhou, “Gastric Stem Cells: Physiological and Pathological Perspectives,” *Front Cell Dev Biol*, vol. 8, Sep. 2020, doi: 10.3389/FCELL.2020.571536.
[106] K. M. Polkoff *et al.*, “LGR5 is a conserved marker of hair follicle stem cells in multiple species and is present early and throughout follicle morphogenesis,” *Sci Rep*, vol. 12, no. 1, Dec. 2022, doi: 10.1038/S41598-022-13056-W.
[107] N. Koike, “The Role of Stem Cells in the Hepatobiliary System and in Cancer Development: a Surgeon’s Perspective,” in *Stem Cells and Cancer in Hepatology*, Elsevier, 2018, pp. 211–253. doi: 10.1016/B978-0-12-812301-0.00011-6.
[108] R. Yamaoka *et al.*, “CD90 expression in human intrahepatic cholangiocarcinoma is associated with lymph node metastasis and poor prognosis,” *J Surg Oncol*, vol. 118, no. 4, pp. 664–674, Sep. 2018, doi: 10.1002/jso.25192.
[109] F. Famili, A. S. Wiekmeijer, and F. J. Staal, “The development of T cells from stem cells in mice and humans,” *Future Sci OA*, vol. 3, no. 3, 2017, doi: 10.4155/FSOA-2016-0095.
[110] K. Baghaei *et al.*, “Isolation, differentiation, and characterization of mesenchymal stem cells from human bone marrow,” *Gastroenterol Hepatol Bed Bench*, vol. 10, no. 3, p. 208, 2017, doi: 10.22037/ghfbb.v0i0.1089.
[111] F. Cialdai, C. Risaliti, and M. Monici, “Role of fibroblasts in wound healing and tissue remodeling on Earth and in space,” *Front Bioeng Biotechnol*, vol. 10, Oct. 2022, doi: 10.3389/FBIOE.2022.958381.
[112] A. R. M. Lobba *et al.*, “High CD90 (THY-1) expression positively correlates with cell transformation and worse prognosis in basal-like breast cancer tumors,” *PLoS One*, vol. 13, no. 6, p. e0199254, Jun. 2018, doi: 10.1371/journal.pone.0199254.

[113] H. Lu *et al.*, "A breast cancer stem cell niche supported by juxtacrine signalling from monocytes and macrophages," *Nat Cell Biol*, vol. 16, no. 11, pp. 1105–1117, Nov. 2014, doi: 10.1038/ncb3041.
[114] L. Kisselbach, M. Merges, A. Bossie, and A. Boyd, "CD90 Expression on human primary cells and elimination of contaminating fibroblasts from cell cultures," *Cytotechnology*, vol. 59, no. 1, pp. 31–44, Jan. 2009, doi: 10.1007/s10616-009-9190-3.
[115] L. Leyton, J. Díaz, S. Martínez, E. Palacios, L. A. Pérez, and R. D. Pérez, "Thy-1/CD90 a Bidirectional and Lateral Signaling Scaffold," *Front Cell Dev Biol*, vol. 7, Jul. 2019, doi: 10.3389/fcell.2019.00132.
[116] W. Wang *et al.*, "Single-Cell Proteomic Profiling Identifies Nanoparticle Enhanced Therapy for Triple Negative Breast Cancer Stem Cells," *Cells*, vol. 10, no. 11, p. 2842, Oct. 2021, doi: 10.3390/cells10112842.
[117] K. Barzaman *et al.*, "Anti-cancer therapeutic strategies based on HGF/MET, EpCAM, and tumor-stromal cross talk," *Cancer Cell Int*, vol. 22, no. 1, p. 259, Aug. 2022, doi: 10.1186/s12935-022-02658-z.
[118] X. Zheng *et al.*, "EpCAM Inhibition Sensitizes Chemoresistant Leukemia to Immune Surveillance," *Cancer Res*, vol. 77, no. 2, pp. 482–493, Jan. 2017, doi: 10.1158/0008-5472.CAN-16-0842.
[119] R. Shome and S. S. Ghosh, "Tweaking EMT and MDR dynamics to constrain triple-negative breast cancer invasiveness by EGFR and Wnt/β-catenin signaling regulation", doi: 10.1007/s13402-020-00576-8/Published.
[120] J. Ni *et al.*, "Epithelial cell adhesion molecule (EpCAM) is associated with prostate cancer metastasis and chemo/radioresistance via the PI3K/Akt/mTOR signaling pathway," *Int J Biochem Cell Biol*, vol. 45, no. 12, pp. 2736–2748, Dec. 2013, doi: 10.1016/j.biocel.2013.09.008.
[121] "EpCAM and WNT signalling pathways. A regulated intramembrane... | Download Scientific Diagram." https://www.researchgate.net/figure/EpCAM-and-WNT-signalling-pathways-A-regulated-intramembrane-proteolysis-RIP-involves_fig4_256451762 (accessed Apr. 18, 2023).
[122] M. P. Motley, K. Banerjee, and B. C. Fries, "Monoclonal antibody-based therapies for bacterial infections," *Curr Opin Infect Dis*, vol. 32, no. 3, pp. 210–216, Jun. 2019, doi: 10.1097/QCO.0000000000000539.
[123] Z. Chen *et al.*, "Antibody-based drug delivery systems for cancer therapy: Mechanisms, challenges, and prospects," *Theranostics*, vol. 12, no. 8, pp. 3719–3746, 2022, doi: 10.7150/thno.72594.
[124] G. KÖHLER and C. MILSTEIN, "Continuous cultures of fused cells secreting antibody of predefined specificity," *Nature*, vol. 256, no. 5517, pp. 495–497, Aug. 1975, doi: 10.1038/256495a0.
[125] H. Hongrong Cai and A. A. Pandit, "Mini Review Article Corresponding Author Therapeutic Monoclonal Antibodies Approved by FDA in 2022," *Journal of Clinical & Experimental Immunology J Clin Exp Immunol*, vol. 8, no. 1, p. 533, 2023, Accessed: Apr. 18, 2023. [Online]. Available: https://www.accessdata.fda.gov/drugsatfda_docs/

[126] J. Charles A Janeway, P. Travers, M. Walport, and M. J. Shlomchik, “Immunobiology,” *Immunobiology*, no. 14102, pp. 1–10, 2001, Accessed: Apr. 18, 2023. [Online]. Available: https://www.ncbi.nlm.nih.gov/books/NBK10757/

[127] J. Charles A Janeway, P. Travers, M. Walport, and M. J. Shlomchik, “The structure of a typical antibody molecule,” 2001, Accessed: Apr. 20, 2023. [Online]. Available: https://www.ncbi.nlm.nih.gov/books/NBK27144/

[128] M. von Mehren, G. P. Adams, and L. M. Weiner, “Monoclonal Antibody Therapy for Cancer,” *Annu Rev Med*, vol. 54, no. 1, pp. 343–369, Feb. 2003, doi: 10.1146/annurev.med.54.101601.152442.

[129] G. P. Adams and L. M. Weiner, “Monoclonal antibody therapy of cancer,” *Nat Biotechnol*, vol. 23, no. 9, pp. 1147–1157, Sep. 2005, doi: 10.1038/nbt1137.

[130] L. C. Tsao, J. Force, and Z. C. Hartman, “Mechanisms of therapeutic anti-tumor monoclonal antibodies,” *Cancer Res*, vol. 81, no. 18, p. 4641, Sep. 2021, doi: 10.1158/0008-5472.CAN-21-1109.

[131] B. Alberts, A. Johnson, J. Lewis, M. Raff, K. Roberts, and P. Walter, “The Generation of Antibody Diversity,” 2002, Accessed: Jul. 02, 2023. [Online]. Available: https://www.ncbi.nlm.nih.gov/books/NBK26860/

[132] C. Keim, D. Kazadi, G. Rothschild, and U. Basu, “Regulation of AID, the B-cell genome mutator,” *Genes Dev*, vol. 27, no. 1, p. 1, Jan. 2013, doi: 10.1101/GAD.200014.112.

[133] J. Charles A Janeway, P. Travers, M. Walport, and M. J. Shlomchik, “The generation of diversity in immunoglobulins,” 2001, Accessed: Jul. 02, 2023. [Online]. Available: https://www.ncbi.nlm.nih.gov/books/NBK27140/

[134] C. Liu, H. Lin, L. Cao, K. Wang, and J. Sui, “Research progress on unique paratope structure, antigen binding modes, and systematic mutagenesis strategies of single-domain antibodies,” *Front Immunol*, vol. 13, p. 1059771, Nov. 2022, doi: 10.3389/FIMMU.2022.1059771.

[135] R. O’Kennedy, C. Murphy, and T. Devine, “Technology advancements in antibody purification,” *Antibody Technology Journal*, vol. Volume 6, pp. 17–32, Aug. 2016, doi: 10.2147/ANTI.S64762.

[136] D. Zahavi and L. Weiner, “Monoclonal Antibodies in Cancer Therapy,” *Antibodies*, vol. 9, no. 3, p. 34, Jul. 2020, doi: 10.3390/antib9030034.

[137] M. A. Firer and G. Gellerman, “Targeted drug delivery for cancer therapy: the other side of antibodies,” *J Hematol Oncol*, vol. 5, no. 1, p. 70, Dec. 2012, doi: 10.1186/1756-8722-5-70.

[138] G. M. Thurber, M. M. Schmidt, and K. D. Wittrup, “Antibody tumor penetration: Transport opposed by systemic and antigen-mediated clearance,” *Adv Drug Deliv Rev*, vol. 60, no. 12, pp. 1421–1434, Sep. 2008, doi: 10.1016/j.addr.2008.04.012.

[139] Z. Shen, R. L. Mernaugh, H. Yan, L. Yu, Y. Zhang, and X. Zeng, “Engineered Recombinant Single-Chain Fragment Variable Antibody for Immunosensors,” *Anal Chem*, vol. 77, no. 21, pp. 6834–6842, Nov. 2005, doi: 10.1021/ac0507690.

[140] M. L. Chiu, D. R. Goulet, A. Teplyakov, and G. L. Gilliland, “Antibody Structure and Function: The Basis for Engineering Therapeutics,” *Antibodies*, vol. 8, no. 4, p. 55, Dec. 2019, doi: 10.3390/antib8040055.

[141] Y. Kiguchi *et al.*, “Clonal array profiling of scFv-displaying phages for high-throughput discovery of affinity-matured antibody mutants,” *Sci Rep*, vol. 10, no. 1, p. 14103, Aug. 2020, doi: 10.1038/s41598-020-71037-3.

[142] Y. Sun, A. Estevez, T. Schlothauer, and A. T. Wecksler, “Antigen physiochemical properties allosterically effect the IgG Fc-region and Fc neonatal receptor affinity,” *MAbs*, vol. 12, no. 1, Jan. 2020, doi: 10.1080/19420862.2020.1802135.
[143] “Immunotoxins: A Review of Their Use in Cancer Treatment,” *J Stem Cells Regen Med*, vol. 1, no. 1, pp. 31–36, Dec. 2006, doi: 10.46582/jsrm.0101005.
[144] S. Baah, M. Laws, and K. M. Rahman, “Antibody–Drug Conjugates—A Tutorial Review,” *Molecules*, vol. 26, no. 10, May 2021, doi: 10.3390/MOLECULES26102943.
[145] A. Shapira and I. Benhar, “Toxin-Based Therapeutic Approaches,” *Toxins (Basel)*, vol. 2, no. 11, pp. 2519–2583, Oct. 2010, doi: 10.3390/toxins2112519.
[146] “Immunotoxins: A Review of Their Use in Cancer Treatment,” *J Stem Cells Regen Med*, vol. 1, no. 1, pp. 31–36, Dec. 2006, doi: 10.46582/jsrm.0101005.
[147] K. Eiklid, S. Olsnes, and A. Pihl, “Entry of lethal doses of abrin, ricin and modeccin into the cytosol of HeLa cells,” *Exp Cell Res*, vol. 126, no. 2, pp. 321–326, Apr. 1980, doi: 10.1016/0014-4827(80)90270-0.
[148] P. Michl and T. Gress, “Bacteria and Bacterial Toxins as Therapeutic Agents for Solid Tumors,” *Curr Cancer Drug Targets*, vol. 4, no. 8, pp. 689–702, Dec. 2004, doi: 10.2174/1568009043332727.
[149] V. Masignani, M. Pizza, and R. Rappuoli, “Molecular, functional, and evolutionary aspects of ADP-ribosylating toxins,” in *The Comprehensive Sourcebook of Bacterial Protein Toxins*, Elsevier, 2006, pp. 213–244. doi: 10.1016/B978-012088445-2/50017-2.
[150] A. Antignani and D. FitzGerald, “Immunotoxins: The Role of the Toxin,” *Toxins (Basel)*, vol. 5, no. 8, pp. 1486–1502, Aug. 2013, doi: 10.3390/toxins5081486.
[151] I. Pastan, R. Hassan, D. J. FitzGerald, and R. J. Kreitman, “Immunotoxin Treatment of Cancer,” *Annu Rev Med*, vol. 58, no. 1, pp. 221–237, Feb. 2007, doi: 10.1146/annurev.med.58.070605.115320.
[152] R. J. Kreitman, “Recombinant Immunotoxins Containing Truncated Bacterial Toxins for the Treatment of Hematologic Malignancies,” *BioDrugs*, vol. 23, no. 1, pp. 1–13, 2009, doi: 10.2165/00063030-200923010-00001.
[153] M. Li *et al.*, “Clinical targeting recombinant immunotoxins for cancer therapy,” *Onco Targets Ther*, vol. Volume 10, pp. 3645–3665, Jul. 2017, doi: 10.2147/OTT.S134584.
[154] A. Rust, L. Partridge, B. Davletov, and G. Hautbergue, “The Use of Plant-Derived Ribosome Inactivating Proteins in Immunotoxin Development: Past, Present and Future Generations,” *Toxins (Basel)*, vol. 9, no. 11, p. 344, Oct. 2017, doi: 10.3390/toxins9110344.
[155] I. Pastan, R. Beers, and T. K. Bera, “Recombinant Immunotoxins in the Treatment of Cancer,” in *Antibody Engineering*, New Jersey: Humana Press, pp. 503–518. doi: 10.1385/1-59259-666-5:503.
[156] P. Wolf and U. Elsässer-Beile, “Pseudomonas exotoxin A: From virulence factor to anti-cancer agent,” *International Journal of Medical Microbiology*, vol. 299, no. 3, pp. 161–176, Mar. 2009, doi: 10.1016/j.ijmm.2008.08.003.
[157] G. M. Rossolini and E. Mantengoli, “Treatment and control of severe infections caused by multiresistant Pseudomonas aeruginosa,” *Clinical Microbiology and Infection*, vol. 11, pp. 17–32, 2005, doi: 10.1111/j.1469-0691.2005.01161.x.

[158] V. S. Allured, R. J. Collier, S. F. Carroll, and D. B. McKay, “Structure of exotoxin A of Pseudomonas aeruginosa at 3.0-Angstrom resolution.,” *Proceedings of the National Academy of Sciences*, vol. 83, no. 5, pp. 1320–1324, Mar. 1986, doi: 10.1073/pnas.83.5.1320.

[159] M.-C. S. Pranchevicius and T. R. Vieira, “Production of recombinant immunotherapeutics for anticancer treatment,” *Bioengineered*, vol. 4, no. 5, pp. 305–312, Sep. 2013, doi: 10.4161/bioe.24666.

[160] J. Hwang, D. J. Fitzgerald, S. Adhya, and I. Pastan, “Functional domains of pseudomonas exotoxin identified by deletion analysis of the gene expressed in E. coli,” *Cell*, vol. 48, no. 1, pp. 129–136, Jan. 1987, doi: 10.1016/0092-8674(87)90363-1.

[161] J. E. Wedekind *et al.*, “Refined crystallographic structure of Pseudomonas aeruginosa exotoxin A and its implications for the molecular mechanism of toxicity 1 1Edited by D. Rees,” *J Mol Biol*, vol. 314, no. 4, pp. 823–837, Dec. 2001, doi: 10.1006/jmbi.2001.5195.

[162] C. B. Siegall, V. K. Chaudhary, D. J. Fitzgerald, and I. Pastan, “Functional Analysis of Domains 11, Ib, and I11 of Pseudomonas Exotoxin*,” *J Biol Chem*, vol. 264, no. 24, p. 1389, 1989, doi: 10.1016/S0021-9258(18)71671-2.

[163] B. Geny and M. R. Popoff, “Bacterial protein toxins and lipids: role in toxin targeting and activity,” *Biol Cell*, vol. 98, no. 11, pp. 633–651, Nov. 2006, doi: 10.1042/BC20060038.

[164] M. Dieffenbach and I. Pastan, “Mechanisms of Resistance to Immunotoxins Containing Pseudomonas Exotoxin A in Cancer Therapy,” *Biomolecules*, vol. 10, no. 7, pp. 1–13, Jul. 2020, doi: 10.3390/BIOM10070979.

[165] J. E. Weldon and I. Pastan, “A guide to taming a toxin--recombinant immunotoxins constructed from Pseudomonas exotoxin A for the treatment of cancer,” *FEBS J*, vol. 278, no. 23, pp. 4683–4700, Dec. 2011, doi: 10.1111/J.1742-4658.2011.08182.X.

[166] R. Mazor and I. Pastan, “Immunogenicity of Immunotoxins Containing Pseudomonas Exotoxin A: Causes, Consequences, and Mitigation,” *Front Immunol*, vol. 11, Jun. 2020, doi: 10.3389/FIMMU.2020.01261.

[167] P. Michl and T. Gress, “Bacteria and bacterial toxins as therapeutic agents for solid tumors,” *Curr Cancer Drug Targets*, vol. 4, no. 8, pp. 689–702, Mar. 2004, doi: 10.2174/1568009043332727.

[168] M. Michalska and P. Wolf, “Pseudomonas Exotoxin A: Optimized by evolution for effective killing,” *Front Microbiol*, vol. 6, no. SEP, p. 151249, Sep. 2015, doi: 10.3389/FMICB.2015.00963/BIBTEX.

[169] G. M. Rossolini and E. Mantengoli, “Treatment and control of severe infections caused by multiresistant Pseudomonas aeruginosa,” *Clinical Microbiology and Infection*, vol. 11, no. 4, pp. 17–32, Jan. 2005, doi: 10.1111/J.1469-0691.2005.01161.X.

[170] R. Mazor, E. M. King, and I. Pastan, “Strategies to Reduce the Immunogenicity of Recombinant Immunotoxins,” *Am J Pathol*, vol. 188, no. 8, pp. 1736–1743, Aug. 2018, doi: 10.1016/j.ajpath.2018.04.016.

[171] C. T. Kuan, L. H. Pai, and I. Pastan, “Immunotoxins containing Pseudomonas exotoxin that target LeY damage human endothelial cells in an antibody-specific mode: relevance to vascular leak syndrome.,” *Clin Cancer Res*, vol. 1, no. 12, pp. 1589–94, Dec. 1995.

[172] R. Hassan *et al.*, "Phase I Study of SS1P, a Recombinant Anti-Mesothelin Immunotoxin Given as a Bolus I.V. Infusion to Patients with Mesothelin-Expressing Mesothelioma, Ovarian, and Pancreatic Cancers," *Clinical Cancer Research*, vol. 13, no. 17, pp. 5144–5149, Sep. 2007, doi: 10.1158/1078-0432.CCR-07-0869.
[173] D. A. Khan, "Hypersensitivity and immunologic reactions to biologics: opportunities for the allergist," *Ann Allergy Asthma Immunol*, vol. 117, no. 2, pp. 115–120, Aug. 2016, doi: 10.1016/J.ANAI.2016.05.013.
[174] P. Hindryckx *et al.*, "Incidence, Prevention and Management of Anti-Drug Antibodies Against Therapeutic Antibodies in Inflammatory Bowel Disease: A Practical Overview," *Drugs*, vol. 77, no. 4, pp. 363–377, Mar. 2017, doi: 10.1007/S40265-017-0693-5.
[175] R. J. Kreitman *et al.*, "Complete Remissions of Adult T-cell Leukemia with Anti-CD25 Recombinant Immunotoxin LMB-2 and Chemotherapy to Block Immunogenicity," *Clinical Cancer Research*, vol. 22, no. 2, pp. 310–318, Jan. 2016, doi: 10.1158/1078-0432.CCR-15-1412.
[176] Y. Grinberg and I. Benhar, "Addressing the Immunogenicity of the Cargo and of the Targeting Antibodies with a Focus on Deimmunized Bacterial Toxins and on Antibody-Targeted Human Effector Proteins," *Biomedicines 2017, Vol. 5, Page 28*, vol. 5, no. 2, p. 28, Jun. 2017, doi: 10.3390/BIOMEDICINES5020028.
[177] "In Vitro Evaluation of Humanized/De-immunized Anti-PSMA Immunotoxins for the Treatment of Prostate Cancer," *Anticancer Res*, vol. 38, no. 1, Jan. 2018, doi: 10.21873/anticanres.12192.
[178] K. Hollevoet, E. Mason-Osann, F. Müller, and I. Pastan, "Methylation-Associated Partial Down-Regulation of Mesothelin Causes Resistance to Anti-Mesothelin Immunotoxins in a Pancreatic Cancer Cell Line," *PLoS One*, vol. 10, no. 3, p. e0122462, Mar. 2015, doi: 10.1371/journal.pone.0122462.
[179] M. C. U. Cheang *et al.*, "Defining Breast Cancer Intrinsic Subtypes by Quantitative Receptor Expression," *Oncologist*, vol. 20, no. 5, pp. 474–482, May 2015, doi: 10.1634/theoncologist.2014-0372.
[180] F. Podo *et al.*, "Triple-negative breast cancer: Present challenges and new perspectives," *Mol Oncol*, vol. 4, no. 3, pp. 209–229, Jun. 2010, doi: 10.1016/j.molonc.2010.04.006.
[181] A. M. Brewster, M. Chavez-MacGregor, and P. Brown, "Epidemiology, biology, and treatment of triple-negative breast cancer in women of African ancestry," *Lancet Oncol*, vol. 15, no. 13, pp. e625–e634, Dec. 2014, doi: 10.1016/S1470-2045(14)70364-X.
[182] W. Kruger and J. Apffelstaedt, "Young breast cancer patients in the developing world: incidence, choice of surgical treatment and genetic factors," *South African Family Practice*, vol. 49, no. 9, pp. 18–24, Oct. 2007, doi: 10.1080/20786204.2007.10873634.
[183] G. J. Morris *et al.*, "Differences in breast carcinoma characteristics in newly diagnosed African-American and Caucasian patients: a single-institution compilation compared with the National Cancer Institute's Surveillance, Epidemiology, and End Results database," *Cancer*, vol. 110, no. 4, pp. 876–884, Aug. 2007, doi: 10.1002/CNCR.22836.
[184] A. Vorobyeva *et al.*, "Radionuclide Molecular Imaging of EpCAM Expression in Triple-Negative Breast Cancer Using the Scaffold Protein DARPin Ec1," *Molecules*, vol. 25, no. 20, Oct. 2020, doi: 10.3390/MOLECULES25204719.

[185] J. Zhang *et al.*, "Efficacy of Anti-mesothelin Immunotoxin RG7787 plus Nab-Paclitaxel against Mesothelioma Patient–Derived Xenografts and Mesothelin as a Biomarker of Tumor Response," *Clinical Cancer Research*, vol. 23, no. 6, pp. 1564–1574, Mar. 2017, doi: 10.1158/1078-0432.CCR-16-1667.
[186] "Transformation of E. coli: Adapted Calcium Chloride Procedure | Microbiology | JoVE." https://www.jove.com/v/10515/transformation-e-coli-cells-using-an-adapted-calcium-chloride (accessed Jul. 05, 2023).
[187] J. Feher, "Osmosis and Osmotic Pressure," *Quantitative Human Physiology*, pp. 182–198, 2017, doi: 10.1016/B978-0-12-800883-6.00017-3.
[188] N. Yagi, K. Satonaka, M. Horio, H. Shimogaki, Y. Tokuda, and S. Maeda, "The role of DNase and EDTA on DNA degradation in formaldehyde fixed tissues," *Biotech Histochem*, vol. 71, no. 3, pp. 123–129, 1996, doi: 10.3109/10520299609117148.
[189] "Common Buffers, Media, and Stock Solutions," *Curr Protoc Hum Genet*, vol. 26, no. 1, Aug. 2000, doi: 10.1002/0471142905.HGA02DS26.
[190] "Alkaline Lysis Method: How it Works in 5 Simple Steps." https://bitesizebio.com/180/the-basics-how-alkaline-lysis-works/ (accessed Jul. 05, 2023).
[191] A. J. Doherty and S. W. Suh, "Structural and mechanistic conservation in DNA ligases," *Nucleic Acids Res*, vol. 28, no. 21, p. 4051, Nov. 2000, doi: 10.1093/NAR/28.21.4051.
[192] B. J. Smith, "SDS Polyacrylamide Gel Electrophoresis of Proteins," *Methods Mol Biol*, vol. 1, pp. 41–56, Nov. 1984, doi: 10.1385/0-89603-062-8:41.
[193] N. W. Roehm, G. H. Rodgers, S. M. Hatfield, and A. L. Glasebrook, "An improved colorimetric assay for cell proliferation and viability utilizing the tetrazolium salt XTT," *J Immunol Methods*, vol. 142, no. 2, pp. 257–265, Sep. 1991, doi: 10.1016/0022-1759(91)90114-U.
[194] R. Martini *et al.*, "African Ancestry–Associated Gene Expression Profiles in Triple-Negative Breast Cancer Underlie Altered Tumor Biology and Clinical Outcome in Women of African Descent," *Cancer Discov*, vol. 12, no. 11, pp. 2530–2551, Nov. 2022, doi: 10.1158/2159-8290.CD-22-0138.
[195] L. A. Newman *et al.*, "Hereditary Susceptibility for Triple Negative Breast Cancer Associated With Western Sub-Saharan African Ancestry," *Ann Surg*, vol. 270, no. 3, pp. 484–492, Sep. 2019, doi: 10.1097/SLA.0000000000003459.
[196] L. A. Newman and L. M. Kaljee, "Health Disparities and Triple-Negative Breast Cancer in African American Women," *JAMA Surg*, vol. 152, no. 5, p. 485, May 2017, doi: 10.1001/jamasurg.2017.0005.
[197] P. Kumar and R. Aggarwal, "An overview of triple-negative breast cancer," *Arch Gynecol Obstet*, vol. 293, no. 2, pp. 247–269, Feb. 2016, doi: 10.1007/s00404-015-3859-y.
[198] "FDA grants regular approval to sacituzumab govitecan for triple-negative breast cancer | FDA." https://www.fda.gov/drugs/resources-information-approved-drugs/fda-grants-regular-approval-sacituzumab-govitecan-triple-negative-breast-cancer (accessed May 09, 2023).
[199] L. A. Carey *et al.*, "The Triple Negative Paradox: Primary Tumor Chemosensitivity of Breast Cancer Subtypes," *Clinical Cancer Research*, vol. 13, no. 8, pp. 2329–2334, Apr. 2007, doi: 10.1158/1078-0432.CCR-06-1109.

[200] M. L. Telli, “Triple-Negative Breast Cancer,” in *Molecular Pathology of Breast Cancer*, Cham: Springer International Publishing, 2016, pp. 71–80. doi: 10.1007/978-3-319-41761-5_6.
[201] J. Sukumar, K. Gast, D. Quiroga, M. Lustberg, and N. Williams, “Triple-negative breast cancer: promising prognostic biomarkers currently in development,” *Expert Rev Anticancer Ther*, vol. 21, no. 2, pp. 135–148, Feb. 2021, doi: 10.1080/14737140.2021.1840984.
[202] M. García-Aranda and M. Redondo, “Immunotherapy: A Challenge of Breast Cancer Treatment,” *Cancers (Basel)*, vol. 11, no. 12, p. 1822, Nov. 2019, doi: 10.3390/cancers11121822.
[203] J. K. Sicklick *et al.*, “Molecular profiling of cancer patients enables personalized combination therapy: the I-PREDICT study,” *Nat Med*, vol. 25, no. 5, pp. 744–750, May 2019, doi: 10.1038/s41591-019-0407-5.
[204] J. L. da Silva, F. R. Rodrigues, G. G. de Mesquita, P. V. Fernandes, L. C. S. Thuler, and A. C. de Melo, “Triple-Negative Breast Cancer: Assessing the Role of Immunohistochemical Biomarkers on Neoadjuvant Treatment,” *Breast Cancer : Targets and Therapy*, vol. 13, p. 31, 2021, doi: 10.2147/BCTT.S287320.
[205] J. Meehan *et al.*, “Precision Medicine and the Role of Biomarkers of Radiotherapy Response in Breast Cancer,” *Front Oncol*, vol. 10, p. 628, Apr. 2020, doi: 10.3389/FONC.2020.00628.
[206] S. M. Hercules *et al.*, “Triple-negative breast cancer prevalence in Africa: a systematic review and meta-analysis,” *BMJ Open*, vol. 12, no. 5, p. e055735, May 2022, doi: 10.1136/bmjopen-2021-055735.
[207] “Advanced Triple-Negative Breast Cancer | KEYTRUDA® (pembrolizumab) | Patients.” https://www.keytruda.com/triple-negative-breast-cancer/ (accessed May 10, 2023).
[208] B. D. Lehmann *et al.*, “Identification of human triple-negative breast cancer subtypes and preclinical models for selection of targeted therapies,” *Journal of Clinical Investigation*, vol. 121, no. 7, pp. 2750–2767, Jul. 2011, doi: 10.1172/JCI45014.
[209] A. M. Brewster, M. Chavez-MacGregor, and P. Brown, “Epidemiology, biology, and treatment of triple-negative breast cancer in women of African ancestry,” *Lancet Oncol*, vol. 15, no. 13, pp. e625–e634, Dec. 2014, doi: 10.1016/S1470-2045(14)70364-X.
[210] R. M. Califf, “Biomarker definitions and their applications,” *Exp Biol Med*, vol. 243, no. 3, p. 213, Feb. 2018, doi: 10.1177/1535370217750088.
[211] L. Li, F. Zhang, Z. Liu, and Z. Fan, “Immunotherapy for Triple-Negative Breast Cancer: Combination Strategies to Improve Outcome,” *Cancers (Basel)*, vol. 15, no. 1, Jan. 2023, doi: 10.3390/CANCERS15010321.
[212] L. Shan, Y. Liu, and P. Wang, “Recombinant Immunotoxin Therapy of Solid Tumors: Challenges and Strategies,” *J Basic Clin Med*, vol. 2, no. 2, p. 1, 2013, Accessed: May 26, 2023. [Online]. Available: /pmc/articles/PMC4192646/
[213] S. J. Isakoff, “Triple Negative Breast Cancer: Role of Specific Chemotherapy Agents,” *Cancer J*, vol. 16, no. 1, p. 53, Jan. 2010, doi: 10.1097/PPO.0B013E3181D24FF7.
[214] A. Lin *et al.*, “Off-target toxicity is a common mechanism of action of cancer drugs undergoing clinical trials,” *Sci Transl Med*, vol. 11, no. 509, Sep. 2019, doi: 10.1126/SCITRANSLMED.AAW8412.

[215] P. Chames, M. Van Regenmortel, E. Weiss, and D. Baty, “Therapeutic antibodies: successes, limitations and hopes for the future,” *Br J Pharmacol*, vol. 157, no. 2, p. 220, May 2009, doi: 10.1111/J.1476-5381.2009.00190.X.
[216] “LGR5 as a potential therapeutic target for breast cancer: A Systematic Review and Meta-analysis - PubMed.” https://pubmed.ncbi.nlm.nih.gov/36239721/ (accessed Jan. 15, 2023).
[217] A. S. Wayne, D. J. FitzGerald, R. J. Kreitman, and I. Pastan, “Immunotoxins for leukemia,” *Blood*, vol. 123, no. 16, p. 2470, Apr. 2014, doi: 10.1182/BLOOD-2014-01-492256.
[218] S. Barth, M. Huhn, B. Matthey, A. Klimka, E. A. Galinski, and A. Engert, “Compatible-solute-supported periplasmic expression of functional recombinant proteins under stress conditions,” *Appl Environ Microbiol*, vol. 66, no. 4, pp. 1572–1579, Apr. 2000, doi: 10.1128/AEM.66.4.1572-1579.2000.
[219] T. Nachreiner, F. Kampmeier, T. Thepen, R. Fischer, S. Barth, and M. Stöcker, “Depletion of autoreactive B-lymphocytes by a recombinant myelin oligodendrocyte glycoprotein-based immunotoxin,” *J Neuroimmunol*, vol. 195, no. 1–2, pp. 28–35, Mar. 2008, doi: 10.1016/J.JNEUROIM.2008.01.001.
[220] J. Kaur, A. Kumar, and J. Kaur, “Strategies for optimization of heterologous protein expression in E. coli: Roadblocks and reinforcements,” *Int J Biol Macromol*, vol. 106, pp. 803–822, Jan. 2018, doi: 10.1016/J.IJBIOMAC.2017.08.080.
[221] J. Ratelade, M.-C. Miot, E. Johnson, J.-M. Betton, P. Mazodier, and N. Benaroudj, “Production of Recombinant Proteins in the lon-Deficient BL21(DE3) Strain of Escherichia coli in the Absence of the DnaK Chaperone,” *Appl Environ Microbiol*, vol. 75, no. 11, p. 3803, Jun. 2009, doi: 10.1128/AEM.00255-09.
[222] W. Schumann, L. Carlos, and S. Ferreira, “Production of recombinant proteins in Escherichia coli”, Accessed: May 31, 2023. [Online]. Available: www.sbg.org.br
[223] L. Briand *et al.*, “A self-inducible heterologous protein expression system in Escherichia coli,” *Sci Rep*, vol. 6, Sep. 2016, doi: 10.1038/SREP33037.
[224] M. Mühlmann, E. Forsten, S. Noack, and J. Büchs, “Optimizing recombinant protein expression via automated induction profiling in microtiter plates at different temperatures,” *Microb Cell Fact*, vol. 16, no. 1, pp. 1–12, Nov. 2017, doi: 10.1186/S12934-017-0832-4/FIGURES/5.
[225] A. Sandomenico, J. P. Sivaccumar, and M. Ruvo, “Evolution of Escherichia coli Expression System in Producing Antibody Recombinant Fragments,” *Int J Mol Sci*, vol. 21, no. 17, pp. 1–39, Sep. 2020, doi: 10.3390/IJMS21176324.
[226] S. Mojtabavi, N. Samadi, and M. A. Faramarzi, “Osmolyte-Induced Folding and Stability of Proteins: Concepts and Characterization,” *Iran J Pharm Res*, vol. 18, no. Suppl1, p. 13, Sep. 2019, doi: 10.22037/IJPR.2020.112621.13857.
[227] B. C. Joseph, S. Pichaimuthu, and S. Srimeenakshi, “An Overview of the Parameters for Recombinant Protein Expression in Escherichia coli,” *J Cell Sci Ther*, vol. 06, no. 05, 2015, doi: 10.4172/2157-7013.1000221.
[228] C. French, E. Keshavarz-Moore, and J. M. Ward, “Development of a simple method for the recovery of recombinant proteins from the Escherichia coli periplasm,” *Enzyme Microb Technol*, vol. 19, no. 5, pp. 332–338, 1996, doi: 10.1016/S0141-0229(96)00003-8.

[229] N. G. Bednarska, J. Schymkowitz, F. Rousseau, and J. Van Eldere, “Protein aggregation in bacteria: the thin boundary between functionality and toxicity,” *Microbiology (Reading)*, vol. 159, no. Pt 9, pp. 1795–1806, Sep. 2013, doi: 10.1099/MIC.0.069575-0.
[230] M. Ashayeri-Panah, F. Eftekhar, B. Kazemi, and J. Joseph, “Cloning, optimization of induction conditions and purification of Mycobacterium tuberculosis Rv1733c protein expressed in Escherichia coli,” *Iran J Microbiol*, vol. 9, no. 2, p. 64, 2017, Accessed: May 31, 2023. [Online]. Available: /pmc/articles/PMC5715279/
[231] M. Lebendiker and T. Danieli, “Production of prone-to-aggregate proteins,” *FEBS Lett*, vol. 588, no. 2, pp. 236–246, Jan. 2014, doi: 10.1016/J.FEBSLET.2013.10.044.
[232] D. M. Francis and R. Page, “Strategies to Optimize Protein Expression in E. coli,” *Curr Protoc Protein Sci*, vol. 61, no. 1, p. 5241, Aug. 2010, doi: 10.1002/0471140864.PS0524S61.
[233] J. Glazyrina *et al.*, “High cell density cultivation and recombinant protein production with Escherichia coli in a rocking-motion-type bioreactor,” *Microb Cell Fact*, vol. 9, p. 42, May 2010, doi: 10.1186/1475-2859-9-42.
[234] K. J. Mukherjee, D. C. D. Rowe, N. A. Watkins, and D. K. Summers, “Studies of Single-Chain Antibody Expression in Quiescent Escherichia coli,” *Appl Environ Microbiol*, vol. 70, no. 5, p. 3005, May 2004, doi: 10.1128/AEM.70.5.3005-3012.2004.
[235] C. Schimek *et al.*, “Extraction of recombinant periplasmic proteins under industrially relevant process conditions: Selectivity and yield strongly depend on protein titer and methodology,” *Biotechnol Prog*, vol. 36, no. 5, Sep. 2020, doi: 10.1002/BTPR.2999.
[236] J. A. Bornhorst and J. J. Falke, “[16] Purification of proteins using polyhistidine affinity tags,” 2000, pp. 245–254. doi: 10.1016/S0076-6879(00)26058-8.
[237] M. E. Kimple, A. L. Brill, and R. L. Pasker, “Overview of Affinity Tags for Protein Purification,” *Current protocols in protein science / editorial board, John E. Coligan ... [et al.]*, vol. 73, no. SUPPL.73, p. Unit, 2013, doi: 10.1002/0471140864.PS0909S73.
[238] “GPC-IR® | High Temperature GPC/SEC System for Polyolefins - Polymer Char.” https://polymerchar.com/products/analytical-instruments/gpc-ir?gclid=Cj0KCQjw4NujBhC5ARIsAF4Iv6c2xr6dmX2XvVCbkLwWsNVWQlY-6Kx-tmrStfvQNsump2r1QVekwqsaAkj-EALw_wcB (accessed Jun. 01, 2023).
[239] Y. Pouny, C. Weitzman, and H. Ronald Kaback, “In vitro biotinylation provides quantitative recovery of highly purified active lactose permease in a single step,” *Biochemistry*, vol. 37, no. 45, pp. 15713–15719, Nov. 1998, doi: 10.1021/BI981519Z.
[240] J. Tucker and R. Grisshammer, “Purification of a rat neurotensin receptor expressed in Escherichia coli,” *Biochem J*, vol. 317 (Pt 3), no. Pt 3, pp. 891–899, Aug. 1996, doi: 10.1042/BJ3170891.
[241] R. R. Burgess, “A brief practical review of size exclusion chromatography: Rules of thumb, limitations, and troubleshooting,” *Protein Expr Purif*, vol. 150, pp. 81–85, Oct. 2018, doi: 10.1016/J.PEP.2018.05.007.
[242] M. Johnson, “Detergents: Triton X-100, Tween-20, and More,” *Materials and Methods*, vol. 3, Jan. 2013, doi: 10.13070/MM.EN.3.163.
[243] J. Hering *et al.*, “The rapid ‘teabag’ method for high-end purification of membrane proteins,” *Sci Rep*, vol. 10, no. 1, p. 16167, Dec. 2020, doi: 10.1038/S41598-020-73285-9.

[244] I. Voráčková, Š. Suchanová, P. Ulbrich, W. E. Diehl, and T. Ruml, "Purification of proteins containing zinc finger domains using Immobilized Metal Ion Affinity Chromatography," *Protein Expr Purif*, vol. 79, no. 1, p. 88, Sep. 2011, doi: 10.1016/J.PEP.2011.04.022.
[245] J. Giacometti and D. Josić, "Protein and Peptide Separations," *Liquid Chromatography: Applications*, pp. 149–184, 2013, doi: 10.1016/B978-0-12-415806-1.00007-3.
[246] V. Riguero *et al.*, "Immobilized metal affinity chromatography optimization for poly-histidine tagged proteins," *J Chromatogr A*, vol. 1629, Oct. 2020, doi: 10.1016/J.CHROMA.2020.461505.
[247] S. Knecht, D. Ricklin, A. N. Eberle, and B. Ernst, "Oligohis-tags: Mechanisms of binding to Ni2+-NTA surfaces," *Journal of Molecular Recognition*, vol. 22, no. 4, pp. 270–279, Jul. 2009, doi: 10.1002/JMR.941.
[248] V. Riguero *et al.*, "Immobilized metal affinity chromatography optimization for poly-histidine tagged proteins," *J Chromatogr A*, vol. 1629, p. 461505, Oct. 2020, doi: 10.1016/J.CHROMA.2020.461505.
[249] S. Łukasiewicz, M. Czeczelewski, A. Forma, J. Baj, R. Sitarz, and A. Stanisławek, "Breast Cancer—Epidemiology, Risk Factors, Classification, Prognostic Markers, and Current Treatment Strategies—An Updated Review," *Cancers (Basel)*, vol. 13, no. 17, Sep. 2021, doi: 10.3390/CANCERS13174287.
[250] S. A. Dass *et al.*, "Triple Negative Breast Cancer: A Review of Present and Future Diagnostic Modalities," *Medicina (B Aires)*, vol. 57, no. 1, pp. 1–18, Jan. 2021, doi: 10.3390/MEDICINA57010062.
[251] S. Cocco *et al.*, "Biomarkers in Triple-Negative Breast Cancer: State-of-the-Art and Future Perspectives," *Int J Mol Sci*, vol. 21, no. 13, pp. 1–33, Jul. 2020, doi: 10.3390/IJMS21134579.
[252] A. C. Parslow, A. H. A. Clayton, P. Lock, and A. M. Scott, "Confocal Microscopy Reveals Cell Surface Receptor Aggregation Through Image Correlation Spectroscopy," *J Vis Exp*, vol. 2018, no. 138, p. 57164, Aug. 2018, doi: 10.3791/57164.
[253] A. D. Elliott, "Confocal Microscopy: Principles and Modern Practices," *Curr Protoc Cytom*, vol. 92, no. 1, p. e68, Mar. 2020, doi: 10.1002/CPCY.68.
[254] D. A. Basiji, W. E. Ortyn, L. Liang, V. Venkatachalam, and P. Morrissey, "Cellular Image Analysis and Imaging by Flow Cytometry," *Clin Lab Med*, vol. 27, no. 3, p. 653, Sep. 2007, doi: 10.1016/J.CLL.2007.05.008.
[255] N. S. Barteneva, E. Fasler-Kan, and I. A. Vorobjev, "Imaging Flow Cytometry: Coping with Heterogeneity in Biological Systems," *Journal of Histochemistry and Cytochemistry*, vol. 60, no. 10, p. 723, Oct. 2012, doi: 10.1369/0022155412453052.
[256] K. M. McKinnon, "Flow Cytometry: An Overview," *Curr Protoc Immunol*, vol. 120, p. 5.1.1, Feb. 2018, doi: 10.1002/CPIM.40.
[257] D. A. Basiji, W. E. Ortyn, L. Liang, V. Venkatachalam, and P. Morrissey, "Cellular Image Analysis and Imaging by Flow Cytometry," *Clin Lab Med*, vol. 27, no. 3, p. 653, Sep. 2007, doi: 10.1016/J.CLL.2007.05.008.
[258] L. M. Granat, O. Kambhampati, S. Klosek, B. Niedzwecki, K. Parsa, and D. Zhang, "The promises and challenges of patient-derived tumor organoids in drug development and precision oncology," *Animal Model Exp Med*, vol. 2, no. 3, p. 150, Sep. 2019, doi: 10.1002/AME2.12077.

[259] P. Mirabelli, L. Coppola, and M. Salvatore, “Cancer Cell Lines Are Useful Model Systems for Medical Research,” *Cancers (Basel)*, vol. 11, no. 8, Aug. 2019, doi: 10.3390/CANCERS11081098.
[260] G. Kaur and J. M. Dufour, “Cell lines: Valuable tools or useless artifacts,” *Spermatogenesis*, vol. 2, no. 1, p. 1, Jan. 2012, doi: 10.4161/SPMG.19885.
[261] R. Mazor, M. Onda, and I. Pastan, “Immunogenicity of therapeutic recombinant immunotoxins,” *Immunol Rev*, vol. 270, no. 1, pp. 152–164, Mar. 2016, doi: 10.1111/imr.12390.
[262] C. Alewine, L. Xiang, T. Yamori, G. Niederfellner, K. Bosslet, and I. Pastan, “Efficacy of RG7787, a next-generation mesothelin-targeted immunotoxin, against triple-negative breast and gastric cancers,” *Mol Cancer Ther*, vol. 13, no. 11, pp. 2653–2661, Nov. 2014, doi: 10.1158/1535-7163.MCT-14-0132.
[263] N. M. Rueth *et al.*, “Underuse of trimodality treatment affects survival for patients with inflammatory breast cancer: an analysis of treatment and survival trends from the National Cancer Database,” *J Clin Oncol*, vol. 32, no. 19, pp. 2018–2024, Jul. 2014, doi: 10.1200/JCO.2014.55.1978.